Alma Mater Studiorum - Università di Bologna

School of Science
Department of Physics and Astronomy
Master Degree Programme in Astrophysics and Cosmology

Tools for Advanced Chain Access Analysis on Satellite Constellations

Graduation Thesis

Presented by:
Luca Pizzuto

Supervisor:
Chiar.mo Prof. Dario Modenini

Co-supervisor:
Samuele Raffa, M. Sc.

Academic year 2023-2024
Graduation date V

Abstract

Keywords: Free Space Optical Communication, Satellite Constellations, Optical Inter-Satellite Links, Network Optimization, Python, DLR

Free Space Optical (FSO) communication between satellites is a new cutting-edge topic that is gaining more and more popularity, due to its possible advantages with respect to standard radio communication. Another interesting and under development field is the one of satellite constellations. Feeder Links for Non Geo-Stationary Orbits (FL4NGSO) is a joint project between DLR, ESA and Kepler Communications wich aims at studying the coverage and access availability performance of two Low Earth Orbit (LEO) constellations that use Optical (Uplink) Feeder links and Optical Inter-Satellite Links (OISL). The goal is to couple the fast, reliable and power efficient FSO communication with the coverage benefits of a LEO constellation.

This work will present the main results of the access availability and inter-satellite links analysis, which make the core part of the project as it was initially designed. However, the main focus will be on the logic and implementation of two Python-based performance optimization tools: a Network Optimization tool and a Flexible OISL tool. This thesis will show how these tools significantly improve the results of the analysis by identifying the most optimal Optical Ground Station (OGS) network and the most optimal OISL architecture to guarantee access availabilities above 99% with the minimum number of OGSs possible.

Across the different sections the reader will see how the access availability performance of each constellation improves by introducing OISL first, and the optimization tools later, as well as the intrinsic differences between constellation A, with a higher orbital altitude and a limited number of satellites, and constellation B, with a lower orbital altitude and a larger number of satellites. It emerged that constellation A needs significantly less OGSs than constellation B to reach an optimal coverage and access availability for all the most important targets. The Flexible OISL tool improves the performance of the constellations by shifting some of the requirements from the ground segment to the space segment, with the net result of reducing the number of OGSs needed to guarantee an operable network.

The results obtained were used to conclude the thesis with a trade-off analysis between the two constellations, considering the access availability performance, the composition of the OGS network, the complexity, the latency and the estimated cost and environmental impact. The conclusion is that the higher altitude constellation is by far more performing for all the trade factors, with the exception of the latency, and is therefore better suited for this project.

Contents

1 Introduction **10**
- 1.1 Thesis Motivation . . . 11
- 1.2 Introduction to FL4NGSO . . . 11
- 1.3 Methodology and structure . . . 12

2 Satellite Communication **14**
- 2.1 Optical Communication: Heritage and Outlook . . . 14
  - 2.1.1 Advantages of FSO Communication . . . 16
  - 2.1.2 Challenges of FSO Communication . . . 19

3 Satellite Constellation Design **20**
  - 3.0.1 Walker constellations . . . 24

4 Chain Access and Availability Analysis **25**
- 4.1 Data PreProcessing . . . 28
- 4.2 OGS Selection . . . 30
- 4.3 Chain Analysis . . . 32
- 4.4 Availability Analysis . . . 35

5 OGS HandOver **39**
- 5.1 HandOver Logic . . . 41
- 5.2 HandOver Results . . . 44

6 Optical Inter-Satellite Links **47**
- 6.1 OISL Logic and Implementation . . . 48
- 6.2 OISL Results . . . 50

7 Chain Duration Analysis **54**
- 7.1 Duration Analysis Implementation . . . 54
- 7.2 Duration Analysis Results . . . 55
- 7.3 90 Percentile cut . . . 56

8 Network Optimization **57**
- 8.1 Logic of the tool . . . 57
- 8.2 Results of the tool . . . 62
  - 8.2.1 Constellation A without OISL . . . 63
  - 8.2.2 Constellation A with OISL . . . 64
  - 8.2.3 Constellation B with OISL . . . 66
  - 8.2.4 General Conclusions . . . 70

9 Flexible OISL **74**
- 9.1 Logic of the tool . . . 75
- 9.2 Flexible OISL Implementation . . . 77
- 9.3 Results of the tool . . . 81
- 9.4 General Conclusions . . . 85
- 9.5 Flexible OISL: Constraints on Payload Allocation . . . 87
- 9.6 Logic and Implementation of the tool . . . 88

9.7 Results of the tool 93
9.8 General Conclusions 99

10 Conclusion **101**
10.1 Executive Summary 101
10.2 Trade-Off 102
10.3 Suggestions for Future Research 105

List of Figures

1 Conceptual topology of Free Space Optical (FSO) integrated network [34]. 10
2 Overview of mission elements between ARTEMIS and SPOT-4 (image credit: CNES). 15
3 Visual representation of EDRS constellation and its communication architecture. . . 16
4 Comparison of optical and RF beam divergence from Mars towards Earth [12]. . . . 17
5 Definition of classical orbital elements [19]. 20
6 Comparison of the coverage footprints of LEO satellite versus MEO satellite [25]. . . 22
7 Visualization of FL4NGSO's Europe target grid. 22
8 Coverage footprint of a satellite as a function of its altitude h [13]. 23
9 Ground swath by successive satellites in the same orbital plane [13]. 24
10 Example of concurrent accesses per OGS plot. 26
11 Example of Access Availability percentage plot. 27
12 Example of Coverage HeatMap plot. 28
13 STK framework: Graphic Windows and Access Report Manager. 29
14 Location of the selected OGSs. 31
15 Basic representation of the concept of Chain Access. 32
16 Chain Access generation process. 33
17 Visualization of the Cloud Filtering process. 34
18 Visualisation of Chain Access definition through access windows overlap. 35
19 Access Availability and Coverage HeatMap implementation. 36
20 Access Availability percentage (a) and Coverage HeatMap (b) for the Best Cloud network in Constellation A. 37
21 Access Availability percentage for the Best Cloud (a) and Western (b) networks in Constellation B. 38
22 Topological Concurrent Accesses histograms for the OGS in Barcelona, for constellation A and B. 39
23 Number of concurrent accesses for Amsterdam OGS in constellation B over a 40 minutes period. 42
24 Flowchart of the HO Chain DB creation. 44
25 Access Availability for the Best Cloud Network in constellation A and B after the implementation of the HO. 45
26 Decrease in Access Availability for the Best Cloud Network in constellation A and B after the implementation of the HO. 45
27 Topology of 1 hop OISL. 47
28 Ground coverage of a single chain with no OISL and with 1 hop OISL. 48
29 Flowchart of the OISL Chain DB creation. 50
30 Northern Network, constellation A. Access Availability with HO , with HO and OISL and Access Availability Improvement due to the introduction of OISL. 51
31 Northern Network, constellation B. Access Availability with HO, with HO and OISL and Access Availability Improvement due to the introduction of OISL. 52
32 Chain Duration CDF and PDF for Munich OGS in constellation A and B with HandOver. 55
33 Chain Duration per target for the Northern network in constellation B with HO without OISL and with OISL. 55
34 Change in Chain Duration and Availability after the introduction of the $90th$ percentile cut. 56
35 Flowchart of the Network Optimization Tool. 61

36 Flowchart of the Trade-Off algorithm. 62
37 Access availability percentage for the best network of 5 OGSs in constellation A. . . 64
38 Access availability for the best network of 9 OGSs for constellation A. 65
39 Access availability for the best network of 11 OGSs for constellation A. 66
40 Access availability for the best network of 5 OGSs for constellation B. 67
41 Access availability for the best network of 9 OGSs for constellation B. 68
42 Access availability for the best networks of 14 and 16 OGSs for constellation B. . . . 69
43 Access availability for constellation B considering all 24 OGSs. 69
44 Constellation A, comparison between the increase in availability performance due to the optimization of the network and the one due to the introduction of a new OGS. 70
45 Constellation B, comparison between the increase in availability performance due to the optimization of the network and the one due to the introduction of a new OGS. 71
46 Availability scores and percentage changes of the best networks with increasing number of OGSs. 72
47 Ground coverage of a single chain with 2 hops OISL. 74
48 Western Network, constellation B. Access Availability with 2 hops and Access Availability Improvement due to the introduction of 1 additional hop. 75
49 Satellites available for flexible OISL. 76
50 Flowchart of the Flexible OISL Tool. 79
51 Flowchart of the trade-off tool to select the satellites to include in the hop of a specific Uplink group. 81
52 Constellation A, Best Cloud Network. Access Availability Percentage with flexible OISL and Percentage Improvement in Access Availability from Classical OISL geometry to Flexible OISL geometry. 82
53 Constellation A, 9 OGSs. Access Availability Percentage with flexible OISL and Percentage Improvement in Access Availability from Classical OISL geometry to Flexible OISL geometry. 82
54 Constellation A. Access Availability percentage of the most performing network of 10 OGSs with Flexible OISL. 83
55 Constellation B, Best Cloud Network. Access Availability Percentage with flexible OISL and Percentage Improvement in Access Availability from Classical OISL geometry to Flexible OISL geometry 84
56 Constellation B, Best 16 OGSs Network. Access Availability Percentage with flexible OISL and Percentage Improvement in Access Availability from Classical OISL geometry to Flexible OISL geometry. 84
57 Constellation B. Access Availability percentage of the most performing network of 16 OGSs with Flexible OISL. 85
58 Artistic representation of two satellites linked via the classic OISL geometry [45]. . . 87
59 Projected visibility cone of an optical terminal for ISL. 88
60 AER access of a random satellite and a central satellite, showed with its velocity vector. 89
61 Satellite 8 visible from the Eastern and Northern decks. 90
62 Flowchart of the Find Deck algorithm. 92
63 Flowchart of the Flexible OISL Tool with payload constraints. 93
64 Access Availability percentage and Coverage Heatmap for the Best Cloud network in constellation A, with Flexible OISL and constraints on payload allocation. 94
65 HeatMap for the Best Cloud network in constellation A, with flexible OISL but without constraints on payload allocation. 95

66 Access Availability percentage change after the introduction of the payload allocation constraint for the Best Cloud network in constellation A. 96
67 Access Availability improvements for the Best Cloud network in constellation A, from classic OISL to Flexible OISL with payload constraints. 97
68 Access Availability percentage (a) and Improvements from Classic to Flexible OISL with constraints (b) for the best 9 OGSs network in constellation A. 98
69 Access Availability improvements for the best 11 OGSs network in constellation A, from classic OISL to Flexible OISL with payload constraints. 99

List of Tables

1 Constellations Characteristics. 12
2 Comparison between an optical and a RF communication system in different link configurations. 17
3 Major Satellite Constellation Parameters. 21
4 Example of a small interval of time (1 second) in which no HO can be guaranteed due to topological constraints. 40
5 Topological outage for constellation B over 1 simulation period. 41
6 Number of networks tested per OGS number and Constellation - OISL logic. 62
7 Composition of the best networks tested per OGS number and Constellation. 63
8 ISL Terminals implementation. 90
9 Example rows from the AER .csv file. 91
10 Comparison between classic OISL and flexible OISL access availability results for networks of 5, 9 and 11 OGSs. 100
11 Average Weighted Availability Gain from classic OISL to flexible OISL for networks of 5, 9 and 11 OGSs. 100
12 Absolute rating values for the trade-off factors. 103
13 Qualitative trade study results. 104
14 Constellations values for each trade factor. 104
15 Quantitative trade study results. 104

List of Acronyms

AER Azimuth Elevation Range

AO Adaptive Optics

CapEx Capital Expenditure

CDF Cumulative Distribution Function

ConOps Concept of Operations

DL Downlink

DLR Deutsches Zentrum fur Luft und Raumfahrt

DSOC Deep Space Optical Communications

EDRS European Data Relay System

ESA European Space Agency

FL4NGSO Feeder Links for Non Geo-Stationary Orbits

FSO Free Space Optical

GEO Geo-Stationary Orbit Orbit

GNSS Global Navigation Satellite System

GPS Global Positioning System

GS Ground Station

HO Hand Over

HM HeatMap

ISS International Space Station

LCT Laser Communication Terminal

LEO Low Earth Orbit

LOS Line Of Sight

MEO Medium Earth Orbit

NASA National Aeronautics and Space Administration

NIR Near Infra Red

NO Network Optimization

OpEx Operational Expenditure

OGS Optical Ground Station

OISL Optical Inter-Satellite Link

OWNs Optical Wireless Networks

PDF Probability Distribution Function

PNT Positioning, Navigation and Timing

RF Radio Frequency

SQL Structured Query Language

STK System Tool Kit

UL Uplink

1 Introduction

Free Space Optical (FSO) communication between satellites is a new cutting-edge topic that is gaining more and more popularity, due to its possible advantages with respect to standard radio communication. Thus far, in wireless communication systems, the Radio Frequency (RF) has remained the dominant technology in both licensed and unlicensed spectra, which has resulted in its wide-scale adoption and the development of a huge number of RF devices. A few fundamental problems with the RF band are limited capacity, high cost in the licensed spectrum technologies and interference in unlicensed spectrum technologies. Owing to an exponential growth of the number of consumer devices, the researchers are exploring new means of wireless communication.
FSO is a wireless communication technology which uses light as a medium for transmission of data at frequencies above 300 GHz, a frequency significantly higher than the ones typically used in satellite communications, which range from 1.5 and 30 GHz [34]. The higher frequency allows for many benefits including being faster, more secure, lighter and more flexible, but it has some challenges, like the higher beam accuracy requirement and the presence of clouds and turbulence from the atmosphere [43].
FSO communication involves three key components: the transmitter, the propagation medium, and the receiver. The transmitter is often a satellite, a Ground Station (GS), or another element of the communication network. The payload of the satellite includes an optical terminal and its adaptive optics. The signal is created as photons from a light source, travels through the propagation medium, and is received by a photodiode in the payload of another satellite or GS. This photodiode converts the signal into an electrical signal, which can then be processed, stored, or forwarded to another receiver [31]. In FSO communication, the propagation medium is the vacuum of space, which is assumed to be free of losses. This means that the signal transmission relies solely on the optical connection between the sender and receiver.

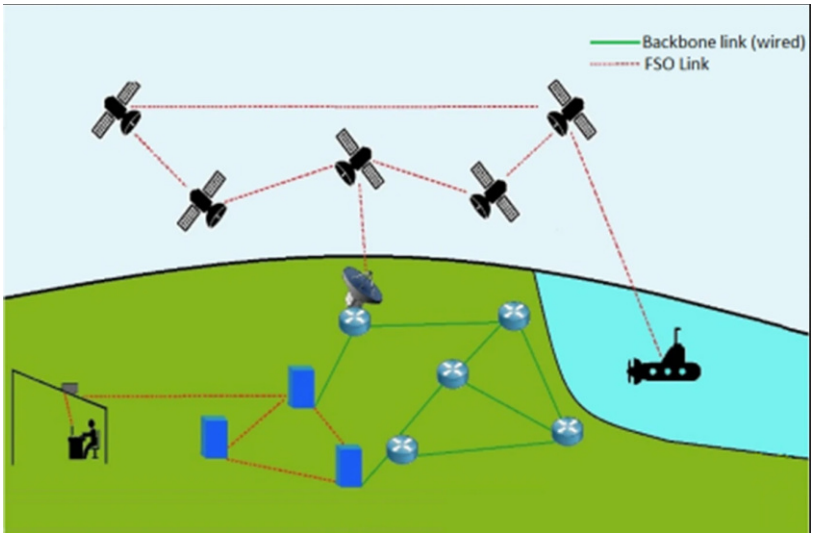

Figure 1: Conceptual topology of Free Space Optical (FSO) integrated network [34].

The FSO networks or Optical Wireless Networks (OWNs) can broadly be classified into four categories depending upon the operational distances and applications. These categories are Optical Wireless Home Networks (OWHNs), Optical Wireless Terrestrial Networks (OWTNs), Optical Wire-

less Satellite Networks (OWSNs), and Optical Wireless Underwater Networks (OWUNs). Figure 1 shows these four categories operational in their respective geographical domains [34].
Another interesting and under development field is the one of satellite constellations. A satellite constellation is a group of artificial satellites, typically placed in sets of complementary orbital planes, working together as a system to achieve a unique objective, in general used to fulfill spatial and temporal coverage and observation requirements which can not be met with a single satellite. The satellites of the constellation are connected to globally distributed ground stations and they may also use inter-satellite communication. The main advantage of using a constellation is that, unlike a single satellite, a constellation can provide permanent global or near-global coverage, such that at any time everywhere on Earth at least one satellite is visible. Examples of important satellite constellations are the Global Navigation Satellite System (GNSS) like the Global Positioning System (GPS) and GALILEO, the former operated by the United States Space Force and the latter by the European Space Agency (ESA), which provide positioning, navigation, and timing (PNT) services on a global or regional basis. Being able to use laser techonology for free-space optical communication in a satellite constellation will provide the benefits of optical communication systems coupled with the higher coverage of a constellation.

1.1 Thesis Motivation

In the moment this thesis is being written, multiple projects are exploring FSO communication technology, supervised by the main space agencies all over the world, like the National Aeronautics and Space Administration (NASA), ESA and the German Aerospace Center (Deutsches Zentrum für Luft und Raumfahrt - DLR). One of the main centers for optical communication research is in Oberpfaffenhofen, Germany, which hosts the group of Optical Technology for Satellite Links, under the Institute of Communication and Navigation. The Optical Technologies for Satellite Links Group deals with research in the area of high-speed optical satellite links interfaces. This includes topics ranging from the study of the atmospheric turbulence and the techniques to counteract its effects to the development of high-speed communications technologies and systems.
This thesis is developed in the context of a new project from the joint collaboration of ESA and DLR, called Feeder Links for Non Geo Stationary Orbits (FL4NGO). The goal of this project is to test the feasibility and performance, in terms of ground coverage and access availability, of two Low Earth Orbit (LEO) satellite constellations that use optical feeder links for the communication with the GS and Optical Inter-Satellite Links (OISL). This study will be used to establish, with a trade-off analysis, which constellation is more suitable for the mission goals, as well as to identify the differences in performance between deployments that incorporate both optical feeder links and radio links, versus those that solely rely on radio links. The first goal is carried out entirely by the DLR, while the radio analysis is carried out by Kepler Communications.
This thesis will present the main results of the access availability analysis and the inter-satellite links analysis, which make the core part of the project as it was initially designed. However, the main motivation of this work is to further develop the project by implementing optimization tools to increase the performance of the constellations, in order to fully exploit the benefits of the optical feeder links while reducing costs and managing the technological challenges of such an ambitious mission. The results presented will undoubtedly show the benefits brought by the different optimization tools and, as a consequence, the huge potential of this project.

1.2 Introduction to FL4NGSO

The two satellite constellations that will be analyzed during this thesis are:

- **Constellation A**: A constellation of 288 satellites equally distributed on 24 planes, at an inclination of 60 degrees and an altitude of 1200 km. During the analysis phase this constellation will be also referred as 'Small LEO', due to the limited number of satellites.
- **Constellation B**: A constellation of 1152 satellites equally distributed on 48 planes, at an inclination of 70 degrees and an altitude of 500km. During the analysis phase this constellation will be also referred as 'Large LEO', due to the higher number of satellites.

The main features of the two constellations are summarized in Table 1.

Table 1: Constellations Characteristics.

	Constellation A	**Constellation B**
Link type	OGSL	
Data rate [Gbps]	25-100	6-24
Altitude [km]	1200	500
Inclination [deg]	60	70
No. Planes	24	48
Satellites per Plane	12	24
Total Satellites	288	1152

where by OGSL it is meant "Optical Ground Station Link". As can be seen, each constellation has two possible data rates; the lower one is the data rate in the case OISLs are not applied, the higher one is the one used in case of a single hop OISL, hence it is 4 times larger since the central satellite will link with four other satellites. Satellites in LEO constellations benefit greatly by being able to communicate with one another because, since they are relatively close to the Earth, they can only access small portions of the ground at one time, making inter-satellite links essential in creating a robust global LEO network. However, since the signal is distributed across satellites instead of going directly from the Optical Ground Station (OGS) to the satellite, it has to travel a longer distance and, as a consequence, it experiences more attenuation and signal degradation, increasing the bit rate requirement. The exact values of the data rates come from the link budget analysis [48].
The entire study will be conducted considering Europe as the only access area, since at the moment FL4NGSO is only a European project and surveying the entire globe will be extremely computationally expensive and time consuming.

1.3 Methodology and structure

The thesis is divided in the current introduction, eight main chapters and the concluding chapter.
In Chapters 2 and 3, an introduction to satellite communication and satellite constellations will be provided and the key benefits and difficulties associated with optical links will be discussed.
In Chapter 4, after a summary description of the preprocessing of the data, the OGSs selection and the target definition, the chain access and availability logic and analysis will be presented. The analysis conducted in this chapter can be considered as a theoretical scenario, since no limitation on the number of teleports per OGS has been implemented, meaning that the same OGS can be connected to as many satellites as possible simultaneously. On the other hand, Chapter 5 will present

a more realistic case, where the OGSs can be linked only with two satellites at a time, switching connection via an Hand Over logic. To mitigate the decrease in performance from the theoretical case to the HO case, OISL are introduced in Chapter 6. This study has been conducted focusing on a 1 hop topology with a constant OISL geometry and 8 different OGSs network have been tested. In Chapter 7, the duration analysis tool is presented to provide more insights on the chain access duration for the two constellations with and without OISL on the single OGSs as well as on the 8 previous OGS networks.
In Chapter 8, a network optimization tool is presented. The goal is to test new OGS networks to make these constellations operable, reaching access availability percentages above 99% for almost all the targets. Different weights on the targets are attributed based on their geographical location and a network score system is defined in order to establish a network ranking. A trade-off tool is then used to suggest improvements on the most performing network of n OGSs. This tool will highlight the weak points of the constellations in terms of availability coverage and OISL geometry, offering important information to compare them and open the road to a new OISL geometry.
In Chapter 9, the flexible OISL tool is presented, with the goal of showing how the constellation performance can benefit from the introduction of a smarter OISL logic, where the central satellite picks the satellites within range to form its hop based on their target coverage and access duration performance, instead of on their position in the constellation. A subsection providing the results of the tool with the additional implementation of payload allocation constraints is present as well.
Finally, Chapter 10 will present the trade-off analysis of the two constellations and the conclusions of this work will be drawn.

2 Satellite Communication

Satellite applications are increasing all the time, from radio communications, astronomy, weather forecasting, mapping and many more. The basic principle of wireless communication systems is simple. At one end, a transmitter encodes or modulates messages by varying the amplitude or frequency of the wave. At the other end, a receiver tuned to the same wavelength picks up the signal and decodes it back to the desired form: sounds, images, data, etc. All wireless communication systems, from the home remote control up to the satellite, are based on this principle, even though increasingly complex technologies are of course used to encode these electromagnetic signals, improve their quality, increase the amount of information or make transmissions secure [47]. The links between satellite and ground station are usually in the radio part of the electromagnetic spectrum, but they cover a wide range, from lower frequencies to higher frequencies. A general breakdown of these frequency bands with their main applications is presented [38]:

- **L-band [1-2 GHz]**: GPS carriers and also satellite mobile phones, such as Iridium; Inmarsat providing communications at sea, land and air; WorldSpace satellite radio.
- **S-band [2-4 GHz]**: Weather radar, surface ship radar, and some communications satellites, especially those of NASA for communication with International Space Station (ISS) and Space Shuttle.
- **C-band [4-8 GHz]**: Primarily used for satellite communications, for full-time satellite TV networks or raw satellite feeds. Commonly used in areas that are subject to tropical rainfall, since it is less susceptible to rain fade than Ku band.
- **X-band [8-12 GHz]**: Primarily used by the military. Used in radar applications including continuous-wave, pulsed, single-polarisation, dual- polarisation, synthetic aperture radar and phased arrays.
- **Ku-band [12-18 GHz]**: Used for satellite communications. In Europe, Ku-band Downlink (DL) is used from 10.7 GHz to 12.75 GHz for direct broadcast satellite services, such as Astra.
- **Ka-band [26-40 GHz]**: Communications satellites, UpLink (UL) in either the 27.5 GHz and 31 GHz bands, and high-resolution, close-range targeting radars on military aircraft.

Lower-frequency bands like L-band and S-band have their own advantages, such as better penetration through atmospheric conditions and vegetation, and lower signal attenuation, making them suitable for long-distance communications. On the other hand, congestion has become a serious issue in the lower frequency bands and many of the limitations of low frequency radio can be overcome using higher frequency. Using shorter wavelengths reduces the effects of the charged particles due to ionosphere and solar plasma and allows for higher bandwidth. New technologies are being investigated so that higher bands can be used, and optical technologies are the most important.

2.1 Optical Communication: Heritage and Outlook

FSO communication has technological similarities with fiber optic, but it is a wireless technology, which transmits data via laser beams, instead of relying on silica fibers. Communication lie in the near infrared (NIR) range, with wavelengths between 700 nm and 2000 nm. As already stated, nowadays different space agencies are testing FSO applications, like NASA's Deep Space Optical Communications (DSOC) experiment, which will be the agency's first demonstration of optical communications beyond the Earth-Moon system [35]. The main historical events for FSO communication

research will be now presented.
The first theoretical study on optical uplink transmission from ground-to-satellite has been studied by Fried in 1967 [1]. Few years later, an uplink transmission using ground-based continuous-wave argon laser towards geodetic Earth orbiting satellite-II (GEOS-II) was demonstrated by Minott [3]. Thereafter, various theoretical studies and successful experiments were performed to investigate optical ground-to-satellite and inter-satellite communications. Some of them showed how atmospheric turbulence affects the optical contact, as described for example in [7]. In 1992, an uplink optical communication to deep space vehicle was demonstrated through Galileo optical experiment (GOPEX) that transmitted a pulsed laser signal from two optical ground stations mounted at California and New Mexico [6]. The results demonstrated the distortion of uplink beam due to atmospheric turbulence. Later in 1995, the first ground-to-space two way communication link was demonstrated in Ground/Orbiter Lasercom Demonstration (GOLD) using argon ion laser [11], [9]. To mitigate the effects of atmospheric turbulence, a bidirectional laser link between Earth and Moon was demonstrated using adaptive optics [10]. The first inter-satellite laser communication link was successfully demonstrated by ESA between the two satellites SPOT-4 and ARTEMIS for optical data-relay services at 50 Mbps [15] [23]. In figure 2 an overview of the mission elements between ARTEMIS and SPOT-4 is showed.

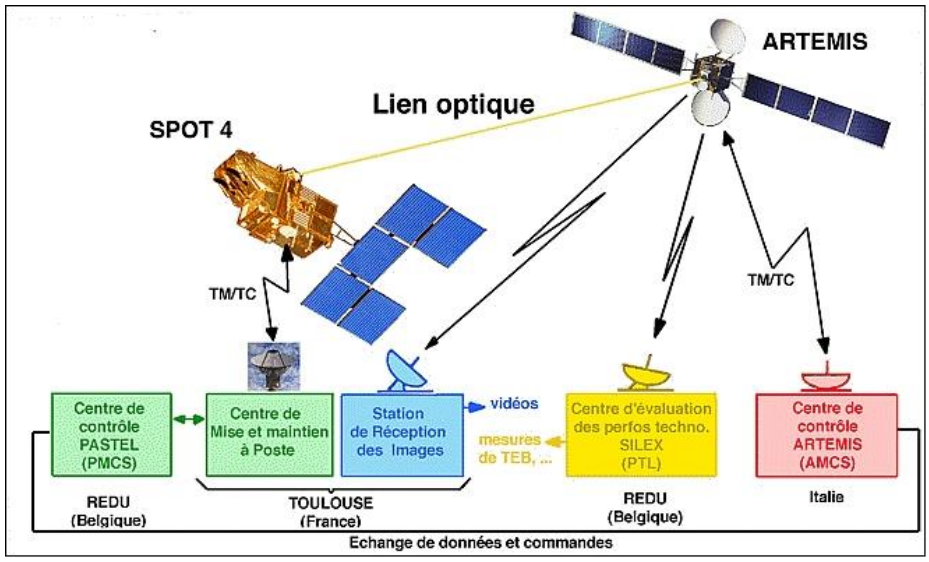

Figure 2: Overview of mission elements between ARTEMIS and SPOT-4 (image credit: CNES).

More recently, a NASA mission, the Laser Communications Relay Demonstration (LCRD), was launched in 2017. This mission showcased the potential of optical relay services for both near-Earth and deep space communications missions [40]. Another notable example of this technology is the European Data Relay System (EDRS) developed by the German Aerospace Center. The EDRS utilizes Geostationary Earth Orbit (GEO) satellites as relays to LEO satellites, primarily for commercial and disaster prevention purposes [36][27].
As of the time of writing, two EDRS payloads have been launched: EDRS-A and EDRS-C. EDRS-A, which includes an optical inter-satellite link and a Ka-band inter-satellite link, is hosted on the EUTELSAT 9B EAST satellite operated by Eutelsat (FR)[21]. EDRS-C, which includes an optical inter-satellite link as well, is hosted on a platform developed on the basis of the SmallGEO, a

public-private partnership scheme between OHB and ESA as part of the ARTES programme [37].

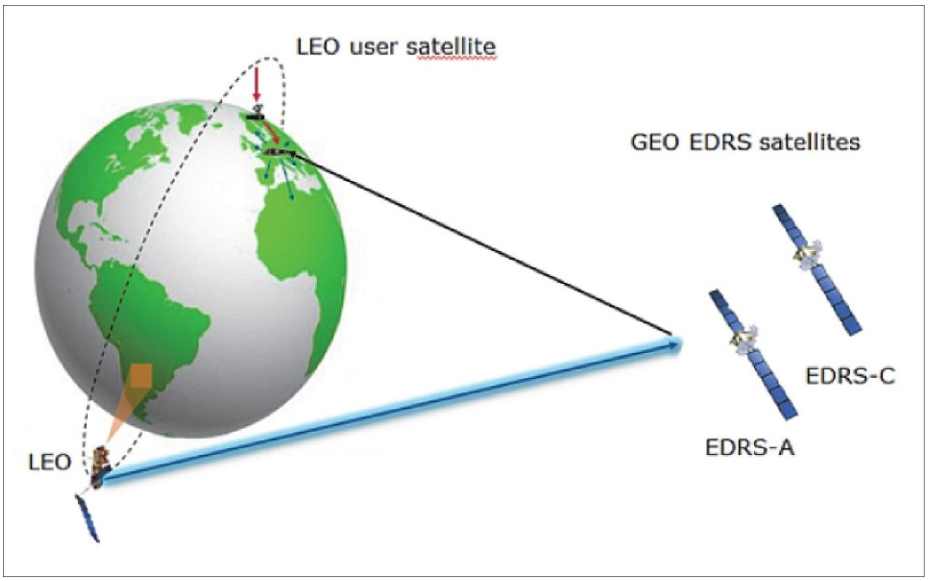

Figure 3: Visual representation of EDRS constellation and its communication architecture (image credit: ESA).

The EDRS A and C form the initial core space infrastructure that provides direct coverage for LEO satellites over Europe, the Middle East, Africa, the Americas, Asia, and the Poles. The initial plan was to develop two further spacecraft to complement the system from 2020 onwards, affording a complete coverage of the Earth and providing long-term system redundancy beyond 2030.

2.1.1 Advantages of FSO Communication

Optical communication systems seek to address the limitations of radio frequency communications. The main advantages of such technology are [23]:

- **Higher bandwidth**: The higher frequency allows for higher bandwidth, increasing the information carrying capacity of the communication system, meaning it is possible to carry more mission data. Ka-band frequency can go up to 40 GHz, while optical carriers in the NIR range can easily be around $10^{16} Hz$. Even if the maximum allowed bandwidth, meaning the maximum amount of data transmitted in given amount of time, was only 1% of the carrier frequency (usually it is around 20% for RF systems) the theoretical bandwidth for the FSO channel would still be around 100 THz. This makes the usable bandwidth at an optical frequency in the order of THz which is almost 105 times that of a typical RF carrier.
- **Less power and mass requirements**: The beam divergence is proportional to λ/D_R, where λ is the carrier wavelength and D_R the aperture diameter. Thus, the beam spread offered by the optical carrier is narrower than that of the RF carrier. This leads to an increase in the intensity of signal at the receiver for a given transmitted power. Fig. 4 shows the comparison of beam divergence for optical and RF signals when sent back from Mars towards Earth.

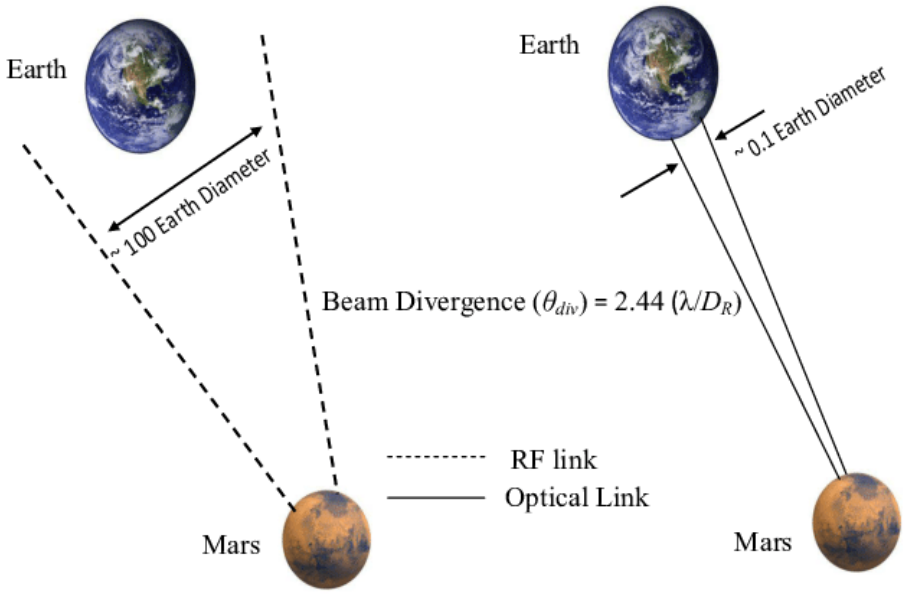

Figure 4: Comparison of optical and RF beam divergence from Mars towards Earth [12].

Thus, a smaller wavelength of optical carrier permits the FSO designer to come up with a system that has smaller antenna than RF system to achieve the same gain, as antenna gain scales inversely proportional to the square of the operating wavelength. The typical size for the optical system is 0.3 m vs 1.5 m for RF spacecraft antenna [8]. Table 2 gives the power and mass comparison between optical and RF communication systems using 10 W and 50 W for optical and Ka band systems, respectively at 2.5 Gbps. The values in parentheses are normalised to optical system parameters [16].

Table 2: Comparison between an optical and a RF communication system in different link configurations.

Link	**Optical**	**RF**
GEO-LEO		
Antenna Diameter	10.2 cm (1.0)	2.2 m (21.6)
Mass	65.3 kg (1.0)	152.8 kg (2.3)
Power	93.8 W (1.0)	213.9 W (2.3)
GEO-GEO		
Antenna Diameter	13.5 cm (1.0)	2.1 m (15.6)
Mass	86.4 kg (1.0)	145.8 kg (1.7)
Power	124.2 W (1.0)	204.2 W (1.6)
LEO-LEO		
Antenna Diameter	3.6 cm (1.0)	0.8 m (22.2)
Mass	23.0 kg (1.0)	55.6 kg (2.4)
Power	33.1 W (1.0)	77.8 W (2.3)

where in a GEO-GEO configuration both satellites are in GEO, in LEO-LEO both in LEO and in GEO-LEO one in GEO and the other in LEO. The biggest improvements are for satellites in LEO orbit, which is the case for both Constellation A and B, where the antenna diameter, mass and power requirements of the satellites are way lower in the optical case than in the RF case.

- **High security**: FSO communication can not be detected by spectrum analyzers or RF meters as FSO laser beam is highly directional with very narrow beam divergence. Any kind of interception is therefore very difficult. Unlike RF signal, FSO signal cannot penetrate walls, therefore can prevent eavesdropping [41].

- **High directivity**: Directivity is a parameter of an antenna or optical system which measures the degree to which the radiation emitted is concentrated in a single direction. The directivity of antenna is closely related to its gain. The advantage of optical carrier over RF carrier can be seen from the ratio of antenna gain as given in the equation below [17]

$$\frac{Gain_{(\mathrm{opt})}}{Gain_{(\mathrm{RF})}} \sim \frac{4\pi/\theta^2{}_{\mathrm{div(opt)}}}{4\pi/\theta^2{}_{\mathrm{div(RF)}}} \tag{1}$$

  where $\theta_{\mathrm{div(opt)}}$ and $\theta_{\mathrm{div(RF)}}$ are the optical and RF beam divergences, respectively and are proportional to λ/D_R. Since the optical wavelength is very small, a very high directivity and improved gain are obtained.

- **Unlicensed spectrum**: In the RF system, interference from adjacent carrier is the major problem due to spectrum congestion. This requires the need for spectrum licensing by regulatory authorities. But on the other hand, the optical system is free from spectrum licensing till now. This reduces the initial set up cost [18].

- **Scalability**: Scalability in the context of optical communication refers to the ability of the system to handle an increasing amount of data or traffic. It is a key attribute of optical communication systems due to several reasons, above all the high bandwidth density, meaning the ability to carry a large amount of data over a small area, the integrated parallelism, meaning that optical communication systems can handle multiple signals simultaneously [28], and the use of ultracompact transceivers integrated on a single chip.

- **Time-frequency transfer**: Time-frequency transfer is a process that involves the transmission of information in both time and frequency domains. It is a crucial aspect of many applications, including precision navigation and timing, clock-based geodesy, long-baseline interferometry, coherent radar arrays, tests of general relativity and fundamental constants, and future redefinition of the second [20]. Optical communication is a powerful tool for time-frequency transfer due to its high precision, low interference, ability to transmit over long distances, lack of spectrum licensing, and scalability.

- **Quantum communication**: Optical communication is an excellent choice for quantum communication due to its high capacity. For instance, Ciena has been able to establish high-capacity optical channels of up to 800 Gbps per channel today and plans to reach 1.6 Tbps per channel next year [39]. This high capacity is crucial for quantum communication, which requires the transmission of large amounts of data to perform quantum computations and to secure quantum communications. Optical communication is also being used to pioneer the path for long-distance quantum-secured communications. This is being done through the development of quantum repeaters, which are still the subject of intense worldwide research. In

addition, optical communication is a significant player in the field of quantum-secured communications.

2.1.2 Challenges of FSO Communication

The ground-to-satellite and satellite-to-ground FSO communications are subject to atmospheric effects. FSO technology uses atmospheric channel as a propagating medium whose properties are random functions of space and time. This makes FSO communication a random phenomena that is dependent upon geographical location and unpredictable atmospheric conditions that can degrade the performance of the system. Various unpredictable environmental factors like clouds, snow, fog, rain, haze, etc., cause strong attenuation in the optical signal and limit the link distance. The main weak points of FSO communication are:

- **Atmospheric turbulence**: Variations of temperature and pressure along the propagation path will result in the formation of turbulent cells, also called eddies, of different sizes and refractive indices. These eddies will act like a prism or lenses and will eventually cause constructive or destructive interference of the propagating beam. The perturbations of the optical beam associated with atmospheric turbulence is referred as atmospheric seeing effect.
- **Cloud blockages**: The presence of opaque clouds may occasionally disrupt the signal or completely block the optical signal from ground-to-satellite or satellite-to-ground rendering the Line Of Sight (LOS) communication useless [30]. These intermittent blockages can last from few seconds to several hours depending on the geographical location and season. Clouds offer significant attenuation as high as tens of dB and therefore require necessary actions to combat the signal loss due to cloud coverage.
- **Beam divergence loss**: Beam divergence loss in optical communication refers to the spreading out of a laser beam as it travels through a medium over a distance. The further the communication distance, the more the beam spreads, and the weaker the signal becomes at the receiving end. Its main cause is the diffraction that the beam experiences when it passes through the receiver's aperture.

Another limiting factor, is the position of the Sun relative to the laser transmitter and receiver. In a particular alignment, solar background radiations can increase and that will lead to poor system performance, as showed in [14]. These factors undoubtedly poses a great challenge to FSO system designers. To mitigate some of these effects, multiple techniques are available:

- **Using Optical Collimators**: These optical devices help maintain a more collimated beam by minimizing divergence. This is achieved by either placing an infinitesimally small source exactly one focal length away from an optical system with a positive focal length or observing the point source from infinitely far away [44].
- **Aperture Averaging**: This technique is used to mitigate the effect of atmospheric turbulence by increasing the size of the receiver aperture that averages out relatively fast fluctuations caused by the small-size eddies and helps in reducing channel fading, which is a phenomenon where the received signal strength decreases with distance from the transmitter, due to the scattering of the signal by atmospheric turbulence.
- **Adaptive Optics (AO)**: AO systems can actively adjust the shape of optical elements to compensate for atmospheric turbulence and reduce beam spread in free-space optical links. In Oberpfaffenhofen an entire department is dedicated on the development of AO techniques to mitigate the aforementioned challenges of FSO communication.

3 Satellite Constellation Design

All existing satellite constellations, whether operational or proposed, are based on a geometric and mathematical study, providing guidelines for the design process and the achievement of fixed objectives. To describe the orbit of a satellite within a constellation six orbital parameters are used:

- **Semimajor Axis**: The semimajor axis (a) of an orbit is the average distance from the center of the orbit to the orbiting body. It is half of the length of the longest radius of the orbit.
- **Eccentricity**: The eccentricity (e) is a measure of how much an orbit deviates from a perfect circle. Along with the semimajor axis the eccentricity describes the shape of the orbit. When the orbit is circular the eccentricy is 0, and when the orbit is parabolic the eccentricy is 1. Larger values from 0 to 1 indicate an orbit more and more elliptic and values larger than 1 are used to describe hyperbolic orbits.
- **Inclination**: The inclination (i) is the angle between the orbit's plane and the reference plane, usually the plane of the equator. Hence, an equatorial orbit will have an inclination of 0 degrees, while a polar orbit will have an inclination around 90 degrees.
- **Longitude of Ascending Node (Right Ascension of the Ascending Node, RAAN)**: The longitude of the ascending node (Ω) is the angle from the reference direction, usually the direction of the vernal equinox, to the direction of the ascending node, the point of the orbit in which the orbiting body crosses the equator moving from south to north. The RAAN determines, along with the inclination, the orientation of the orbit.
- **Argument of Periapsis (Argument of Pericenter)**: The argument of periapsis (ω) is the angle from the reference direction, usually the direction of the ascending node, to the direction of the orbiting object at periapsis, the closest approach to the central body. It is measured in the direction of motion.
- **True Anomaly**: The true anomaly (ν) is the angle between the direction of periapsis and the current position of the body. Along with the argument of periapsis, it is uded to describe the position of the body along its orbit.

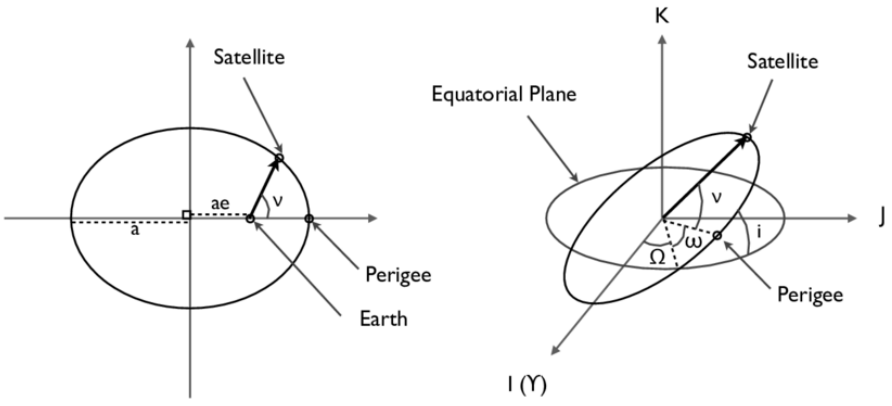

Figure 5: Definition of classical orbital elements [19].

Figure 5 shows all six orbital parameters and their role in defining the orbit of a satellite and its position in it. The satellites in a constellation are disposed in orbital planes that share the same semimajor axis, eccentricity and inclination but differ for the argument of the pericenter.
Depending on the orbital altitude , there are three different types of satellite constellations: GEO, MEO, and LEO. Each type has its specifics and is important for a particular purpose, so let's consider how these three compare.
GEO stands for a geostationary (or geosynchronous equatorial) orbit, and it hosts hundreds of satellites nowadays. Geostationary swarms derived their name from their Earth-rotation mode: they synchronize with our planet's movement, thus hovering all the time over the same point. It happens because GEO swarms fly over the equator, and each rotation takes 24 hours. GEO is a typical orbit for weather satellite constellations. Others broadcast TV and provide low-speed communication services. Thanks to its altitude of around 36,000 km, an individual GEO satellite can capture 40% of the Earth's surface. Thus, a group of three units 120 angular degrees apart is enough to keep an eye on the whole world.
MEO is an acronym for Medium Earth (or mid-Earth) Orbit, and these constellations operate at the altitudes from around 5,000 to 20,000 km. They are traditionally used for navigation purposes, typical examples being the GPS, Galileo, and GLONASS. MEO constellations also provide high-bandwidth connectivity in locations where terrestrial infrastructure is poor or not feasible. This particularly refers to maritime and aerospace industries, offshore platforms, and rescue team operations in remote areas.
LEO stands for Low Earth Orbit, and these orbits make the densest space population, operating at altitudes from 500 to 1,200 km. The derived data is widely used by governmental bodies, as well as commercial and non-commercial organizations. Low Earth orbit satellite constellations primarily support research, telecommunication, and Earth Observation (EO) needs of environmental monitoring, disaster response, forestry, and agri-sector. Such swarms may have circular or elliptical orbits . Circular orbits are at the same altitude, while elliptical orbits contain the apogee (the highest point) and the perigee (the lowest one). Swarms with circular orbits revolve around our planet within 1.5 to several hours and typically fly nearly above the geographic poles. As for elliptical orbits, they are passed slower at the apogee and faster at the perigee points [46].
Table 3 summarizes the principal features of the 3 types of orbits.

Table 3: Major Satellite Constellation Parameters.

Parameter	**GEO**	**MEO**	**LEO**
Altitude	36,000 km	5,000 to 20,000 km	500 to 1,200 km
Coverage area	Vast	Medium	Narrow
Downlink and uplink rate (signal speed)	Slow	Medium	Fast
Ground station spacing	Distant	Regional	Local
Antenna	Stationary	Dual-tracking	Complex tracking and terrestrial network

Of particular importance is the relation between the altitude of the constellation and the covered area; the higher the altitude, the vaster the covered area and thus the lower the number of satellites needed to provide the coverage of the area of interest.

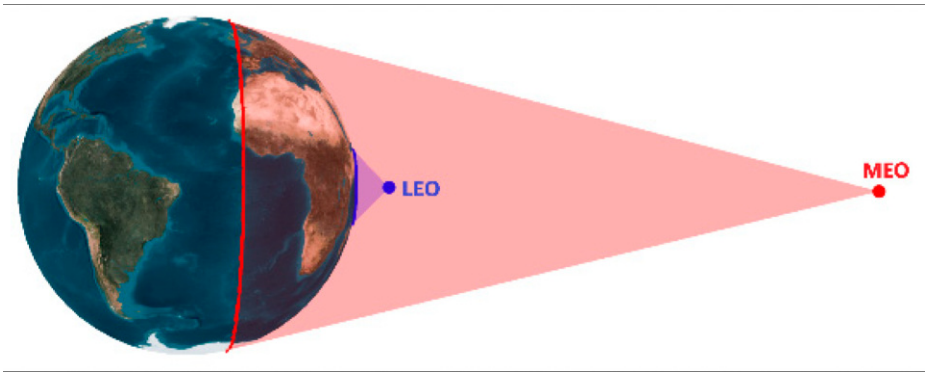

Figure 6: Comparison of the coverage footprints of LEO satellite versus MEO satellite [25].

Figure 6 shows a comparison in the coverage footprints between two satellites at different altitudes. This directly applies to the two constellations of this study: constellation B is a low LEO constellation, so the number of satellites is way larger than the one of constellation A, which is a high LEO constellation, to account for the narrower coverage footprint.
In terms of constellation coverage, it is possible to target a global coverage of the planet, a zonal coverage or a local coverage for well identified users. Zonal coverage objectives can be shaped according to complex and tortuous boundaries (e.g. for a country or a region) but they are more often defined as simple latitude ranges. In our case, the target area of interest is the European area, defined simply as a square, divided in 64 sub-targets, as can be seen from figure 7

Figure 7: Visualization of FL4NGSO's Europe target grid.

As can be expected, the coverage goals of a constellation will influence its design, since the design methods rely on geometrical coverage considerations. In designing a satellite constellation, a major consideration is to provide the specified coverage area with the fewest number of satellites. To tackle

this problem, the concept of the elevation angle is critical. The elevation angle is the angle between a satellite and the observer's (ground station's) horizon plane. The range of elevation ranges from 0 to 90 degrees. When the elevation angle is equal to 0 degrees, the instantaneous coverage area of a satellite is at its maximum. Any point located within this coverage area will be within the geometric visibility to the satellite. However, close to zero elevation angle is not operable due to the high blocking and shadowing effects. This leads to the concept of minimum elevation angle [13]. The minimum elevation angle is defined as the elevation angle required for the satellite to be within 'operational visibility'. For a given minimum elevation angle, the only factor affecting the coverage area is the satellite altitude. Figure 8 shows a typical circle of coverage by a satellite at an altitude h.

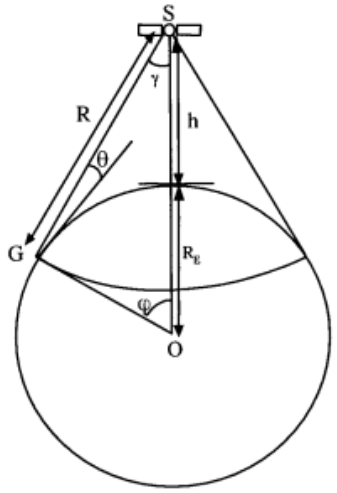

Figure 8: Coverage footprint of a satellite as a function of its altitude h [13].

The value of the minimum elevation angle varies according to the mission goals and the communication protocol. For an optimal constellation of satellites, the most efficient plan is to have the satellites equally spaced within a given orbital plane and the planes equally spaced around the equator. The coverage obtained by successive satellites in a given orbital plane is described by a ground swath or street of coverage as shown in Figure 9. Total Earth coverage is achieved by overlapping ground swaths of different orbital planes.

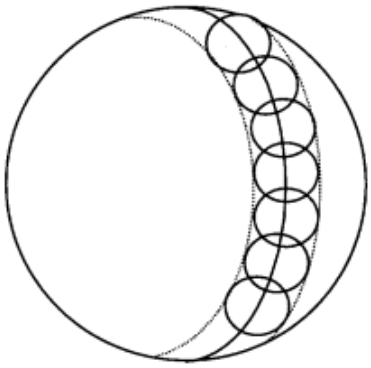

Figure 9: Ground swath by successive satellites in the same orbital plane [13].

Another point of consideration in the design of a satellite constellation is the number of satellites being visible at any one time within a coverage area in order to support certain applications or to provide a guaranteed service. For instance, GPS requires at least four satellites to provide accurate positioning data [22].

3.0.1 Walker constellations

Out of all the possible satellite constellation designs, our two constellations follow the design formulated by Walker [2]. The Walker class of constellations developed by Walker was initially used for MEO constellations but was subsequently applied to LEO satellites as well.
The main feature of all the Walker patterns consists in circular orbits of equal period and same inclinations for all planes of the constellation; elliptical orbits are advantageous for coverage limited areas, but the more uniform patterns provided by circular orbits appear preferable for whole-Earth coverage [4]. The notation to describe these orbits as defined by walker [5] is the following: i: t/p/f with i being the inclination, t the total number of satellites, p the number of planes and f the phasing parameter, which is the relative spacing between satellites in adjacent planes. The change in true anomaly, in degrees, for equivalent satellites in neighbouring planes is equal to f $\times$ 360 / t. According to this notation, Constellation A is a 60: 288/24/1 Walker constellation, while Constellation B is a 70: 1152:48:1 Walker constellation. The symmetric properties of the Walker constellations will come to be really useful in the design of the optimization tool for flexible OISL, as presented in chapter 9.

4 Chain Access and Availability Analysis

In this section, the core of the project's analysis is presented: the Chain Access Analysis and the Availability and Coverage Analysis of both constellations. Starting from the preprocessing of the data, the OGS selected for the analysis will be presented, in order to provide the entire background for the subsequent chain generation. The resulting databases, obtained through a double level filtering process, will be used to extract the most important information for this project: the access availability map.
Since multiple concepts and definitions used during the study might result unfamiliar to the reader, this section aims at providing some guidance. In particular:

- **Access**: Every time window in which it is possible to establish a link between OGS, constellation and target. In order to have an access, there are different requirements for the uplink and the downlink:
  - **Uplink**: topological requirement, meaning that the satellite must be at least at 30 degrees elevation angle for the OGS, and cloud requirement, meaning that for the entire duration of the access the sky must be sufficiently clear. These requirements are specific to the FSO communication technology; the higher elevation angle is chosen to reduce as much as possible the degrading effect of the sky and the cloud requirement is added since optical light tend to be absorbed, scattered and diffused more readily by atmospheric particles and other materials, reducing its penetration depth.
  - **Downlink**: only topological requirement, with the minimum elevation angle for the access to the targets defined at 25 degrees, according to required elevation for RF downlink as computed by Kepler Communication. Since the wavelength here is way higher, the clouds don't constitute a problem anymore and the minimum elevation angle can be reduced.

  When used in the context of satellite to satellite access, it is meant as the interval of time during which the satellites are within the range constraint for the analysis and thus are available to establish inter-satellite links.
- **Availability**: Number of concurrent accesses possible at a given time for a specific target or OGS. Most of the times the targets have an availability value of 2, meaning that there are at least two satellites that satisfy both the uplink and downlink requirements. Such analysis can be fine-tuned by down-selecting the accesses by only looking at longer duration times, which would lead to less concurrent accesses, but would guarantee the best link times.
- **Chain Access Analysis**: By chain access it is meant the available link formed by $OGS \rightarrow Satellite \rightarrow GroundTarget$. The analysis has been done in terms of coverage and access duration for each target.
- **Access Availability Map**: The end result of the Availability analysis is the Access Availability map, which quantifies the percentage of the simultion time during which at least one active chain access is available for each target.
- **Coverage HeatMap**: The coverage HeatMap (HM) is another output that gives a qualitative feedback on the coverage overlap for chain access, using as a metric the aggregated summed time of each chain available for a target.
- **Uptime**: The uptime of a specific target is the percentage of the simulation time during which it is possible to access that target.

- **OutageTime**: The outage time of a specific target is the percentage of the simulation time during which it is not possible to access that target. It is of course the complementary of the uptime.

Following, we can see examples of each of these products:

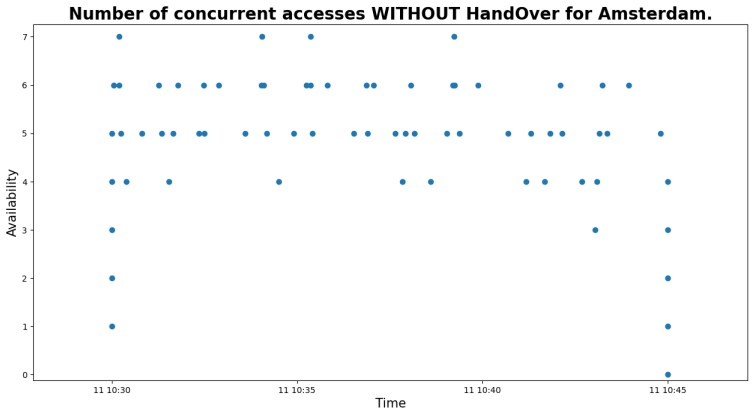

Figure 10: Number of concurrent accesses for the OGS in Amsterdam, Constellation B. A value of 5 indicates that, in that specific moment, the OGS can theoretically have 5 uplinks active with 5 different satellites.

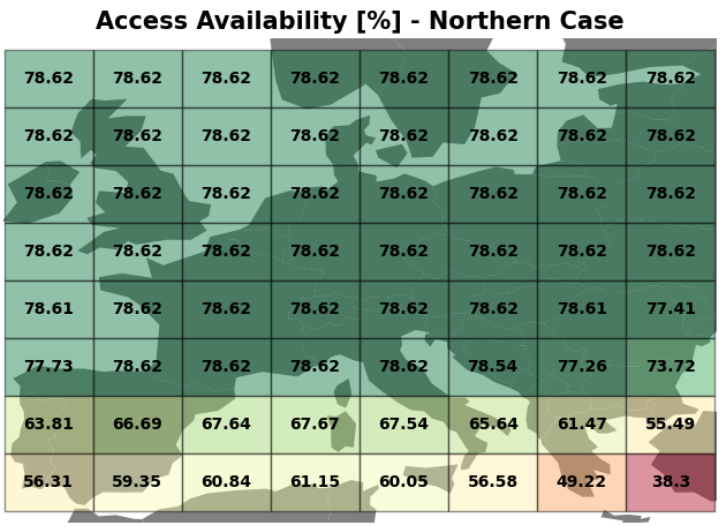

Figure 11: Access Availability percentage for the Northern OGS configuration in constellation A. A value of 78% indicates that a specific target has at least one full active chain for 78% of the simulation time.

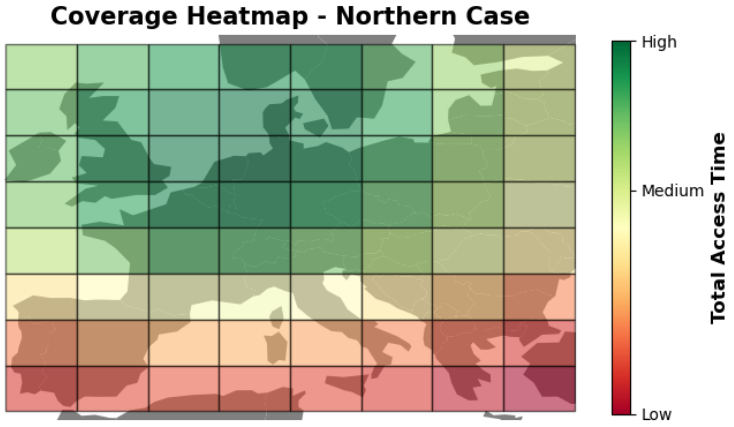

Figure 12: Coverage HeatMap for the Northern OGS network in constellation A. The scale of color ranges from green, for the targets with a high coverage, to red, for the targets with a low coverage.

4.1 Data PreProcessing

The preprocessing of the data has been done using the AGI System Tool Kit (STK) software. This software allows to easily simulate the constellation networks and propagate the satellites orbits, as well as to obtain access reports and to visualize every moment in a nice 2d and 3d graphic window.

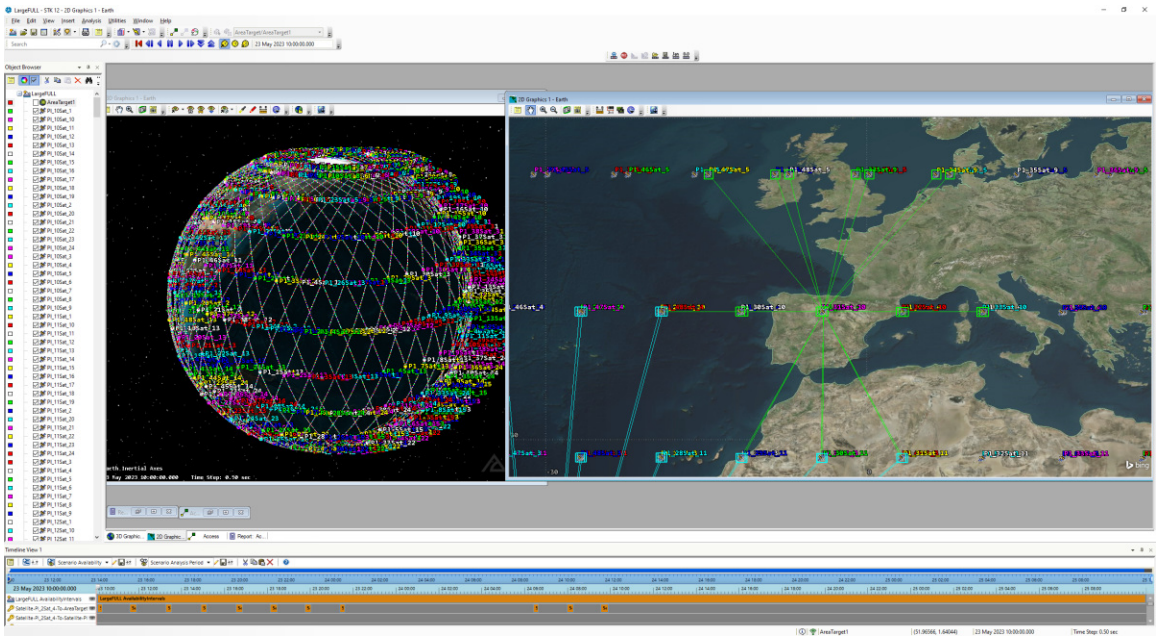

(a) STK 3D and 2D graphic windows framework.

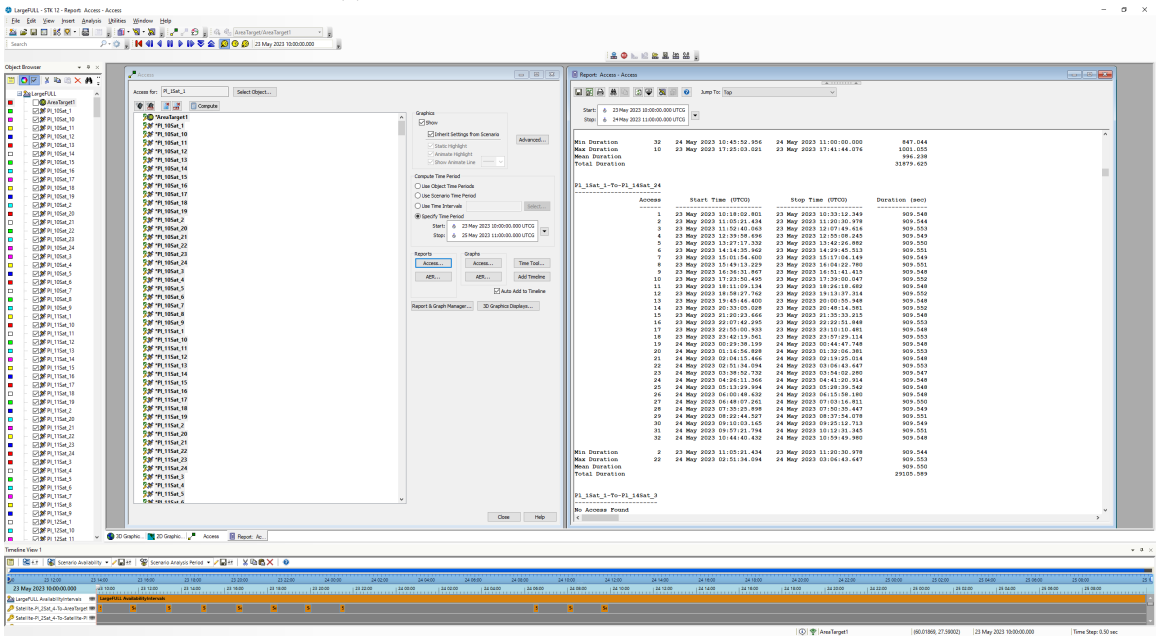

(b) STK Access Report manager and example of created access report.

Figure 13: STK framework. 3D and 2D graphic windows (a) to visualize the satellites orbits and accesses at any moment and Access Report Manager (b) to create reports and visualize them.

Figure 13 shows the STK working environment used to perform this pre-analysis.
Via STK all the inputs needed in postprocessing, with the exception of the cloud databases, were

obtained, and they include:

- **Uplink databases** for all the 24 OGSs containing the accesses of every OGS to the satellites of the constellation, with their start times, end times and durations. Since these DBs are huge and the satellites orbits were shown to be somehow periodic, they were obtained only for 1 'constellation period', which is defined as the interval of time in which the orbits of the satellites repeat themselves, not as the time it takes for a satellite to complete one orbit. Such constellation period coincides to be almost 8 days for constellation A and almost 17 days for constellation B, and then they were propagated during the post process analysis respectively 46 and 22 times, to reach the simulation time of 1 year. While this approach can present some limitations and introduce uncertainties in the long run, it was the best trade-off between analysis accuracy and computational requirements.
- **Downlink database** containing the accesses of the satellites of the constellation to the different targets, with their start times, end times and durations. Again, these DBs were cut to one period of almost 8 days for constellation A and almost 17 days for constellation B, and then propagated during the postprocessing analysis.
- **Satellite to Satellite access reports** containing the accesses of every satellite with respect to the other satellites of the constellation, with a range constraint of 3923 km for constellation A and 1796 km for constellation B. While these reports are not required to perform the access availability analysis they are needed to implement the flexible OISL tool that will be described in chapter 9.

STK was also used to produce some of the images that will be shown in this thesis, as well as short videos used for PowerPoint presentations.

4.2 OGS Selection

For this analysis, a collection of OGS locations were selected across Europe. These locations were chosen according to good access to high-speed ground network, site diversity and acceptable proximity w.r.t. COLT Network access points. The COLT network provides IP Access On Demand services in various locations across Europe. These services are supported on standard On Demand ports in data centers and enterprise locations [42]. The only exceptions are Athens and Catania, which were chosen due to good Clear Sky availability. The OGS considered in this study are located in:

- Porto
- Lisbon
- Madrid
- Barcelona
- Sevilla
- Marseille
- Paris
- Bordeaux

- Geneva
- Rome
- Munich
- Berlin
- Amsterdam
- Vienna
- Warsaw
- Zagreb
- Sofia
- Dublin
- London
- Copenhagen
- Milan
- Stockholm
- Catania

and they can be seen, over the Europe map, in figure 14.

Figure 14: Location of the selected OGSs.

To get the availability access plots these locations have been combined in different hypothetical OGS Networks of 5 OGSs each:

- **Best Cloud Availability network**: Catania, Sevilla, Lisbon, Athens, Porto.
- **Best Cloud Availability per Quadrant network**: Catania, Sevilla, Copenhagen, Paris, Marseille.
- **Northern network**: London, Dublin, Amsterdam, Copenhagen, Stockholm.
- **Southern network**: Lisbon, Barcelona, Catania, Athens, Rome.
- **Western network**: Dublin, Porto, London, Bordeaux, Barcelona.
- **Eastern network**: Athens, Sofia, Warsaw, Stockholm, Zagreb.
- **Central network 1**: Marseille, Milan, Paris, Vienna, Amsterdam.
- **Central network 2**: Geneva, Munich, Zagreb, Berlin, Marseille.

These are simply logical combinations that bias the OGSs allocation toward specific European areas. For example, in the Southern case all the OGSs are in southern Europe, while in the Central cases the OGSs are chosen in central Europe. Furthermore, the Best Cloud and Best Cloud per Quadrant (or simply Best Quadrant) network pick the OGS on the basis of their weather conditions, instead of their geographical locations, but since the sky generally tends to be clearer the more we move toward southern Europe, these networks end up picking the majority of their OGSs at lower European latitudes as well.

4.3 Chain Analysis

By chain analysis it is meant the computation of all possible accesses for a specific OGS, taking into account the topological and cloud requirements for the uplink and the downlink segments. The output of the analysis is a chain database that, along with the chain databases of the other OGS in the network, is the building block of the network database. A valuable access will form a chain only if the full link between OGS, SAT and Ground Target is available.

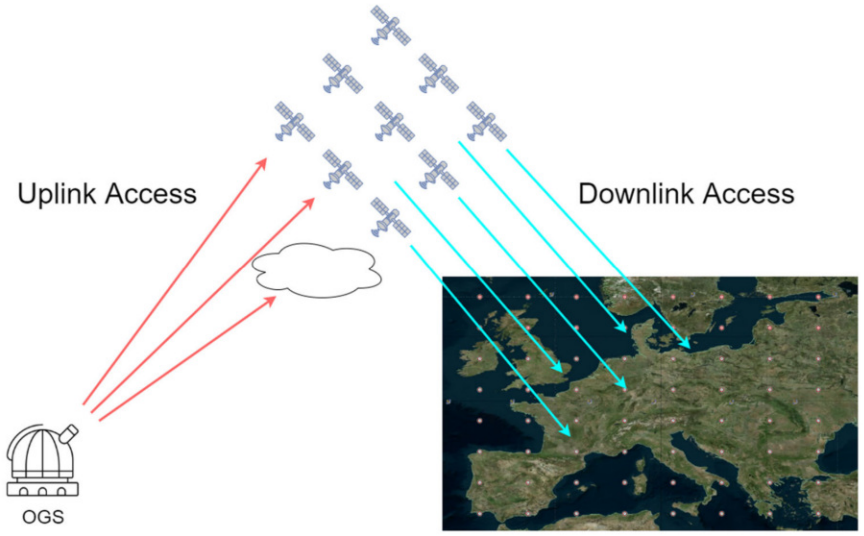

Figure 15: Basic representation of the concept of Chain Access.

Regarding the ground targets, the target grid of figure 7 was defined as an 8x8 array of STK Target objects evenly distribute over Europe. These targets are the end point of the access chain, and represents the targets for the downlink. This link is assumed to be performed in the RF, thus no filtering on clouds is required. The only requirement is the minimum elevation angle of 25 degrees, as already explained. Figure 15 gives a schematic representation of the access concept.
The inputs for this analysis are:

- Target database: the DB containing the propagation of the orbits of the satellites in the constellation for a constellation period, as already explained in the preprocessing section. This DB is the downlink DB, and its columns are the Satellite Name, the accessed target name, the start of the access and the end of the access.
- Uplink database: the DB containing the uplink information. One DB for each OGS has been created, following the guidelines described in the preprocessing section. Its columns are: Satellite Name, Access start, Access End and Duration of the access.
- Cloud database: a DB containing the clear sky data retrieved and distributed by the University of Lille, showing the time windows in which the level of clearness of the sky is above a specific threshold. The threshold value was established on the basis of the previous ESA project ONUBLA; on a scale of 1 (best condition) to 4 (worst condition, maximum turbulence) if the sky is above or equal to 2, the optical link can be established, if the topological requirement is satisfied as well, of course [26]. The temporal resolution is 15 minutes. As for the uplink DBs, 24 total cloud DBs have been created, one for each OGS.

The output of the analysis is a Chain DB containing all the chain accesses for a specific OGS for the entire one year simulation period. It is important to specify that during this first analysis no requirements on link duration and number of concurrent accesses per OGS have been imposed. We can therefore consider these results as some kind of upper limit for the subsequent analysis.
The chain analysis was performed by breaking up the chain in two segments: OGS-TO-SAT segment (Uplink segment) and SAT-TO-Target segment (Downlink segment). The final DB is then produced after having cross-checked the two segments data to find the time overlap between uplink and downlink that share the same satellite, which represents the central node of the chain.

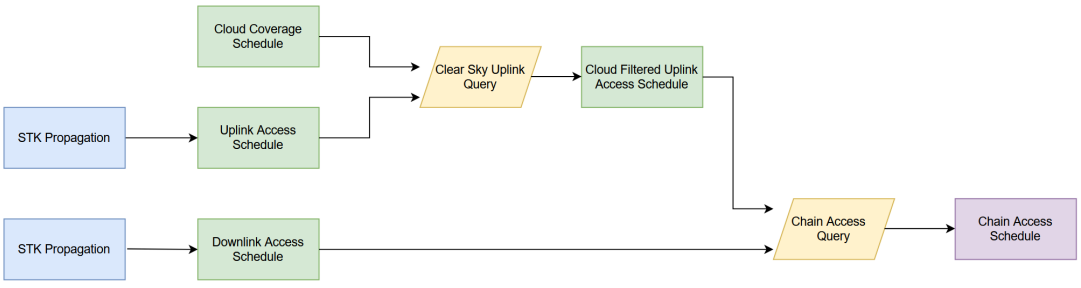

Figure 16: Chain Access generation process.

Given the fact that both the UL and DL DBs contain simply a small sample of the entire simulation interval, the filtering processes were performed on 22 (Large LEO) and 46 (Small LEO) subsets of data, each one equals to the previous one plus a time shift of 7 days, 23 hours, 30 minutes and 11

seconds (Small LEO) and 16 days, 22 hours, 52 minutes and 15 seconds (Large LEO). In the end these sub-chain-DBs will be concatenated to form the final DB. To decrease the execution time, the query of the cloud and uplink DBs was performed on SQL, using the sqlite3 library of Python.
To obtain the final Chain DB two filtering processes are required: cloud filtering and downlink filtering. The filtering process is translated into a simple query that merges two DBs into a single one, selecting the regions where a temporal overlap is present. In the case of the cloud filtering, what we are looking for is the overlap between the uplink from a specific OGS and a condition of clear sky above the same OGS. Physically, we are just considering the cloud constraint, meaning that the optical uplink can be established from an OGS only if the sky over that OGS is sufficiently clear. The output of the analysis is a cloud filtered uplink DB for each OGS, which will be used for the rest of the analysis and will be simply referred as 'Uplink Database'.

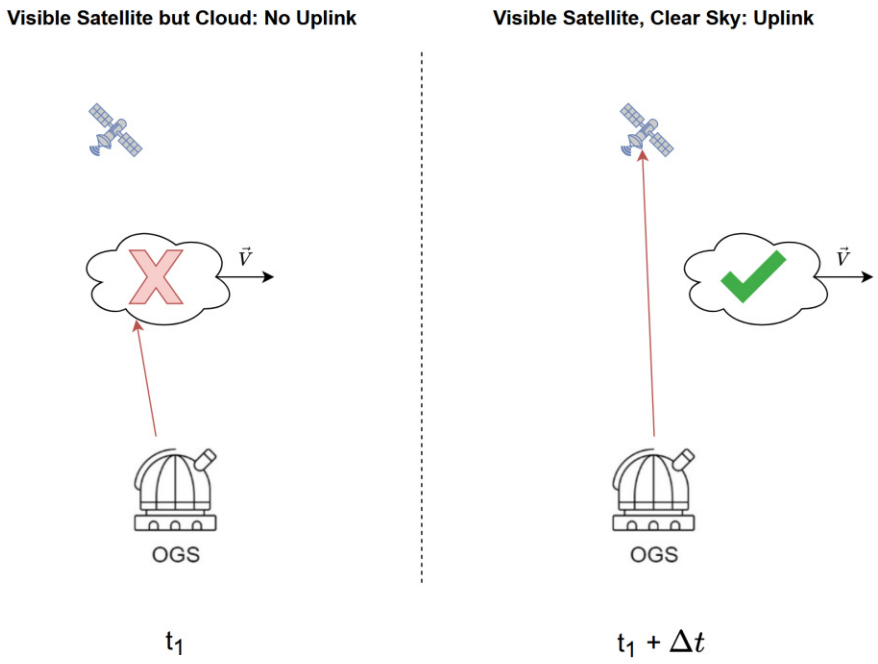

Figure 17: Visualisation of the Cloud Filtering process. At t_1 the sky over the OGS is not clear, so the uplink cannot be established even though the satellite is visible. At $t_1 + \Delta t$, instead, the cloud has moved making the sky clear and the uplink possible.

Figure 17 shows a visualization of the cloud filtering process.
At this point the filtering on the clouds is finished, and the downlink segment can be considered.
To generate the chain DB the same logic is applied: we move to SQL, perform the query and save the results in a series of arrays that will lately be concatenated. This time the query will include a further condition for the merge: the UL and DL chains must of course share the same satellite. After this a correction for the overlap is done, to avoid having a chain that starts before the effective start of the uplink or ends after the effective end of the uplink. A visual representation of the overlap we are looking for is showed in figure 18

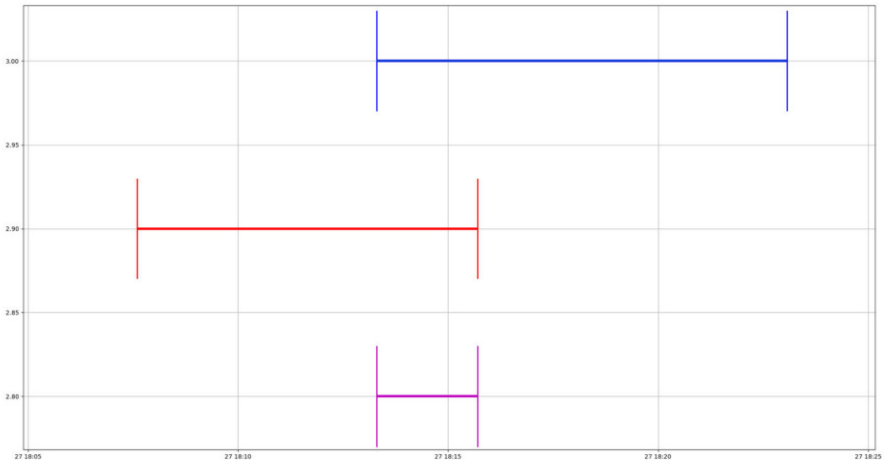

Figure 18: Visualisation of Chain Access definition through access windows overlap. The blue segment represents the time interval over which the downlink is available. The red segment represents the time interval over which the uplink is available. The violet segment is the intersection over which the chain access is available.

The entire chain generation process is summarized and can be visualized in figure 16.

4.4 Availability Analysis

Once the chain DBs for all the OGSs have been created, the final part of the analysis is the computation of the access availability of each network of OGSs. This part of the analysis is processed by a different script, which relies on parallel computing using the multiprocessing library of Python. The inputs are:

- Chain DBs for each of the 5 OGSs in the selected network configuration.
- The 8x8 target grid representing the 64 targets in which the European area has been divided.

The output consists of two plots:

- Access Availability plot: showing, for each target of the grid, the percentage of the simulation time during which at least one active chain access is available that specific target.
- Coverage HeatMap plot: giving a qualitative feedback on the coverage overlap for chain accesses, using as a metric the aggregated summed time of each chain available for a Target.

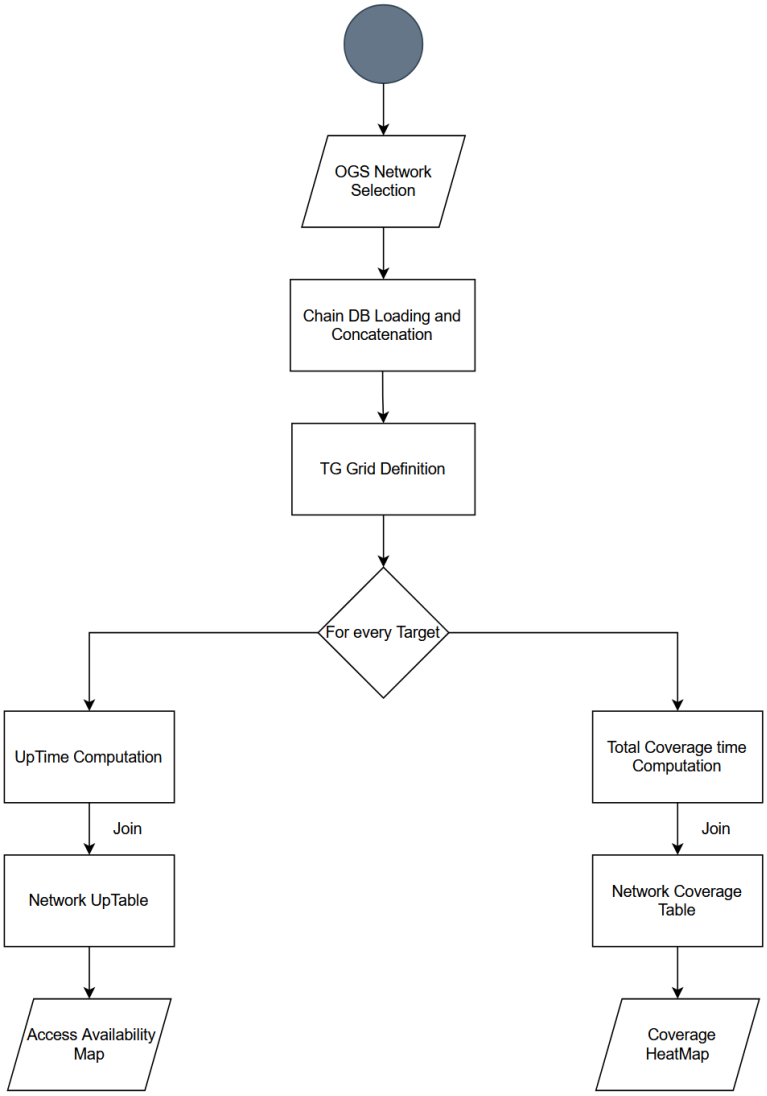

Figure 19: Access Availability and Coverage HeatMap implementation.

The analysis is built upon the following steps:

1. The chain DBs for the OGSs of the selected network are loaded and concatenated together.
2. The target area is defined as an 8x8 grid made of 64 total targets.
3. For each of the 64 targets, a method is called to obtain its Uptime and total coverage time. The former is computed as the sum of the durations of the accesses to the target, the latter as the seconds of the simulation time in which at least one active chain to the target is present. The method queries the full chain DB to select only the chains that end at the specific target, then returns the aforementioned times.

4. The target uptime array is converted first into percentages values and then into a table, which will be plotted over the Europe map to make the Access Availability percentage plot. The total coverage time, instead, is used to derive the coverage table that will be used to produce the HeatMap of the network.

The flowchart of the tool can be visualized in figure 19. In figure 20 an example of these results is showed for constellation A and the OGS network made of Catania, Sevilla, Lisbon, Athens and Porto. These OGSs are all located in the south of Europe, hence the higher availability at the lower latitudes. We can see that, due to topological constraints, the higher latitudes are not sufficiently covered with this network configuration. The analysis of the respective HeatMap shows exactly how the majority of the total access time is concentrated in the south western areas of Europe, where the HM displays a green color, while the north-eastern areas of Europe have less total access time, as highlighted by the red color of the HM.

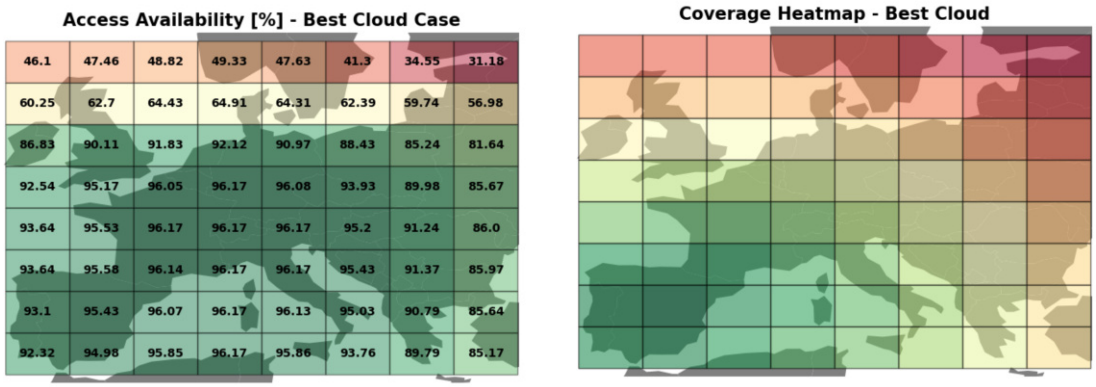

(a) Access Availability percentage.

(b) Coverage HeatMap.

Figure 20: Access Availability percentage (a) and Coverage HeatMap (b) for the Best Cloud network in Constellation A.

Two access availability plots for constellation B are showed in figure 21. The left plot shows the result for the Best Cloud network, while the right plot shows the result for the Western network, made of the OGSs in Barcelona, Bordeaux, Duplin, Porto and London. By looking at these two plots it emerges clearly the difference in the coverage and availability percentage: they both perform well for the south-western targets, but the best cloud has availability holes in the northern part of Europe while the western in the eastern part of Europe, as expected looking at the OGSs distribution. Also, we can appreciate the difference between the best cloud network in constellation A and in constellation B: the former has clearly a better coverage and availability performance. This result can be explained with the wider visibility cones of the satellites in constellation A, due to their higher orbital altitude, which allows them to be visible at the same time by multiple targets, even in area further away from the OGS that sends the uplink. This difference is more evident in the weak points of the network.

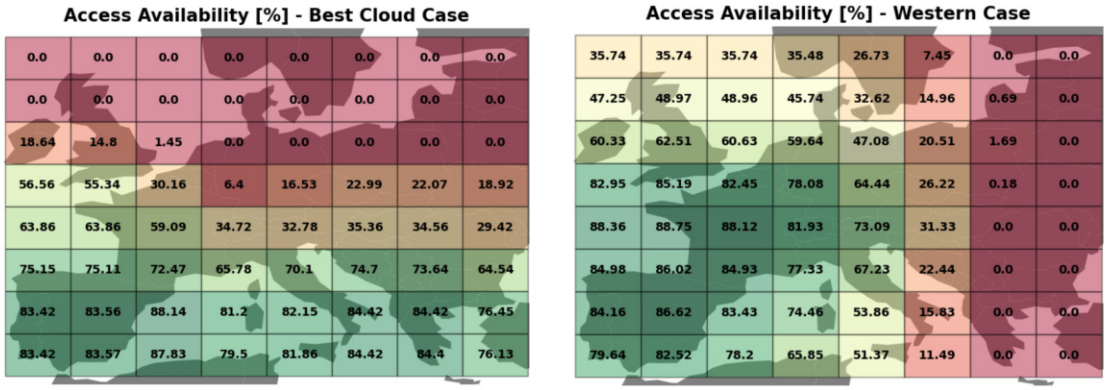

(a) Best Cloud Network.

(b) Western Network.

Figure 21: Access Availability percentage for the Best Cloud (a) and Western (b) networks in Constellation B.

Lastly, it is important to specify that for this first analysis no limitation on the number of teleports per OGS was implemented, meaning that the same OGS can have up to 6 or 7 concurrent accesses, and so can be connected to up to seven different satellites at a time, an unrealistic situation. By imposing a limit on the number of satellites the OGS can be connected with at a given time, a performance decrease in terms of access availability is expected. On the other hand, no significant changes are expected in terms of coverage distribution.
The next section will present the results of an HandOver (HO) logic, in which the OGSs have only two optical terminals and can establish only two uplinks with two different satellites at a time.
The resulting chain DBs will be used for the rest of the analysis.

5 OGS HandOver

The OGS HandOver (HO) is a process in satellite communication where a ground station switches its connection from one satellite to another, deploying different terminals. This process is critical in maintaining a continuous connection between the ground segment and the constellation, especially in LEO satellite systems, where satellites move quickly and frequent handovers can occur [32].
Indeed, the satellite ground track speed (V_{trk}) of a LEO satellite is much greater than Earth's rotation speed and the user's speed, as shown by the following simple computation:

$$V_{trk} = v \cdot \cos(i) \tag{2}$$

with

$$v = \sqrt{\frac{G \cdot M}{r}}. \tag{3}$$

For Large LEO constellation (i = 70 degrees, h = 500km) this results to $2604.98 m/s$, while for the Small LEO constellation (i = 60 degrees, h = 1200) results to $3627.91 m/s$, both significantly larger than the Earth's rotation speed of about $460 m/s$.
Due to the constant rotation of the LEO satellites, the visibility period of a satellite in a target cell can be very small. For this reason, having an HO technique is fundamental to increase the link duration and the total access availability time. In this study a so called Inter-Satellite HandOver is introduced, meaning that the OGS will switch terminals before the current connected satellite will be outside of the visibility of the current terminal, guaranteeing continuity in the communication between the OGS and the satellites of the constellation [24]. This HO technique is possible and this is evident looking at the histogram of the number of concurrent accesses for the two constellations:

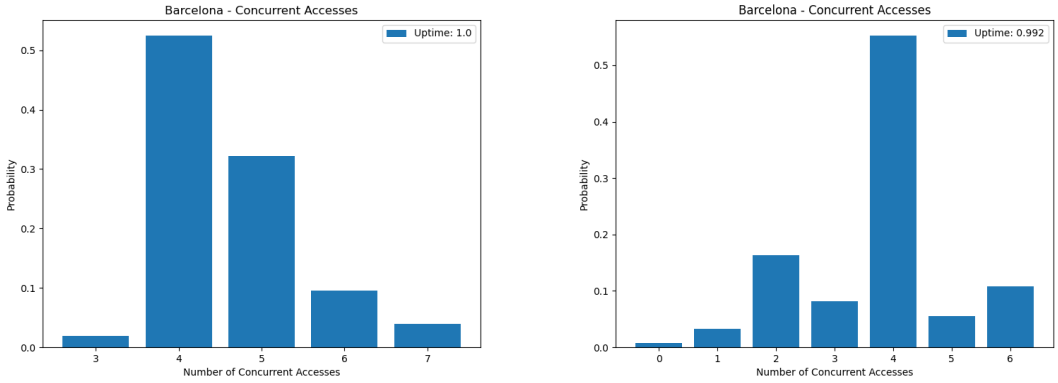

(a) Constellation A.

(b) Constellation B.

Figure 22: Topological Concurrent Accesses histograms for the OGS in Barcelona, for constellation A (a) and B (b). The Uptime value indicates the fraction of the simulation time in which the OGS is connected to at least one satellite.

What appears evident from figure 22 is that in such case, the OGS can always access at least three satellites in constellation A, while for constellation B, with the exception of some moments in which no satellite is accessible, which are only 0.08% of the total simulation time, at least 1 satellite is always in sight, but for the majority of the time more than 2 satellites are available, with the highest

probability for 4 satellites. Having two satellites in the visibility window allows for the link HO at OGS site, from one satellite to another. Not having included any access logic at the moment, with the current assumption it can be stated that a link HO is possible at any given time, with the exception of few OGSs in constellation B, including Barcelona. Indeed, for these particular OGSs, the HO analysis described in the following section highlighted the fact that even outside of a cloud blockage there are few instants of time, in the order of 10^3 over a simulation period, in which an HO cannot be guaranteed due to topological constraints. Constellation A is not affected by this limitation, probably due to its lower altitude and higher inclination, while constellation B is. One example for Porto in constellation B is showed in table 4:

Table 4: Example of a small interval of time (1 second) in which no HO can be guaranteed due to topological constraints. After 00:09:06 the next access starts at 00:09:07, when all the other accesses are over.

Sat	Start	End
Pl30Sat20	2024-05-12 00:05:27	2024-05-12 00:07:13
Pl11Sat2	2024-05-12 00:05:34	2024-05-12 00:07:21
Pl28Sat20	2024-05-12 00:06:14	2024-05-12 00:08:54
Pl9Sat2	2024-05-12 00:06:24	**2024-05-12 00:09:06**
Pl29Sat19	**2024-05-12 00:09:07**	2024-05-12 00:12:42
Pl30Sat19	2024-05-12 00:09:11	2024-05-12 00:11:30

The OGS influenced by this topological outage are those located in correspondence of the symmetry points of constellation B, so the OGS located at a latitude of around 41 degrees: Barcelona, Porto and Rome. An analysis on the entity of these limitations was conducted to quantify the impact of such 'topological zeros' on the availability over 1 period. The results are summarized in table 5. The columns from left to right are:

- Outage(s): total number of seconds in which no accesses are available for the specific OGS.
- Outage(%): outage percentage over the simulation duration.
- Net Outage(%): outage percentage over the simulation duration, without considering cloud blockages. This is also the percentage of the cloud filtered uplink database in which no accesses are available.

Table 5: Topological outage for constellation B over 1 simulation period.

OGS	Outage(s)	Outage(%)	Net Outage(%)
Amsterdam	0.0	0.000e+00	0.000e+00
Athens	0.0	0.000e+00	0.000e+00
Barcelona	7457.0	5.091e-01	7.055e-01
Berlin	0.0	0.000e+00	0.000e+00
Bordeaux	0.0	0.000e+00	0.000e+00
Catania	0.0	0.000e+00	0.000e+00
Copenhagen	0.0	0.000e+00	0.000e+00
Dublin	0.0	0.000e+00	0.000e+00
Geneva	0.0	0.000e+00	0.000e+00
Lisbon	0.0	0.000e+00	0.000e+00
London	0.0	0.000e+00	0.000e+00
Madrid	0.0	0.000e+00	0.000e+00
Marseille	0.0	0.000e+00	0.000e+00
Milan	0.0	0.000e+00	0.000e+00
Munich	0.0	0.000e+00	0.000e+00
Paris	0.0	0.000e+00	0.000e+00
Porto	628.0	4.287e-02	7.540e-02
Rome	2142.0	1.462e-01	3.664e-01
Sofia	0.0	0.000e+00	0.000e+00
Sevilla	0.0	0.000e+00	0.000e+00
Stockholm	0.0	0.000e+00	0.000e+00
Vienna	0.0	0.000e+00	0.000e+00
Warsaw	0.0	0.000e+00	0.000e+00
Zagreb	0.0	0.000e+00	0.000e+00

As we can see these topological outages have a low impact on the entire simulation period, reaching at maximum 0.5% of outage and 0.7% of net outage in the case of Barcelona. Their impact on the availability access will therefore be really small.
The following section will describe how the HO has been implemented.

5.1 HandOver Logic

For this analysis, two Laser Communication Terminals (LCT) have been considered per OGS, LCT1 and LCT2. The OGS will switch between these terminals with the goal of having always at least an active chain, but no more than two. At the start of a cloud blockage the number of accesses will be brought to zero while after the cloud blockage will be 1 again. The last access assigned to a terminal will be referred as the 'last booked access'. A typical trend is shown in figure 23

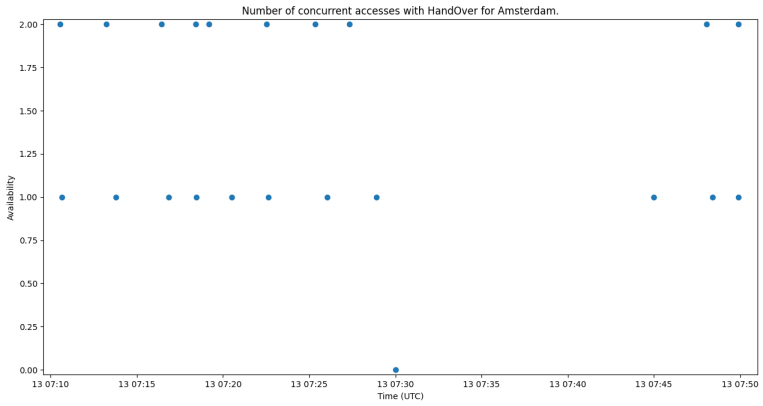

Figure 23: Number of concurrent accesses for Amsterdam OGS in constellation B over a 40 minutes period.

The number of accesses, so the number of active chains that starts from the OGS, oscillates between 1 and 2 and reaches zero at the start of a cloud blockage, during which no active chains are available. The script goes through the following steps for each OGS:

1. Loading the cloud filtered UL database for the selected OGS.
2. Cleaning the DB to remove the accesses with a duration of 0 that were accidentally added by the cloud filtering procedure and removing the consecutive rows with the same value for the end of the access. This is done to avoid considering as candidates the accesses that finish in correspondence of the start of the cloud blockage. Since the DB is ordered by the access start, keeping only the first of these accesses means keeping the longest one, hence the one that guarantees the higher probability of HO and, at the same time, maximizes the link duration bringing it till the very start of the cloud blockage.
3. The first access will be assigned to LCT1. The variable LCT1 flag will become 1, indicating the algorithm that the next access will be assigned to LCT2.
4. After the first access, each subsequent access will be analyzed in terms of its start time with respect to the end time of the current booked access: if the current access starts before the end of the booked one, then it is a candidate for HO, and it is added to the candidate list. If, on the other hand, it starts after the end of the last booked, then the program iterates though the selected candidates and selects the one whose time end is larger than the start of the next (i+1) access, to guarantee an HO.
   In case no candidate is present, a typical scenario that follows a cloud blockage, the current access will be added to the free terminal.
5. The last access will simply be added to the free terminal, concluding the analysis.

This simple algorithm would work fine only for the majority of the cases, but the analysis showed the existence of multiple 'special cases' that must be taken into account.

- If there are multiple accesses starting at the same time, which it the typical situation after a cloud blockage, the program must be able to select the longest of those accesses, which can

guarantee an HO. If the program chose simply the first, it could happen that no HO can be guaranteed.

- It can happen that none of the candidates can guarantee an HO with the next access, but some of those can form an HO with the current access, which can itself make an HO with the next one. So, the program is able to recognize these situations and pick the candidate who can guarantee an HO with the current access, and then immediately switch again to the current access, leading to an HO.
- It can happen that the last access of the DB cannot guarantee an HO with the previously booked access, so in this case the program switches to the last access which can still guarantee an HO with the previously booked access.

In addition, due to the high amount of computational load the script has to handle, parallel computing has been implemented to improve significantly the execution time.
The simplified flowchart of the tool is showed in the following figure 24.

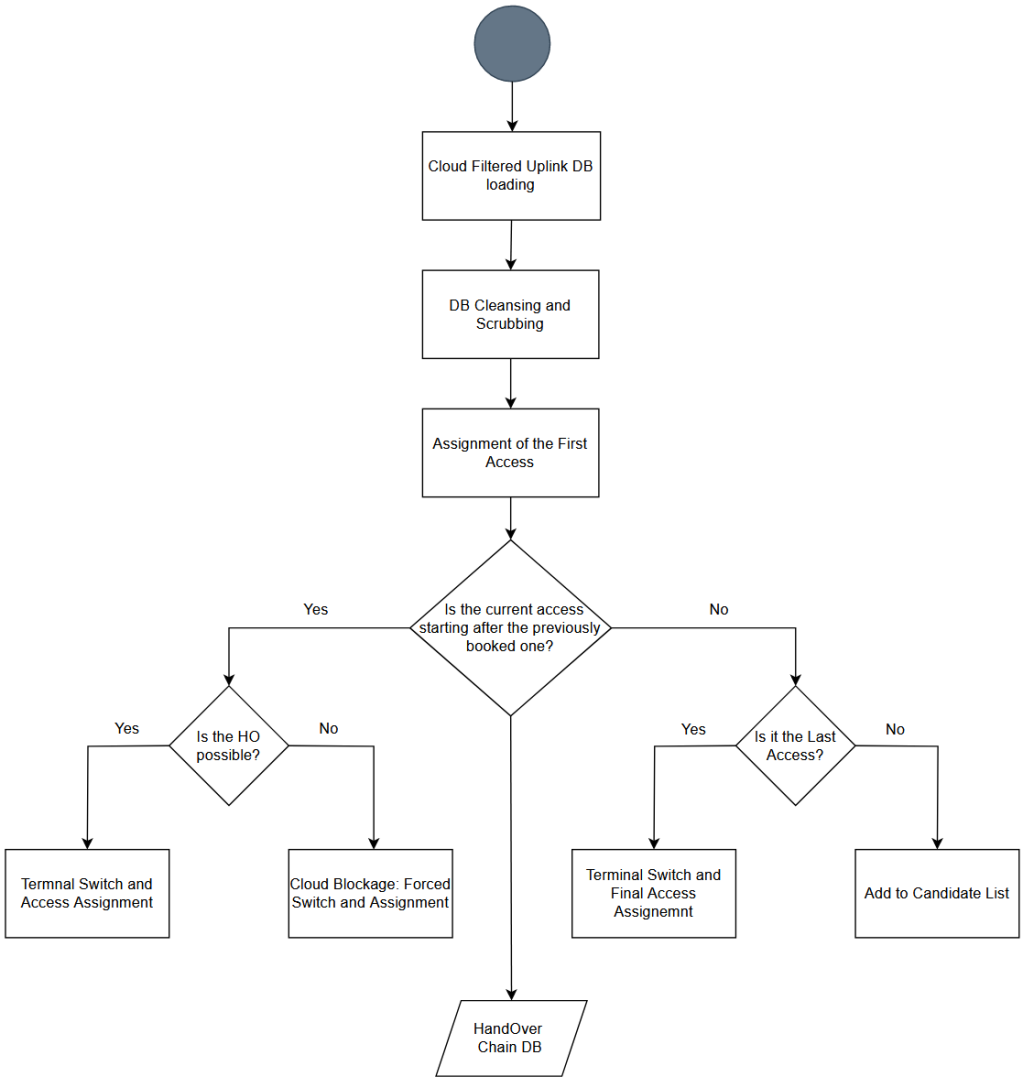

Figure 24: Flowchart of the HO Chain DB creation.

5.2 HandOver Results

The implementation of the OGS HO brings two outputs: an accesses database, containing the start and the end of each access in chronological order, and the chain database, which is now way shorter than the previous one due to the limitation on the total number of concurrent accesses. The former was mostly useful to perform debugs of the code and check that no additional zeros, meaning zeros that are not present in the cloud filtered database, were produced by the script. The latter instead is used to produce the final access availability output. Due to the limitation on the number of concurrent accesses, we expect a decrease in the availability percentage on each OGS network

scenario, with more significant changes in the Large LEO constellation due to the lower altitude and the higher number of total satellites. This is indeed confirmed by the availability analysis, whose outputs are shown in figure 25.

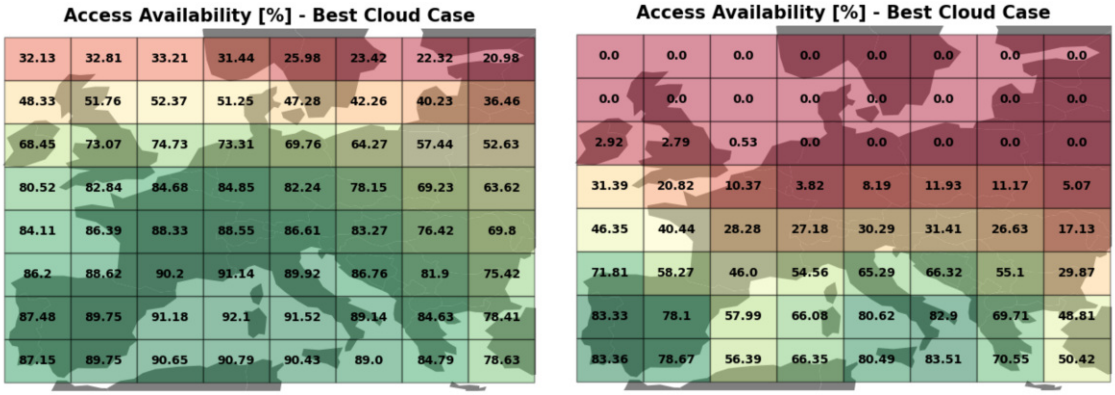

(a) Constellation A. (b) Constellation B.

Figure 25: Access Availability for the Best Cloud Network in constellation A (a) and B (b) after the implementation of the HO.

To have a more immediate grasp on the change in the access availability percentage after the introduction of the HO, figure 26 shows the percentage of the drop in access availability per target.

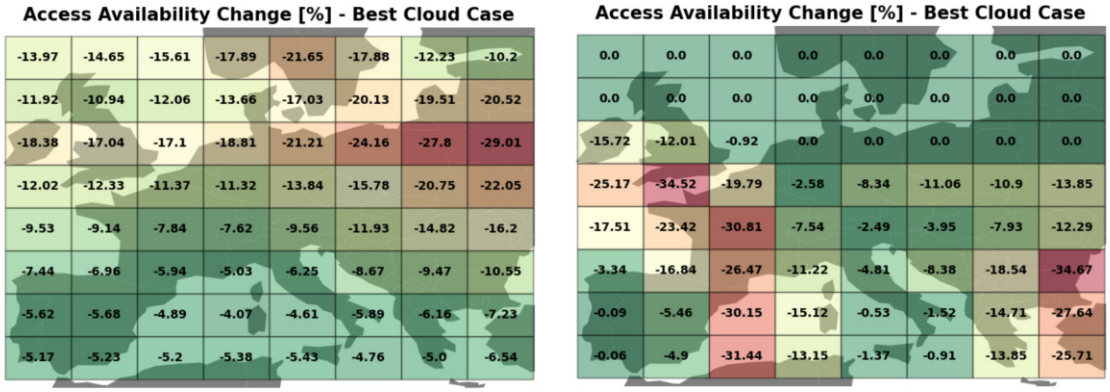

(a) Constellation A. (b) Constellation B.

Figure 26: Decrease in Access Availability for the Best Cloud Network in constellation A (a) and B (b) after the implementation of the HO.

As can be seen from figure 26, for constellation A in the Best Cloud network the area most influenced by the change is the northern area, with drops up to 29%, while in the southern area the drops are smaller than 10%, since all the OGSs are located in the south and it is therefore easier to perform the HO. For constellation B the apparent negligible change in the northern area is due to the fact that the initial availability was zero, and so it stayed the same. If we move to the southern area, however, the entity of the drop is more evident than in constellation A, with values significantly

higher for most targets.
In the next section the results of the introduction of Optical Inter-Satellite Links will be presented. The goal of this analysis is to prove that with OISL the access availability percentage can improve significantly, especially in the most critical areas of each configuration.

6 Optical Inter-Satellite Links

For each constellation, OISL capability was investigated, to understand what is the potential of enabling satellite hops in terms of coverage on ground, link duration and the number of available OISLs given a satellite in the constellation (link availability). The analysis will help figuring out the limitations of such approach, due to link distance and pointing and tracking requirements. The OISL considered are divided in two groups: intra-planar and inter-planar. Intra-planar links are performed between satellites on the same plane, so between the central satellite and its leading and following ones. The quasi-constant range allows to consider these links as static. Inter-planar links are performed between satellites on different planes, so between the central satellite and its two adjacent twins. These links are much more dynamic since the range changes significantly. To start the analysis, a constraint on the link distance was considered. The link distance was set as equivalent to the linear distance between a satellite and its leading/following one, in the same orbital plane. This will guarantee the intra-planar hop for the OISL and, given the fact that the range between a given satellite and its "twin" on the adjacent plane is much shorter, these hops are also guaranteed. The maximum link distances for the two constellations are [48]:

- Constellation A: 3923 km.
- Consellation B: 1796 km.

The central satellite of the hop is the one that receives the uplink from the OGS, and when it is no longer inside the visibility cone of the OGS, the hop will change. The topology of a single hop OISL is showed in figure 27.

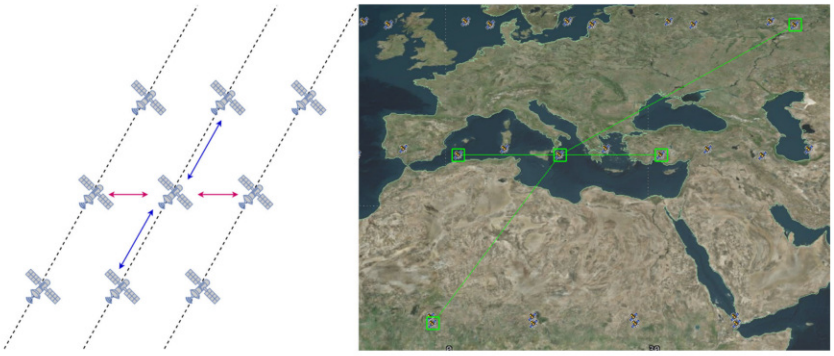

Figure 27: Topology of 1 hop OISL. The central satellite (here visualized over south Italy) receives the uplink and connects with the four satellites of its hop.

The hop "structure" can be repeated by the desired number of hops, allowing for a larger reach from the core satellite. Enabling more hops will of course guarantee a larger ground coverage, but will bring more challenges as well. Concept of Operations (ConOps) for the constellations envisions that the downlink will be operated through an RF Link. For this analysis, 60-degree full divergence cone sensors were attached to the satellite to visualize its ground coverage. With this assumption, the images below show ground coverage for satellite with no OISL (a) and with 1 hop OISL (b).

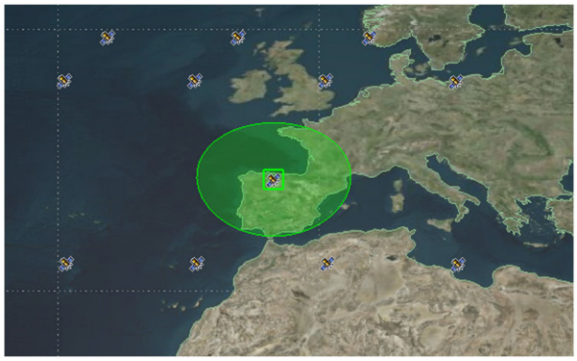

(a) Single Satellite, no Hops.

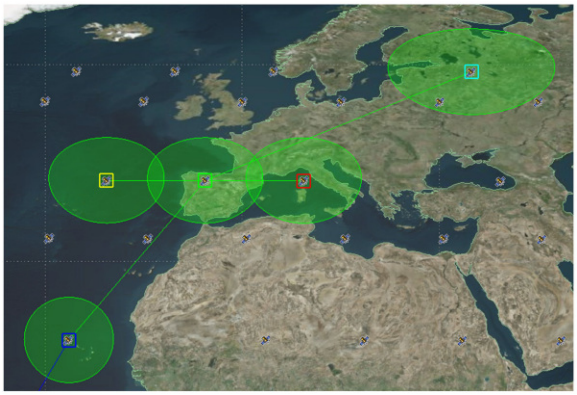

(b) 1 Hop.

Figure 28: Ground coverage of a single chain with no OISL and with 1 hop OISL.

6.1 OISL Logic and Implementation

To implement the OISL links with Python the following logic was followed:

1. Loading the input databases for the analysis: downlink database and cloud filtered uplink database. The downlink database is the same DB used to produce the topological Chain DBs, so it covers only one 'constellation period' and is then propagated for a specific number of periods to reach 1 year. The cloud filtered Uplink DB has been created during the chain analysis and contains data for the entire simulation period of one year.

2. At this point, two cloud filtered UL DBs exist: the topological one and the HandOver one, respectively without limitations on the OGS terminals and with a limitations of two terminals per OGS. For simplicity, they will both be referred as OGS DB. Independently on the OGS DB used, they both have a length of 1 year, and so the application of a mask to the OGS DB is needed to select only the rows within the current downlink period.

3. Substituting the satellite in the OGS DB with its hop. This process is fundamental to guarantee the proper functioning of the query that will follow.

4. Making the proper transformations to be able to transfer the two DBs on SQL via the sqlite3 library.

5. Querying the two databases to look for the time overlap between Uplink and Downlink. In the OISL analysis, the two tables don't need to share the same satellite; the requirement is now less stringent, since we just need that the downlink satellite is one of the satellites in the hop of the central UL satellite. For example, given the uplink with the satellite '10_1', which stands for the first satellite in the 10th plane, the target we want to access doesn't necessarily have to be in the visibility of the same satellite, but can have one of its twins and intra-planar satellites, so one of the following: '10_1', '10_2' (forward), '10_2' (backward for Constellation A), '9_1' and '11_1' (twins).

6. Creating the chain DB for the current period.

The previous procedure is iterated for the required number of periods to reach one year, and the sub-databases are then concatenated into a single final Chain DB for each OGS. The flowchart of the entire procedure is showed in figure 29.

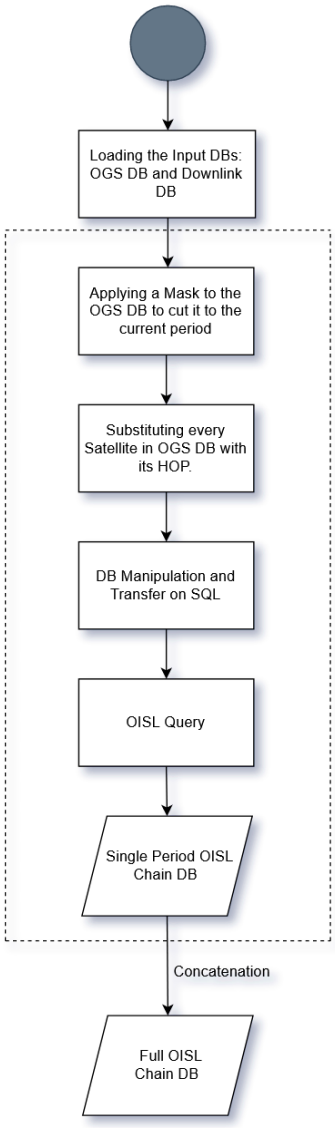

Figure 29: Flowchart of the OISL Chain DB creation. The procedure within the dashed profile is iterated for the 46 (constellation A) and 22 (constellation B) constellation periods. The results are then concatenated into a single 1 year long Chain OISL DB.

6.2 OISL Results

The results will be presented taking the Northern Network as example. First, in figure 30 we can see the improvements due to the introduction of OISL on the HO access availability percentage, in constellation A. We can see that the introduction of OISL does not add much to the northern area, where this network guarantees a good availability by definition, but significantly increases the performance in the southern area, where the improvements are in the order of the $20 - 30\%$.

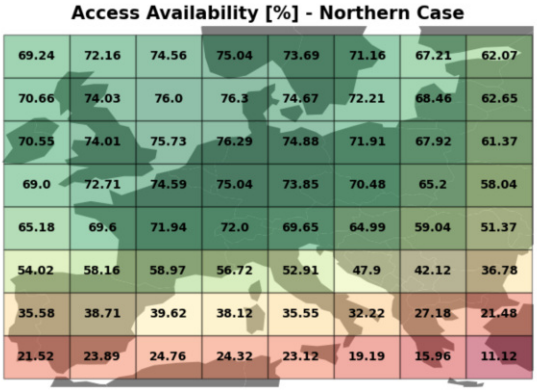

(a) Access Availability with HO.

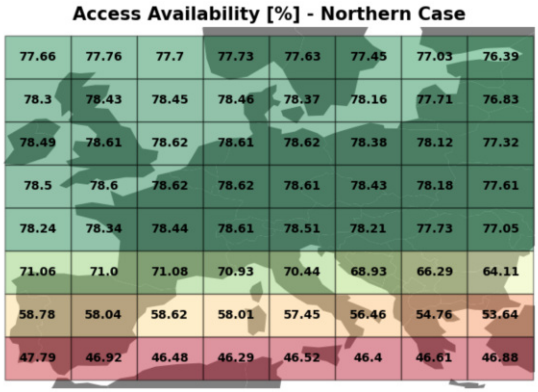

(b) Access Availability with HO and OISL.

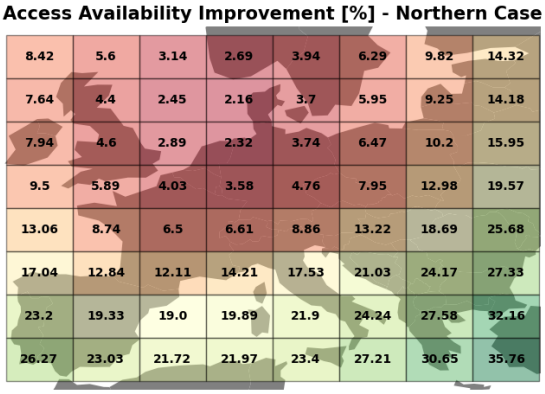

(c) Access Availability Improvement.

Figure 30: Northern Network, constellation A. Access Availability with HO (a), with HO and OISL (B) and Access Availability Improvement due to the introduction of OISL (c).

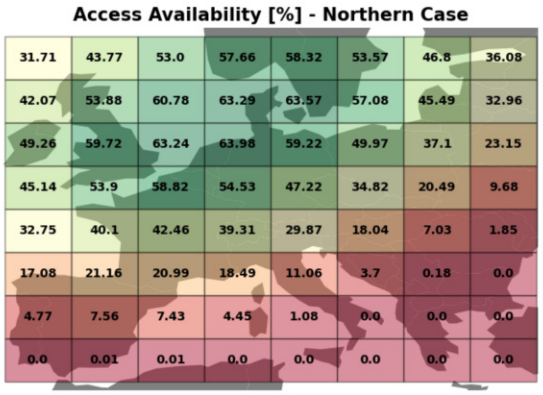

(a) Access Availability with HO.

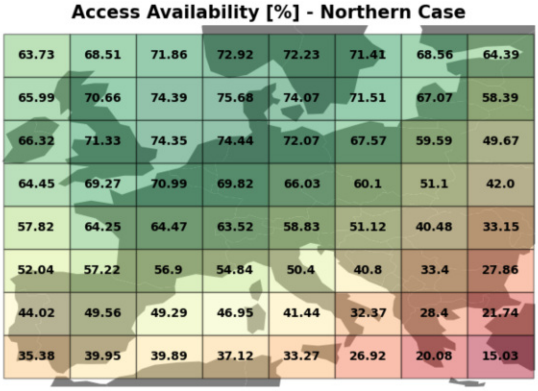

(b) Access Availability with HO and OISL.

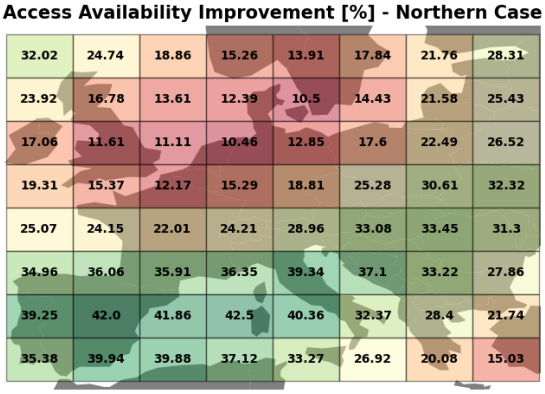

(c) Access Availability Improvement.

Figure 31: Northern Network, constellation B. Access Availability with HO (a), with HO and OISL (B) and Access Availability Improvement due to the introduction of OISL (c).

In figure 31 we can see the constellation B case. Here we appreciate that the lower region moves from a general absence of coverage to availability values in the order of 30%. Nonetheless, for both constellations in this specific network, the availability in the souther area is still not good enough, suggesting that the introduction of multiple hops or the increase in the number of OGSs may be potentially necessary for this specific network.
From the OISL implementation the following conclusions can be drawn:

- As already seen from the Topological and HO results, the availability and coverage performance of Constellation B (Large LEO) is lower than the one of Constellation A (Small LEO).
- The net result of the OISL implementation is an overall increase in access availability for every target of the network, especially for constellation B, and a decoupling between the geographical locations of the OGSs and the availability score per target.

- For both constellations, out of the 8 networks tested so far the ones that perform better are the ones with a more favorable cloud condition: Best Cloud, Best Cloud per Quadrant and Southern networks. This is to be expected since a better sky condition allows to establish more uplinks over the simulation period, which of course leads to a higher number of chain accesses.

The next steps of the analysis will be focused on improving the performance of the networks even more, with the goal of reaching access availabilities values as close as possible to 99% over the majority of the targets. To achieve this, an increase in the number of OGSs is needed, along with an optimization of the networks and the ISL, in terms of selection of the best OGSs and implementation of more efficient OISL geometries. The tools that will be presented from now on work in synergy to optimize the availability and coverage performance of the two constellations, while being as computationally efficient as possible and as configurable to the user's need as possible.

7 Chain Duration Analysis

In order to fully evaluate the two constellations and the performance of the different OGSs configurations, another parameter has been added to the access availability percentage: the total chain duration per target. The goal is to have an idea on the average duration of a full chain access per target, meaning the total time in which both the uplink and the downlink are available for that specific target. Being constellation B located at a lower altitude, a smaller average chain duration with respect to constellation A is expected. The inputs required by the tool are simply the Chain DBs for the scenario we want to analyze. From them, in a fraction of seconds a network is evaluated and a graphical output is produced. The tool has multiple configurable versions that yield different outputs: chain duration distribution per OGS, average chain duration per target per network, chain duration change with the introduction of HO and or OISL. The user can easily select the version according to the goal and apply constraints on the accesses duration.

7.1 Duration Analysis Implementation

The duration analysis has been implemented using one script that takes as input the full one year chain database previously generated and produces as output an 8x8 table, containing the average chain duration per target. The duration analysis covers the entire simulation period to account for cloud blockages and have as much variability as possible. The multiple versions of the script work for both the single OGSs case and the entire network case. All the versions of the script are based on the following iterative process:

- Retrieve the chain databases previously generated, and merge them in case of the analysis of a configuration.
- Create 64 sub-databases based on the 'TG' column, and extract the mean of the 'Duration' table for each of these sub-databases:

```
sub_db = DB.groupby('TG')
avg_duration_per_TG = DB.groupby('TG')['Duration'].mean()
avg_duration_per_TG = avg_duration_per_TG.reset_index()
```

- In case some OGSs or configurations don't have accesses for some targets, which is likely to happen for the most inhomogenously distributed networks and for the Large LEO constellation, the script assigns an average chain duration of 0 to those targets.
- The resulting table is taken and plotted on top of the Europe map for more immediate visualisation, or used to create histograms.

7.2 Duration Analysis Results

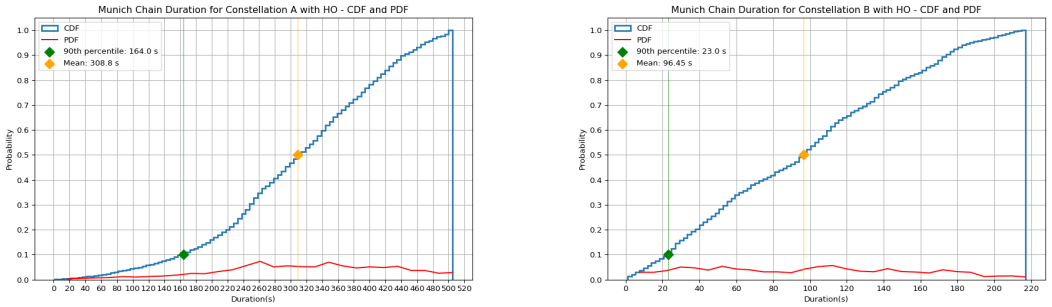

(a) Small LEO

(b) Large LEO

Figure 32: Chain Duration CDF and PDF for Munich OGS in constellation A (a) and B (b) with HandOver.

In figure 32 the Cumulative Distribution Function (CDF) and the Probability Distribution Function (PDF) of the access duration are displayed and the $90th$ percentile and the mean of the distribution are highlighted respectively with the green and yellow vertical lines. In those figures it is evident the difference in the Chain Duration distribution between constellation A and B: selecting the same OGS, constellation B has significantly shorter chains than constellation A, with the average of the latter being more than 3 times larger than the average of the former.

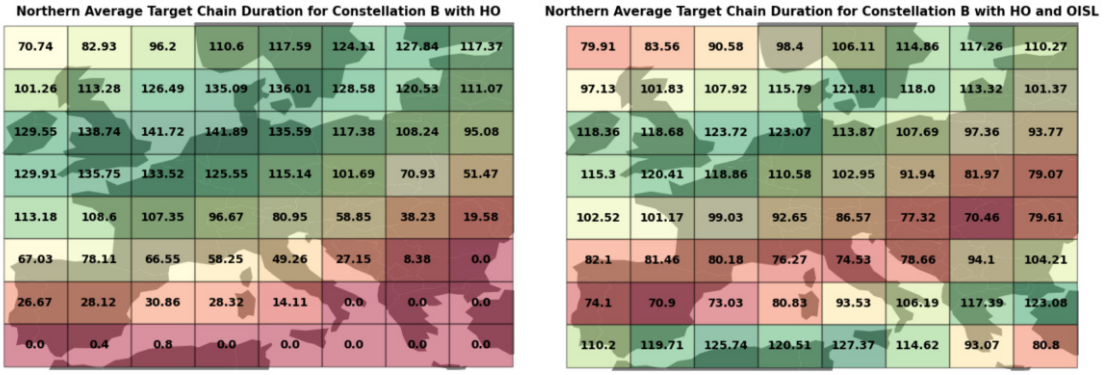

(a) No OISL

(b) OISL

Figure 33: Chain Duration (s) per target for the Northern network in constellation B with HO without OISL (a) and with OISL (b).

In figure 33 is is presented the Average Chain duration per target for the Northern network in constellation B. Figure 33(a) shows the result after the implementation of the HO, but without OISL. Clearly, due to the non uniform distribution of the OGSs, the southern area has an average duration of 0, since no accesses are available. The maximum durations are in correspondence of the location of the OGSs, as expected. In figure 33(b) it can be seen that after the addition of OISL the

situation changes, as now the southern area has average chain durations comparable to the ones in the north.

7.3 90 Percentile cut

One easy way to increase the average chain duration will be to cut all accesses with a duration shorter than the $90th$ percentile of the duration distribution. Being the average sensitive to the presence of outliers, we expect that the removal of very short accesses will improve the result. Of course, the overall availability is expected to decrease by a small amount. The cut to the $90th$ percentile can be considered worth it when the decrease in availability is negligible and the increase in average duration is significant.

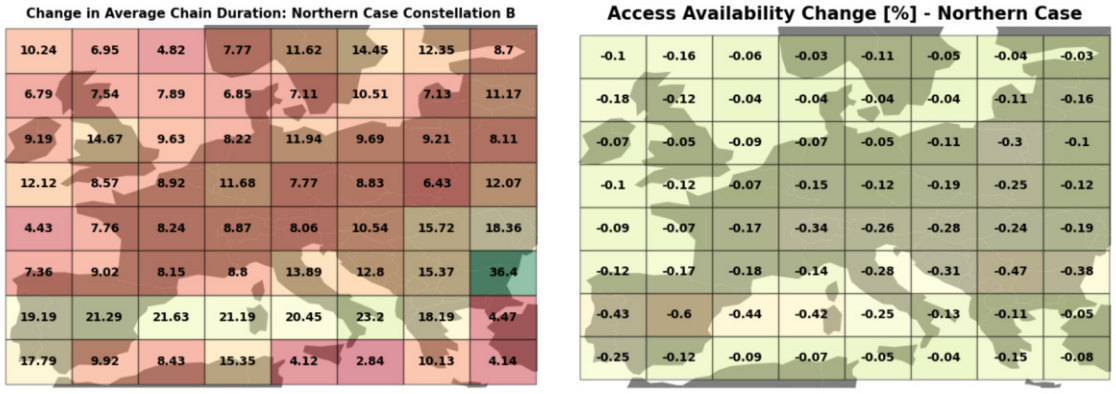

(a) Duration Change (s).

(b) Access Availability Change (%).

Figure 34: Change in Duration per target (a) and availability percentage per target (b) for the Northern network in constellation B with HO and OISL after the introduction of the $90th$ percentile cut.

From figure 34 we can see that the decrease in availability percentage caused by the $90th$ percentile cut is indeed almost negligible, inferior to 0.45% for every target, while the gain in average chain duration is in the order of 5 to 10% per target.

8 Network Optimization

The next step of the analysis is the optimization of the networks. Indeed, for these constellations to be operable by the user, the access availability percentages should be as close as possible to 100%, since even a value of 98%, which may seem, and indeed is, really good, would mean that a specific target will have around 7 total days without service in the arc of one year. Also, it has been shown that not all network configurations are equal in terms of performance. Taking the example of the Northern case, where all the 5 OGSs are located at the higher latitudes, we notice a really good performance in northern Europe but a really bad performance with respect to the lower latitudes. The more homogeneously distributed networks, like Central networks 1 and 2 and Best Quadrant, offer better performance in terms of homogeneity of the availability, even if they might be slightly inferior in terms of maximum target specific availability reached. Dealing with optical uplinks, the cloud distribution plays an important role as well: the performance of the Northern scenario is inferior to the one of the Southern scenario, because southern Europe experiences better weather conditions. All the above considerations bring to two questions:

- What is the minimum number of OGSs needed to reach availability percentages as close to 100% as possible?
- Where should the n OGSs of an n-sized network be located in order to guarantee the best performance?

The solutions to these questions will differ for the two constellations and will help in the trade-off phase of the analysis. To find these answers, a new Network Optimization (NO) tool has been developed. This section aims at describing its implementation and presenting its powerful results.

8.1 Logic of the tool

The Network Optimization tool is based on the following principles:

- **Score system**: to evaluate whether one network performs better than another a score system must be established. Three sub-scores are created: availability score, average chain duration score and homogeneity score. The final score is the weighted mean of these three sub scores, and it is a number between 0 and 1. The weights are configurable, but since the access availability percentage is our main concern, its score has by far the highest weight. The homogeneity score follows, and lastly the duration score, since it mostly depends on the type of constellation and presence or absence of HO and OISL, rather than OGSs selection.
- **Evaluation of old networks**: the old 8 network configurations of 5 OGSs provide a good way to test the efficiency of the tool, since it is evident that some configurations, like Northern and Southern, will have lower homogeneity scores than the Best Quadrant one, and in some cases it can be easily seen that the Best Quadrant configuration performs best also for overall availability score. The fact that the tool is able to confirm these evidences is a requirement that must be satisfied before its usage to test new and larger networks.
- **Number of OGSs**: the networks tested so far assumed a number of OGSs equal to five. However, this number of OGSs is not sufficient to guarantee availabilities in the order of 99%. Without including OISL this is mostly due to the limited coverage of the networks, while with OISL this is mostly due to the cloud blockages; indeed, in the arc of one year there are multiple occasions in which the sky over all the 5 OGSs is unclear at the same time, making any uplink impossible for the entire network. Also, even when the sky is clear only in one or two OGSs,

still not all the targets will be reached, even with OISL and especially for the lower altitude constellation. The task of finding the minimum number of OGSs that guarantees an efficient network is therefore far from being easy.

- **Duration constraint**: applying a duration constraint can be important to identify the networks that seems to perform well but have a high number of very short accesses, for example shorter than the hypothetical time required to switch between terminals and thus impeding the HandOver.

- **Minimum distances between OGSs**: with n possible OGSs in a network of r OGSs, the total number of possible combinations without repetition is given by:

$$C_{\mathrm{n,r}} = \frac{n!}{r!(n-r)!}$$

  which, for 24 possible OGSs in groups of 5, equals to 42504, while for 10 OGSs it reaches the value of 1961256. Testing all these networks requires time, and is in many cases useless: assuming a minimum distance for cloud variability of 300km, taking two OGSs that are closer to each other than this absolute minimum distance is useless. Also, given the high coverage that a single OGSs can provide, especially in constellation A, we can assume a minimum distance between the OGSs in the network, to avoid picking up networks whose performance will inevitably be bad due to low network diversity. Also, especially when the number of possible combinations gets really high, we can assume that having two almost identical networks that differ only for 1 OGS, which is closer than a minimum configurable distance to the one present in the other network, will produce similar results and can therefore be avoided.

- **Target weights**: some of the targets are located in the middle of the sea or in low populated areas, while others are located in areas with a high density of population. Attributing different weights to these targets is a smart way to discriminate between two apparently equally performing networks.

- **Efficiency**: since obtaining the access availability of one network is a long process that requires going through the chain DBs of every OGS in the network, joining them and computing the uptime, and given the fact that the possible OGSs have the same Chain DB for every network, it is more efficient to compute the uptime of each OGS, saving it to a file, and then simply join them together without overlapping the accesses. In this way, for a specific constellation, the majority of the time consuming computations are done only once per OGS, reducing significantly the analysis time required when larger networks are tested.

- **Trade-off**: a trade-off mechanism should be able to select the top 10 best networks, given a number of OGS and a constellation, in terms of overall score and availability score. Not only, it should be able to suggest improvements on the network analyzing the targets where the availability is lower and the cloud blockages, picking up the OGSs that can potentially be included in order to improve the performance.

Every principle is translated into a configurable parameter located in the config.py file, so that the tool can flexibly adapt to different scenarios. The road-map of the tool is the following:

1. Defining the main inputs of the analysis in the config.py script: constellation id, number of OGSs per network, target weights and constraints on the location of the OGSs inside the networks.

2. The configurable parameters defined in the config.py script are taken as input, along with the chain databases of all the OGSs, by the analysis.py script, which is the core of the tool. This script proceeds with the networks validation to exclude the OGSs combinations that do not satisfy the requirements.

3. On the validated networks, the single OGSs are analyzed in terms of access availability performance, producing a file containing their availability vectors in a compressed form. By single OGS availability vector it is meant a vector that contains the temporal availability information, meaning the intervals in which at least 1 full access chain is originating from the OGS, with a time-step of 1 second. It is by definition a long vector, hence the need of manipulating it in a compressed string notation to avoid memory issues. This step allows the tool to be more efficient, since the availability per target information of each OGS is computed only once and can be retrieved every time a new network containing that OGS is analyzed. However, this operation is not corny at all, and so it is performed by a separate script. The output is a .pickle file, which is a byte stream created by pickle, a Python module that can serialize objects to files on a disk.

4. On the validated networks, the access availability and duration analysis are performed, exploiting the single OGSs .picke files to make the access analysis faster. Indeed, a simple merge of the single OGS files is needed, although taking into account the time overlap is necessary since we are interested in the availability performance, not in the total access duration per target. For each OGS in each of the networks analyzed, if the pickle file exists already, it is simply loaded and combined with the ones of the other OGSs in the network. In case it doesn't exist already, it is created by the pre analysis method.

5. To properly combine the .pickle files they must be re-opened and the information must be converted in Uptime per target again, in order to compute the access availability percentage. The resulting tables are saved and they constitute the basis for the network evaluation, along with the average chain duration per target tables, created in the next step with a procedure almost identical to the one already described in the duration analysis section.

6. Every network is scored based on the results of the access availability and duration analysis and its results are written in a .csv file. The columns of the file are the different scores and the rows are the different networks tested for that specific number of OGSs.

7. This file is taken as input by the tradeoff.py script to perform an optimization analysis of the most performing networks, in order to suggest improvements and identify the most performing OGSs.

8. A .csv file is produced to store the top 10 most performing networks. At this point, the user can decide to obtain the access availability plots of some of the networks, or to re-start the analysis cycle implementing the biases and suggestions of the tradeoff.py script.

Of particular interest is the method used to score the networks. This method produces the availability score as the average of the availability per target if the weights on the targets are not applied, as the weighted average otherwise. Then the duration score is obtained with reference to an upper limit of 500 seconds, since no chain can overcome this value of duration. In terms of the homogeneity score, it is computed as the normalised standard deviation of the availability table. The three scores are combined and the final score is a weighted average with the following weights:

- Availability score: 8. The availability is the main parameter we want to optimize, given the fact that no constellation, independently of its duration and homogeneity scores, would be operable with availabilities smaller than 98 or 99%.
- Duration score: 2. The lowest weight is attributed to the duration score since the average chain duration mostly depends on the scenario we are considering, i.e the constellation and the presence or absence of OISL, rather than the disposition of the OGSs.
- Homogeneity score: 3. This parameter, despite being important, is still less important than the availability score, thus the lower weight.

These weights are configurable and indeed for some configurations different weights have been used, but the relative importance remained the same.
The structure of the tool is summarized in diagram 35, with a specific section dedicated to the scoring method:

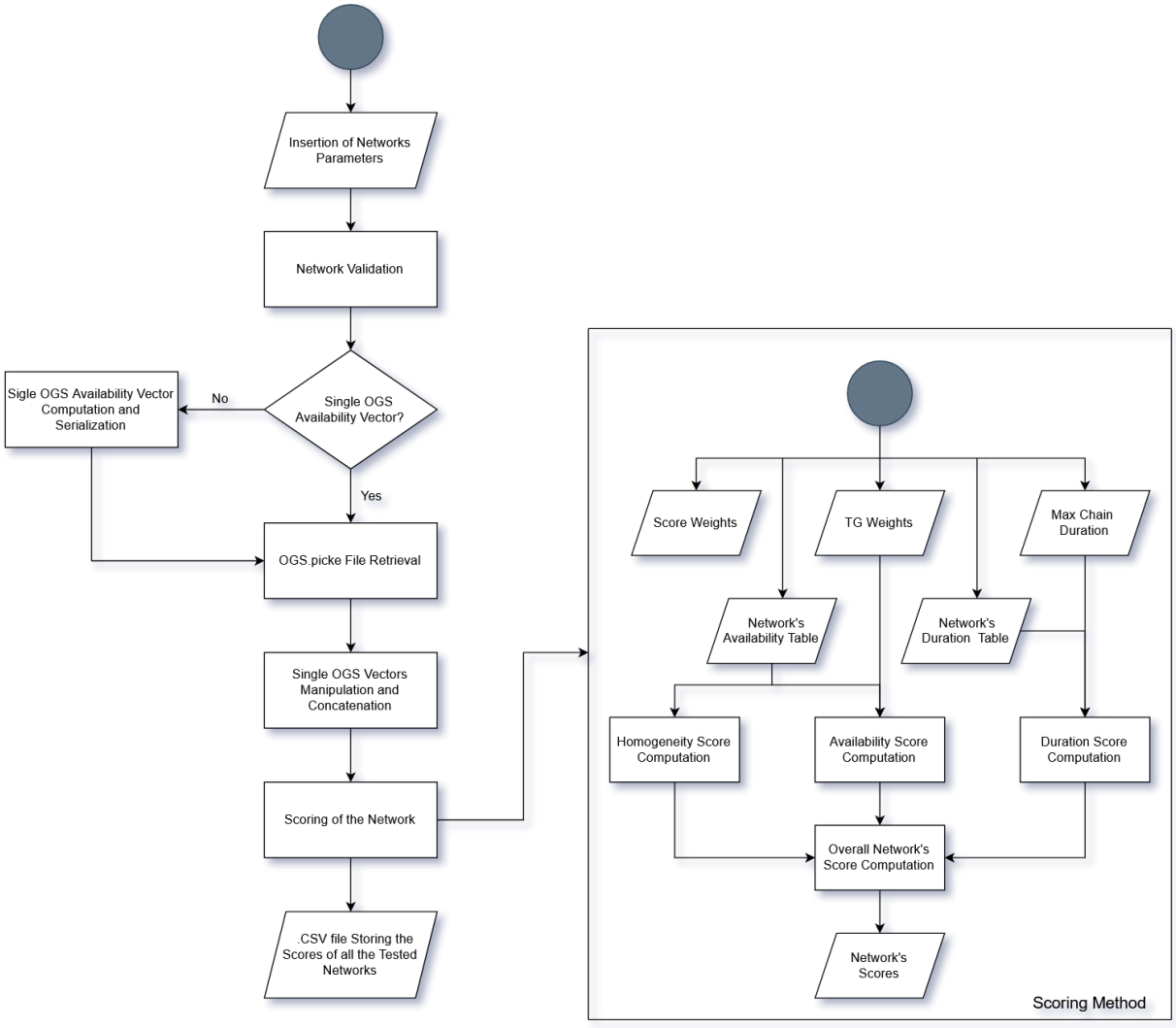

Figure 35: Flowchart of the Network Optimization Tool.

In the end there will be a great number of network analyzed, so a trade-off method is needed to discriminate between them. The trade-off tool selects the top 10 best networks for overall score and the top 10 for availability score and then identifies the most important OGSs, meaning the OGSs that are present in all or the majority of the networks, both for the overall and availability rankings. Then, it suggests to bias the networks toward these OGSs in order to find the best network faster. Also, a more detailed analysis is conducted on the top availability network, for whom the weak areas are computed along with the total outage time due to the clouds, in order to find the OGSs that can fill this time gap for as long as possible, resulting in an increase in the network's uptime and, as a consequence, of its access availability performance.
A specific flowchart for the tradeoff.py script is showed in figure 36, along with a specific section for the cloud outage algorithm.

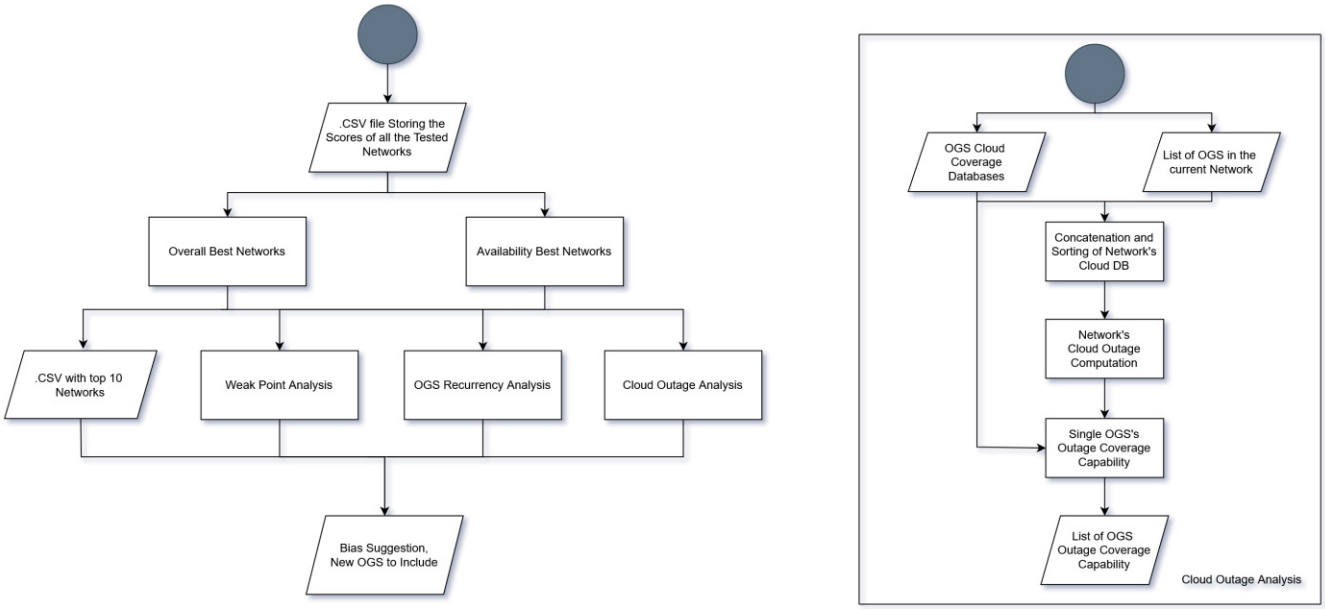

Figure 36: Flowchart of the Trade-Off algorithm.

8.2 Results of the tool

In this section some of the main results of the tool will be presented and analyzed.

Table 6: Number of networks tested per OGS number and Constellation - OISL logic.

OGS number	A - Classic	A - Flexible	B - Classic	B - Flexible
5	370	8	389	28
6	131	0	37	45
7	54	72	54	0
8	111	15	289	0
9	184	3	136	0
10	15	1	121	0
11	1	0	14	0
14	0	0	66	0
15	0	0	10	1
16	0	0	19	1
18	0	0	13	0
24	0	0	1	0

Table 6 shows the number of networks tested by the tool per each OGS number and constellation. Classic refers to the classic OISL geometry presented before, while Flexible stands for the flexible OISL geometry that will be presented in chapter 9. In general, the number of network tested for the Flexible case is significantly lower than for the Classic one, since it was chosen to focus on testing that tool on the best networks identified for the classic geometry, in order to have a grasp on the improvements brought by a different OISL logic, rather than a further optimization of the OGSs

choice. For Small LEO the analysis was stopped at 11 OGSs, since that number of OGSs has shown to be sufficient to reach an optimal performance.

Table 7: Composition of the best networks tested per OGS number and Constellation.

OGS number	Constellation A	Constellation B
5	Catania, Marseille, Sevilla, Sofia, Stockholm	Barcelona, Catania, Copenhagen, Marseille, Sofia
6	Athens, Catania, Copenhagen, Marseille, Lisbon, Sevilla	Barcelona, Catania, Copenhagen, Marseille, Rome, Sofia
7	Athens, Catania, Copenhagen, Marseille, Rome, Sevilla, Stockholm	Athens, Barcelona, Catania, Copenhagen, Marseille, Rome, Sofia
8	Athens, Barcelona, Catania, Copenhagen, Marseille, Rome, Sevilla, Stockholm	Athens, Barcelona, Catania, Copenhagen, Marseille, Porto, Rome, Sofia
9	Athens, Barcelona, Catania, Copenhagen, Marseille, Rome, Sevilla, Sofia, Stockholm	Athens, Barcelona, Catania, Copenhagen, Marseille, Porto, Rome, Sofia, Stockholm
10	Athens, Barcelona, Catania, Copenhagen, Lisbon, Marseille, Rome, Sevilla, Sofia, Stockholm	Athens, Barcelona, Catania, Copenhagen, Marseille, Porto, Rome, Sofia, Stockholm, Vienna

Table 7 shows the OGSs that make the best networks for a given number of OGSs. It is immediately visible how the majority of the OGS are located at the lower latitudes, and some OGS, like Catania and Marseille, are present in all the best networks.

8.2.1 Constellation A without OISL

This tool was initially tested on constellation A without OISL since these chain DBs are by far the smallest and thus the fastest to process. Out of the 8 networks previously analyzed, the best one was the Best Quadrant network which was awarded a total score of 0.667 and an availability score of 0.784. This tool tested 380 networks and the best one, made of the OGSs Catania, Marsiglia, Porto, Sofia and Stockholm, totaled a score of 0.675 and an availability score of 0.795.

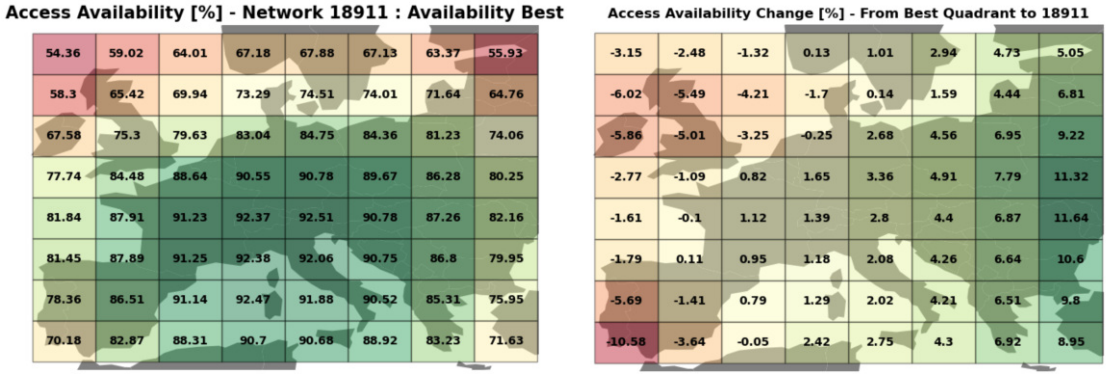

(a) Access Availability percentage.

(b) Access availability percentage change.

Figure 37: Access availability percentage for the network made of Catania, Marseille, Porto, Sofia and Stockholm (a) and change in access availability percentage from Best Quadrant network (b).

In figure 37 the access availability percentage for this network is shown and compared with the one of the best quadrant network. We see that without OISL the performance is still too low and there is no such thing as an overall improvement of all areas, since without links between satellites the coverage and availability per target is limited by the position of the OGSs. Looking at the availability change we see that the western area experienced a decrease, while the eastern area experienced a quite significant increase. This is the result moving from the OGSs Sevilla and Paris to the OGSs Stockholm and Sofia, which is a necessary consequence of prioritizing some targets with respect to other targets; indeed, western Europe hosts more targets in unpopulated or low populated areas, while the opposite is true for eastern Europe.

8.2.2 Constellation A with OISL

Since the importance of the OISL has been proved already to a large extent, the majority of the tests were performed on this scenario. Starting from networks of 5 OGSs, one OGS at a time has been added following the results of the trade-off analysis with the goal of finding the number of OGSs that allows to reach an availability of 99% on at least one target. It turned out that 9 is the minimum number of OGSs required for this purpose. 185 networks were tested and the best one, with a weighted availability score of 0.984, is formed by the following OGSs: Athens, Barcelona, Catania, Copenhagen, Marseille, Rome, Sevilla, Sofia and Stockholm.

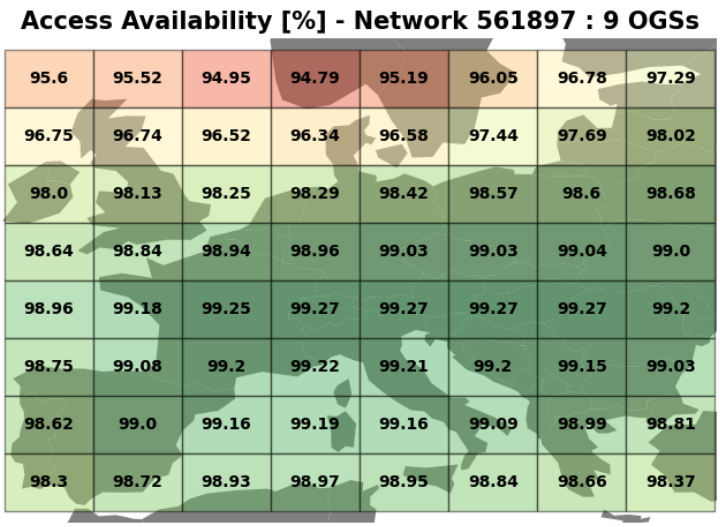

Figure 38: Access availability for the best network of 9 OGSs for constellation A.

Even if this network performs already really well at lower latitudes, there are important urban areas at higher latitudes with lower scores, so the number of OGSs needs to increase again. It turned out that, in order to reach an operable network with huge performance, the key number of OGSs is 11. So, after having found the best network of 9 OGSs the trade-off script was used to suggest the best network with 10 OGSs and after that with 11 OGSs, which turned out to be made of the following OGSs: Athens, Barcelona, Catania, Copenhagen, Marseille, Paris, Rome, Sevilla, Sofia, Stockholm and Warsaw. Its access availability plot is shown in figure 39.

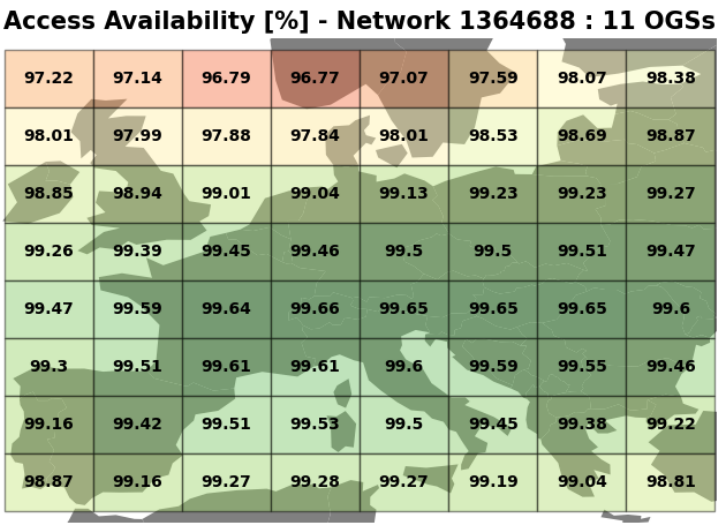

Figure 39: Access availability for the best network of 11 OGSs for constellation A.

Since with this network all the most important targets have values of availability above 99%, extending up to almost 99.7%, the analysis on Constellation A with OISL was stopped, since the benefits brought by a further increment in OGSs number would not be sufficient to justify the higher cost and mission complexity.

8.2.3 Constellation B with OISL

The same process has been applied on constellation B on the OISL chain databases, with the expectation that some of the features of the most performing networks for constellation A will be confirmed, while some differences will arise. Starting with 5 OGSs, the previously best was the Southern network, with an availability score of 0.84. After having tested 380 networks the best came out to be the one with the OGSs Barcelona, Catania, Copenhagen, Marseille and Sofia, with a score of 0.848.

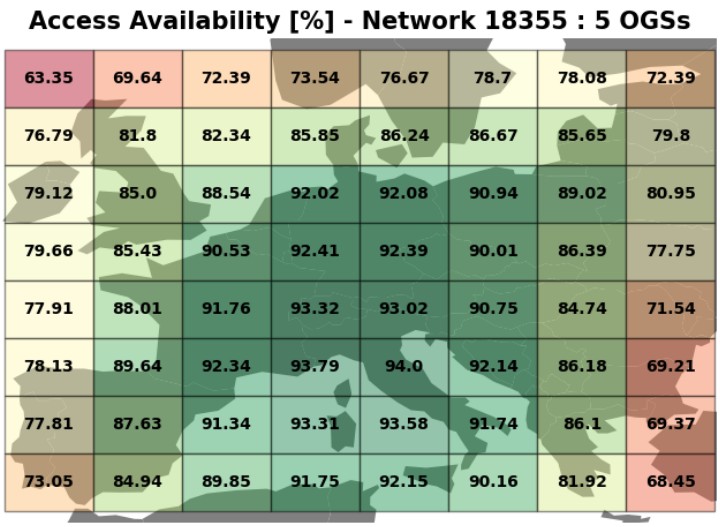

Figure 40: Access availability for the best network of 5 OGSs for constellation B.

Increasing the number of OGSs and giving more importance to the availability score, networks of more OGSs were tested up to a number of 16 total OGSs.

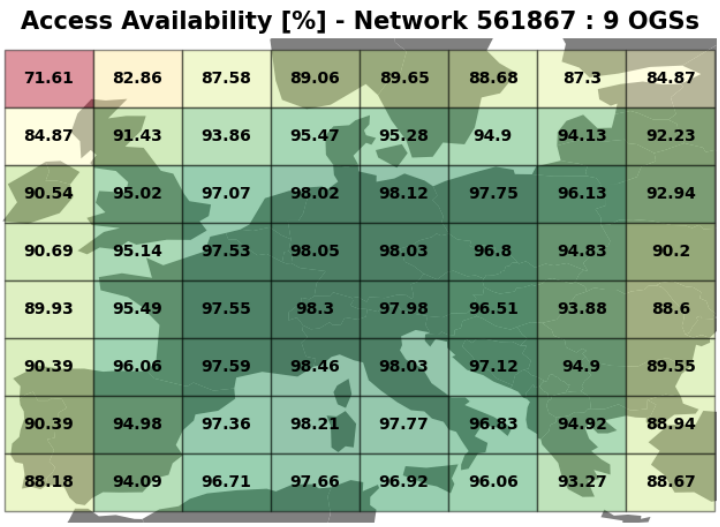

Figure 41: Access availability for the best network of 9 OGSs for constellation B.

Confronting figure 38 and figure 41 we can see the difference in performance between the Small LEO and Large LEO constellations on their best networks of 9 OGSs. A huge gap separates the two constellations, since for constellation B the network of figure 41 still has important weak areas. Increasing the size of the networks, it emerged that with constellation B 11 OGSs are not sufficient to produce availabilities of 99%, while for constellation A they were enough to produce an operable network. On the light of this finding, 66 networks of 14 OGSs and 19 networks of 16 OGSs were tested and the best ones are shown in figure 42. Their weighted score of respectively 0.9692 and 0.9753 are still inferior to the weighted score of 0.984 of the best network of 9 OGSs for constellation A.

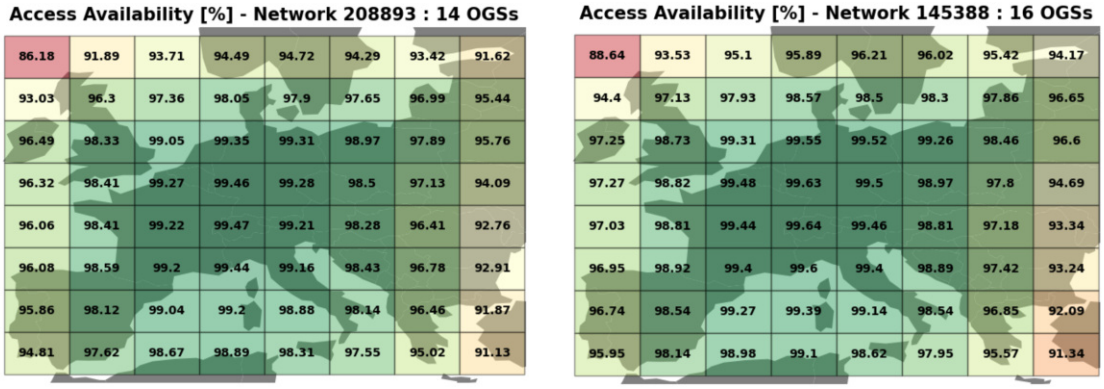

(a) Best network of 14 OGSs.

(b) Best network of 16 OGSs.

Figure 42: Access availability for the best networks of 14 (a) and 16 (b) OGSs for constellation B.

Since even networks of 16 OGSs were shown to be less performing than the 9 and 11 OGSs network of constellation A, a test was done considering all 24 OGSs.

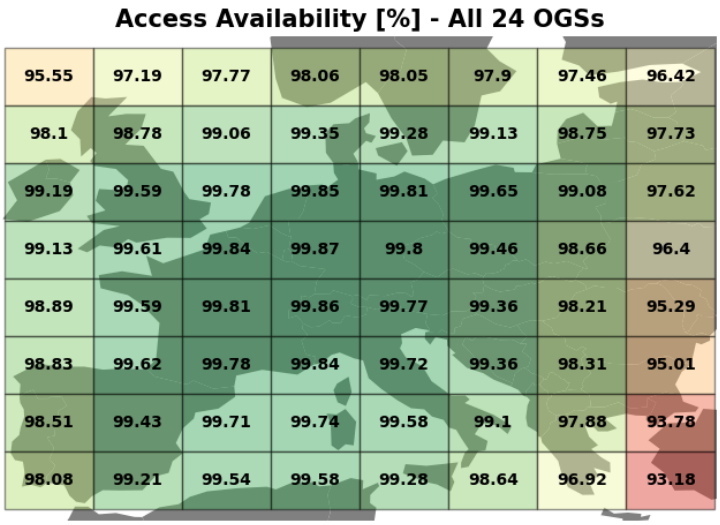

Figure 43: Access availability for constellation B considering all 24 OGSs.

This test is considered to be an hypothetical upper limit, since deploying 24 OGSs would be unfeasible in terms of costs and mission complexity. However, analyzing the performance of such a large network provides important information for the trade-off analysis that will follow: the weighted availability score of this network, which is equal to 0.9857, came out to be still lower than the availability score

of the best 11 OGSs network of constellation A, which is equal to 0.991.

8.2.4 General Conclusions

For both constellations a comparison between the increase in access availability performance due to the optimization in the choice of the OGSs in a fixed size network and the one due to the introduction of a new OGS to the network was made, and the results can be seen in figure 44 for Small LEO and figure 45 for Large LEO. The increase in performance due to the optimization of the network done by the NO tool was quantified as the difference in weighted availability score between the best and the worst networks tested, while the increase in performance due to the addition of a new OGS was quantified as the difference between the average of the maximum and minimum availability scores for the n+1 OGSs case and the n OGSs case. For example, in 44, the two histograms at OGS number equal to 5 represent the benefits of the NO tool for a network of 5 OGSs (green histogram) and the average benefit due to the introduction of a $6th$ OGS to the same network (blue histogram). To improve the readability of the plots, the values have been normalized to the highest Network Optimization performance increase.

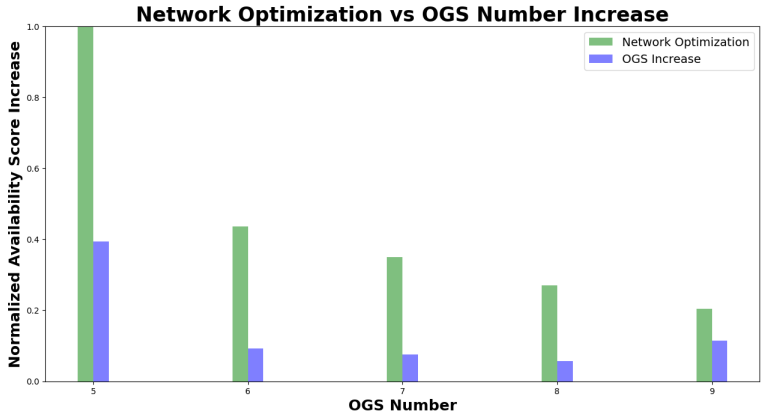

Figure 44: Constellation A, comparison between the increase in availability performance due to the optimization of the network and the one due to the introduction of a new OGS.

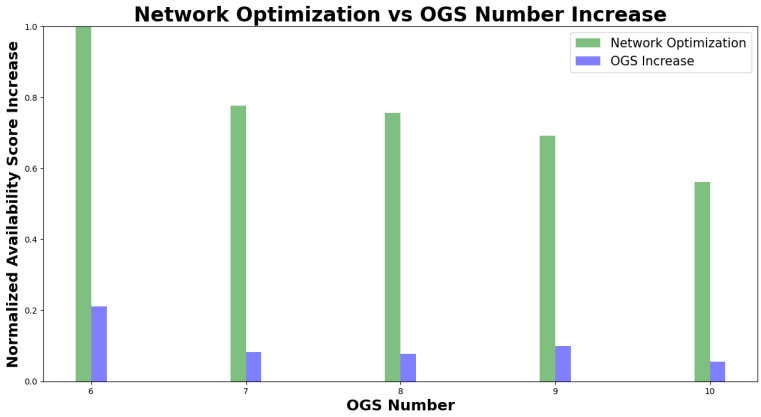

Figure 45: Constellation B, comparison between the increase in availability performance due to the optimization of the network and the one due to the introduction of a new OGS.

The results displayed are of course very dependent on the number of networks tested; a higher improvement is to be expected as the number of n sized networks tested increases since the probability of finding both the absolute best and absolute worst networks is higher. For this reason, the performance increases for the same comparison term at different OGSs number are not on scale; for example, looking at the last two blue histograms in figure 45, the increase in performance due to the introduction of a $9th$ OGS to an 8 sized network seems to be smaller than the one due to the introduction of a $10th$ OGS to a 9 sized network, but this would be a wrong conclusion, since this result is just due to the fact that the discrepancy in the total number of tested network for OGS number 8 and 9 is larger than the discrepancy in the total number of tested network for OGS number 9 and 10. However, what is of interest is the relation between the two comparison terms. Due to how the two improvement scores were computed, this relation is reliable, and points to the conclusion that the optimization of the network is by far more beneficial than its size increase. This is especially true for constellation B, where the choice of the OGS locations highly influence the availability output due to the narrower visibility cones of the satellites. The main reason behind this phenomena lies in the uplink requirements; indeed, what distinguishes one good network from a bad one is mainly the ability of getting around the cloud blockages to establish more uplinks, and thus producing more accesses. If the uplink was at RF, the output would be way different, with a less significant dependence between the geographical location of the OGSs and the availability performance, since the topological requirement would be the only variable to consider.
Furthermore, this tool allowed us to draw these important conclusions:

1. The performance of constellation B is by far lower than the one of constellation A. It has been proved that while for constellation A 11 OGSs are sufficient in creating an operable network with high performance, for constellation B even the upper limit case, which is the one considering all 24 OGSs, has still an inferior performance, while having more capital and operational fees and overall higher mission complexity.

2. With the introduction of OISL and the subsequent improvement in coverage, it has been shown that the best performing networks host the majority of their OGSs in southern Europe, with Catania, Marseille, Sofia and Athens being present in almost all the best networks. The reason behind this geographical bias hides not only in the superior weather conditions of south

Europe with respect to northern Europe, but also in the topology of the OISL implemented so far, which tends to produce more accesses within Europe if the central satellite is at lower latitudes than at higher latitudes, where some of the satellites in the hop are outside of Europe's visibility.

3. The idea of the trade-off tool to bias the networks toward the OGSs that can minimize the overall outage time due to cloud blockage seems to perform well, since the best performing networks found via a brute force combination test coincide with those suggested by the tool in the majority of the case, and have performances almost identical to those in the rest of the cases.

4. The increase in access availability is not scaling linearly with the number of the OGSs added, as can be seen from figure 46. Indeed, the addition of one OGS is way more beneficial when the total number of OGSs is lower rather than when the number of OGSs is already pretty large.

5. Overall, the best performing networks can pretty easily reach availabilities of 99% at lower and middle latitudes, but they all struggle at higher latitudes, where the uppermost targets have significanlty lower availabilities wrt to their souther counterparts. Again this is due to the geographical and topological biases described in point 2.

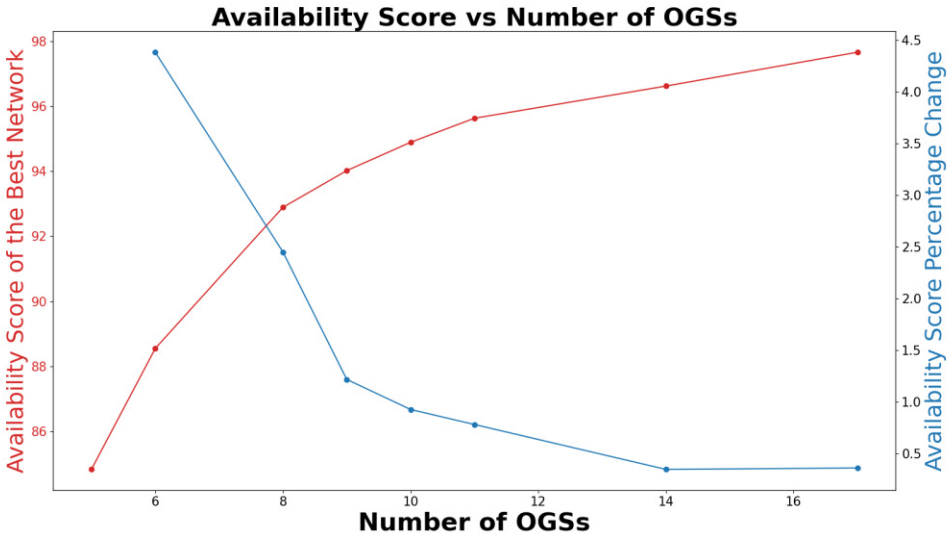

Figure 46: Constellation B, availability scores and percentage changes of the best networks with increasing number of OGSs.

Leading from the conclusions 2 and 5 it emerges that the OISL logic implemented so far, where the central satellite connects with its lateral twins and its 2 closest intra-planar satellites, is not ideal in many cases and thus can be improved. This is because, especially at the borders of our

square area target, the central satellite links with satellites that are mostly outside of Europe for the majority of their visibilities, leading to the aforementioned difficulty of reaching high availabilities values at higher latitudes. For this reason a new OISL geometry, a so called flexible OISL logic, was implemented and will be described in the next session.

9 Flexible OISL

As it has just been shown, constellation A can achieve a really good performance with 11 OGSs, while constellation B struggles to be operable in some target areas even with all 24 OGSs. Moved by this finding, the next question is how can these results be improved. Two approaches have been tested: two hops OISL and flexible OISL. The first method is pretty self-explanatory: the central satellite links with the forward and backward satellites in the same plane and with the adjacent twins satellites, and each of these satellites becomes the center of a new hop. In this way, the total number of satellites per hop moves from 5 to 13, and the ground coverage significantly increases, as can be seen from figure 47.

Figure 47: Ground coverage of a single chain with 2 hops OISL.

The expected result is an increase in the constellation performance, at the expense, however, of the mission complexity and latency, which will both drastically increase. Indeed, allowing two hops ISLs implies that the signal would have to travel twice the distance to reach the destination satellite, which can be a significant delay, especially for real-time applications. Also, the signal strength is more subject to degradation as it travels a longer distance through the air. The signal may require amplification, which can increase the complexity and cost of the system. This method was tested with the 8 original networks of 5 OGSs each, since the resulting chain DBs are extremely large due to the larger number of overall accesses. The results and improvements with respect to 1 hop OISL for constellation B are shown in figure 48.

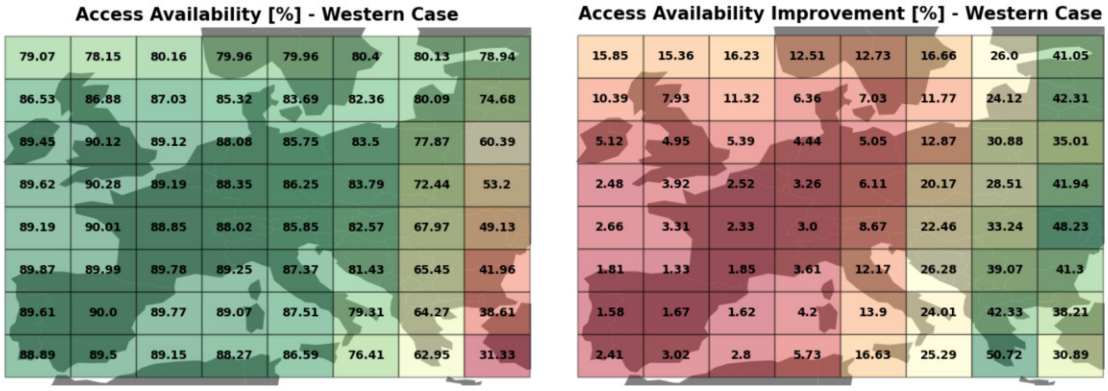

(a) Access Availability with 2 hops OISL.

(b) Improvements in Access Availability from 1 to 2 hops.

Figure 48: Western Network, constellation B. Access Availability with 2 hops (a) and Access Availability Improvement due to the introduction of 1 additional hop (b).

Increasing the hop number improved the performance of the network, especially in the area where it was under performing. However, managing this huge number of accesses leads to chain access databases that are almost three times larger than in the single hop case, with all the negative implications of longer computational time and higher mission complexity and cost. So the second method, that is a flexible OISL geometry, has been implemented.
The basic motivation is that, in the previously tested OISL geometry, some of the satellites in the hop are not covering any target, or they create short accesses. It is visible from figure 28(b) how 2 of the 4 satellites in the hop are outside of the European region, and also in the middle of the sea. In figure 47 the number of 'useless' satellites increases significantly. This is also the reason why the previously tested networks can achieve 99% availabilities in the central area pretty easily, but they all struggle at higher latitudes, where the OISL geometry is not favorable.

9.1 Logic of the tool

The tool aims at using a 'flexible' geometry, meaning that the central satellite is not forced to link with the same 4 satellites every time, but it can select, among the satellites within the link range constraint, the best ones to connect with based on the following criteria:

- **Target coverage**: the satellites in the hop should cover the highest number of targets possible during the entire chain. This excludes the satellites that are outside of the Europe area during the majority of the uplink window, limiting the number of useless links and trying to increase the target coverage.
- **Target weight**: as already discussed in the network optimization section, not all targets should be treated equally, since some of them are in the middle of the sea or in low populated areas, while others can be in extremely densely populated areas. A similar configurable weight system is therefore implemented.
- **Chain duration**: the duration of the resulting chain, which in this case will be *OGS - CENTRAL SATELLITE - HOP SATELLITE - TARGET*, should be as long as possible. Between a satellite that covers a lot of targets for only few seconds and a satellite that covers less targets, but for way longer, the second will lead to better performance.

- **Overlap control**: if two satellites in the same hop cover the same targets in the same time window, one of them is practically useless, and so should be excluded from the hop in favour of another one. This should increase the overall uptime and thus the network's performance.

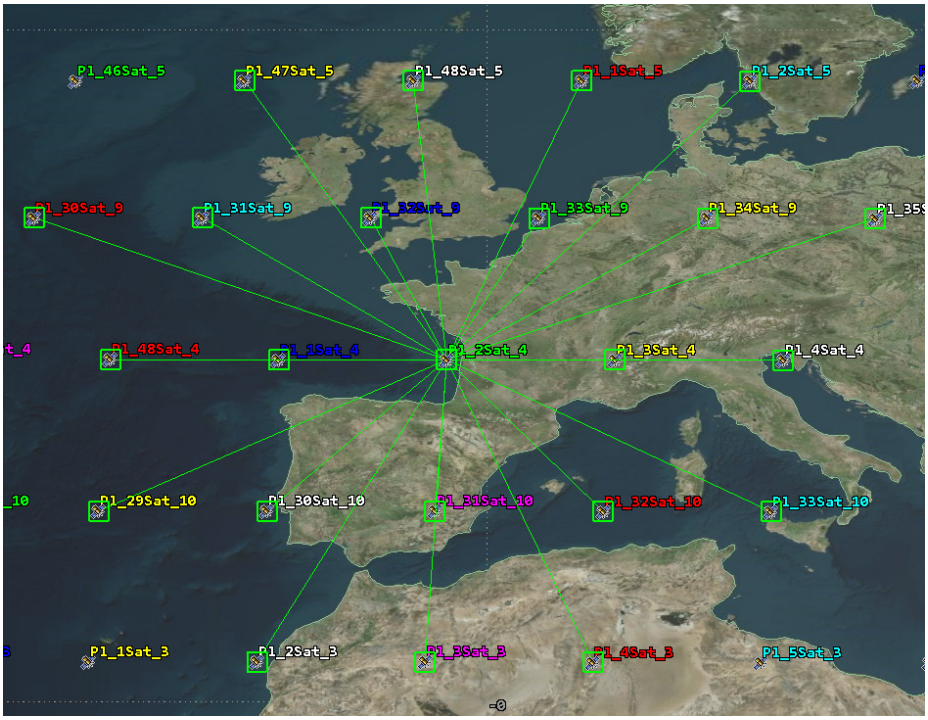

Figure 49: Constellation B. Satellites in the range of 1796km from the central satellite (Pl_2Sat_4) and thus satellites available for flexible OISL.

The range constraint for constellation A is set to 3923 km, while for constellation B is set to 1796km, which are the aforementioned distances between the central satellites and its leading and following satellites on the same plane. In figure 49 we can see all the satellites that satisfy the range constraint and thus can be selected for an OISL. Since the choice is pretty wide, a scoring system was created, based on the combined performance of each satellite in the target coverage and chain duration, taking into account the accesses overlaps. In particular:

- Targets weight: a weight of 1 is attributed to the targets located in densely populated regions, 0.8 in mid populated regions, 0.4 for those in low populated ones and only 0.1 for those located in un-populated areas.
- For every satellite, the total number of target covered during the chain access is computed, and then multiplied by 0.3.
- A minimum target variance and a maximum allowed overlap duration are established and fixed to respectively 30 and 50%. This means that the satellites in the hop are expected to reach a wide variety of targets, instead of the same targets over and over, and the total overlap duration is limited to 50% of the chain access duration.

The satellites within range are given a score based on their target coverage and chain duration, and then out of those only 4 are selected based on the minimum target variance and maximum allowed overlap parameters. In case, with the maximum overlap parameter set to 50%, a full hop of 5 satellites cannot be formed, the selection is repeated but with a threshold value 10% lower and so on, until the value becomes eventually 0%.
An important caveat is that in this first implementation possible constraints on optical payload allocations were not considered: this means that in this simulation the laser terminals responsible for the OISL are able to reach every satellite within range, independently on its position. Of course in a real implementation the terminals will have a fixed position and so they have a limited visibility cone and cannot access satellites which are in the opposite direction of the one where they point.

9.2 Flexible OISL Implementation

The first step for the flexible OISL implementation was to obtain information on which satellites are within range at any given time and for how long. Given the fact that the simulation period is 1 year, and the number of satellites is 288 for constellation A and 1152 for constellation B, computing this for every satellite and for the entire simulation time would be extremely long and inefficient. A better approach is to exploit the symmetry of the constellations to derive some important trends that can be extended to all the satellites in the constellation. To do so, STK was used again to impose the range constraint on a few satellites per constellation, obtain their access reports and confront them to find the trends that will simplify the postprocessing analysis.
After the analysis of few reports, the following conclusions were found:

- Every satellite has access to only a limited number of satellites in the constellation, those within the range constraint, and they are the same throughout the entire simulation. The satellites within possible range can be identified and a scheme can be made and extended to all the satellites of the constellation. In this way, from a single report it is possible to build hops for the entire constellation.

- Within the aforementioned accessible satellites, only few of them are accessible at any moment, like the twins satellites in the adjacent planes and the leading and following satellites on the same plane. The majority of the accessible satellites have 'access windows' of fixed duration, that depends on their orbital position with respect to the central satellite. The further the satellite, the smaller the access duration, and vice-versa. These satellites will enter and exit from the ISL range, making the creation of the hop more complicated.

- The accesses of the non always accessible satellites are separated by a fixed interval of time, equal to almost half the orbital period T:

$$T = \sqrt{4 \cdot \pi^2 \cdot a^3/u} \tag{4}$$

  For constellation A, with an altitude of 1200km, this equals to a period of around 109 minutes and thus an access period of around 54 minutes. For constellation B, with an altitude of 500km, this equals to a period of around 95 minutes and thus an access period of around 47 minutes.

- Given the access schedule of the first satellite of a plane, the access schedule of the N_{th} satellite in that same plane is the same but scaled by $(SAT_N - 1) \cdot \frac{T}{12}$ for constellation A and $(SAT_N - 1) \cdot \frac{T}{24}$ for constellation B.

These findings were used to write a Python script able to extract the data from the STK access report of the Satellite 1 in Plane 1 of both constellations and create a table, called Access.csv, that can be used to derive the satellites in the hop of any given central satellite at any given moment, with their duration and starting time. At this point, the main script is used to create the Chain DB, applying the same structural logic of the previously described OISL script, but with a difference in the hops creation methodology.
The hops generator method takes as input the central satellite, the constellation id, the number of hops and the uplink window, and returns a list containing the satellites in the hop of the central satellite in that given time window. To each uplink window a group is associated, since later in the script a comparison between these satellites will be done in order to select 4 of them, and a unique group identifier is needed to retrieve them from the numerous accesses produced by that central satellites across the simulation time. The function adds automatically the satellites always within range and for every other satellite checks if there is an overlap between the access window and the uplink window, and in the positive case that satellite is added as well. Since at the moment of the start of the simulation some of the periodic accessible satellites have an ongoing access with the central satellite, the script takes that into account and looks for the real start of those accesses. Considering that the Access.csv database only contains the access duration and the first access time start, in order to look for an overlap the first access is propagated until the end of the uplink window. After this, the script goes on performing the SQL query and returning a DB containing all the possible accesses. In the next phase, out of all the accesses of a group, only the accesses of the 5 satellites in the hop are selected. In this way, multiple chain DBs are produced, which are later concatenated to form the final Chain DB for that specific OGS. Figure 50 shows the flowchart of the entire flexible OISL tool, with a focus on the hops generator method.

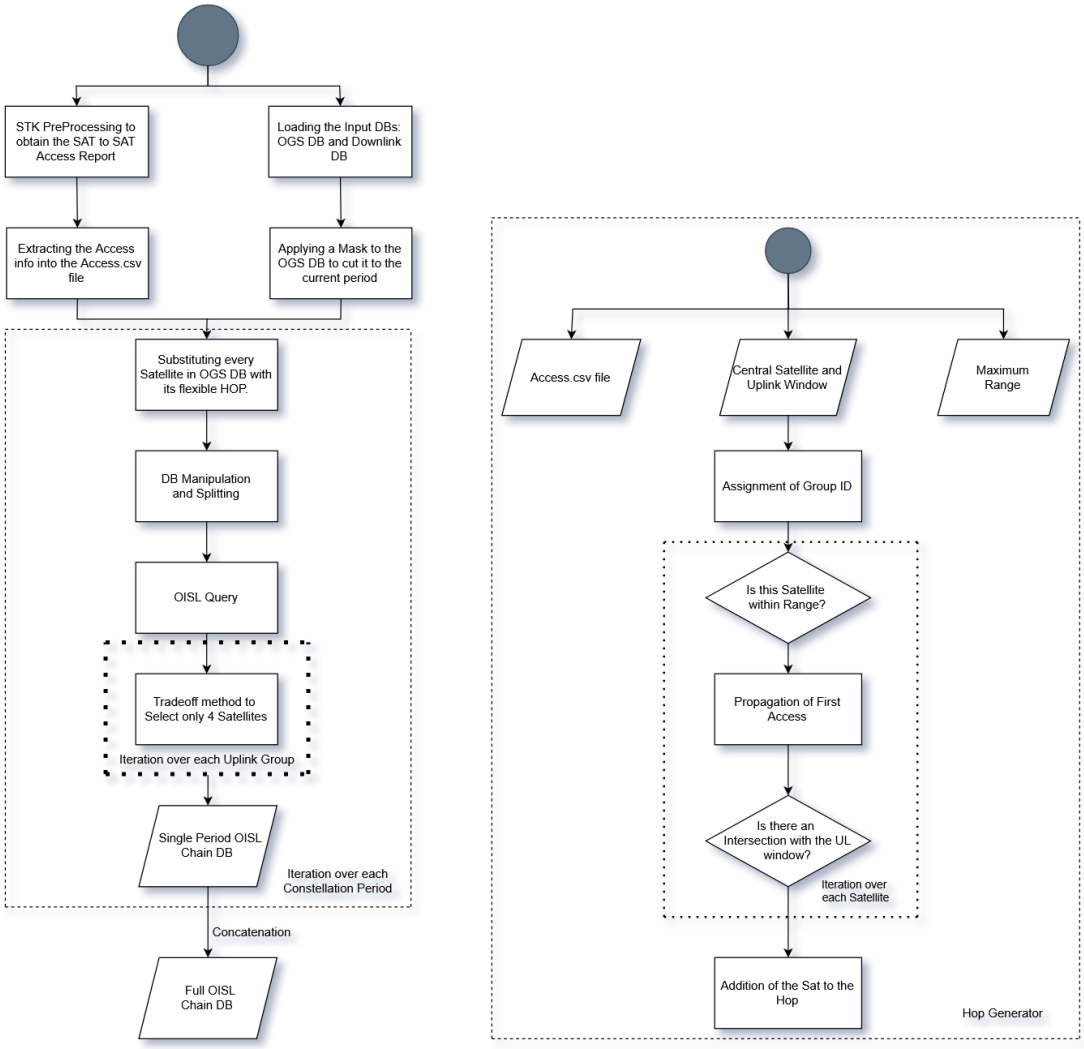

Figure 50: Flowchart of the Flexible OISL Tool. The dashed figure encloses the main iteration while the dotted figure encloses the secondary iteration.

On the left chart the dashed shape encloses the for loop on the constellation periods, while the dotted shape encloses the for loop on each uplink group to select 4 satellites out of all the possible candidates. On the right chart, the dotted shape represents the iteration over all the satellites in the current constellation period.
In order to find the best 4 satellites to include in the hop, the *trade-off OISL* method is called on the group sub-database. Based on the already explained selection logic, the trade-off method is used to draw up a ranking of the accessible satellites, called tradeoff_list, from which 4 satellites are extracted by the *find best sats* method.
Usually the 4 winning satellites are found without problems, but it can happen, although very seldom, that the script is not able to return a full hop of 5 satellites since the trade-off list itself can

contain less than 4 satellites. The reason is because this trade-off selection is done after the SQL query, and so it can be that the majority of the accessible satellites are outside of the Europe target area, and thus are not included in the group DB. In this case, a smaller hop is returned. To attribute a score to the satellites the *score sat* method is called. This method is simply the implementation of the logic already described; the satellites are evaluated based on the number of targets that they access, their quality and the resulted access durations. The final product is a dictionary that will be inserted in the trade-off list.
To select the winning satellites that will form the hop, the *find best sat* method is used upon the trade-off list, with an additional variable parameter given by the maximum overlap percentage which, as already stated, can eventually be increased in case the number of 4 satellites is not reached at the first iteration.
If the minimum target variance parameter is satisfied, the satellite is immediately added to the winning lists. In case this does not happen, the overlap is checked and the satellite is addded to the winning list only if the total overlap due to its addition is below the limit currently set. Out of the winning list, the top 4 satellites (or all the satellites, in case is was not possible to select 4 or more candidates) are selected and the final hop is created. All the accesses of the discarded satellites are removed from the database. In figure 51 the flowchart of the trade-off tool with a zoom on the *find best satellite* method is showed.

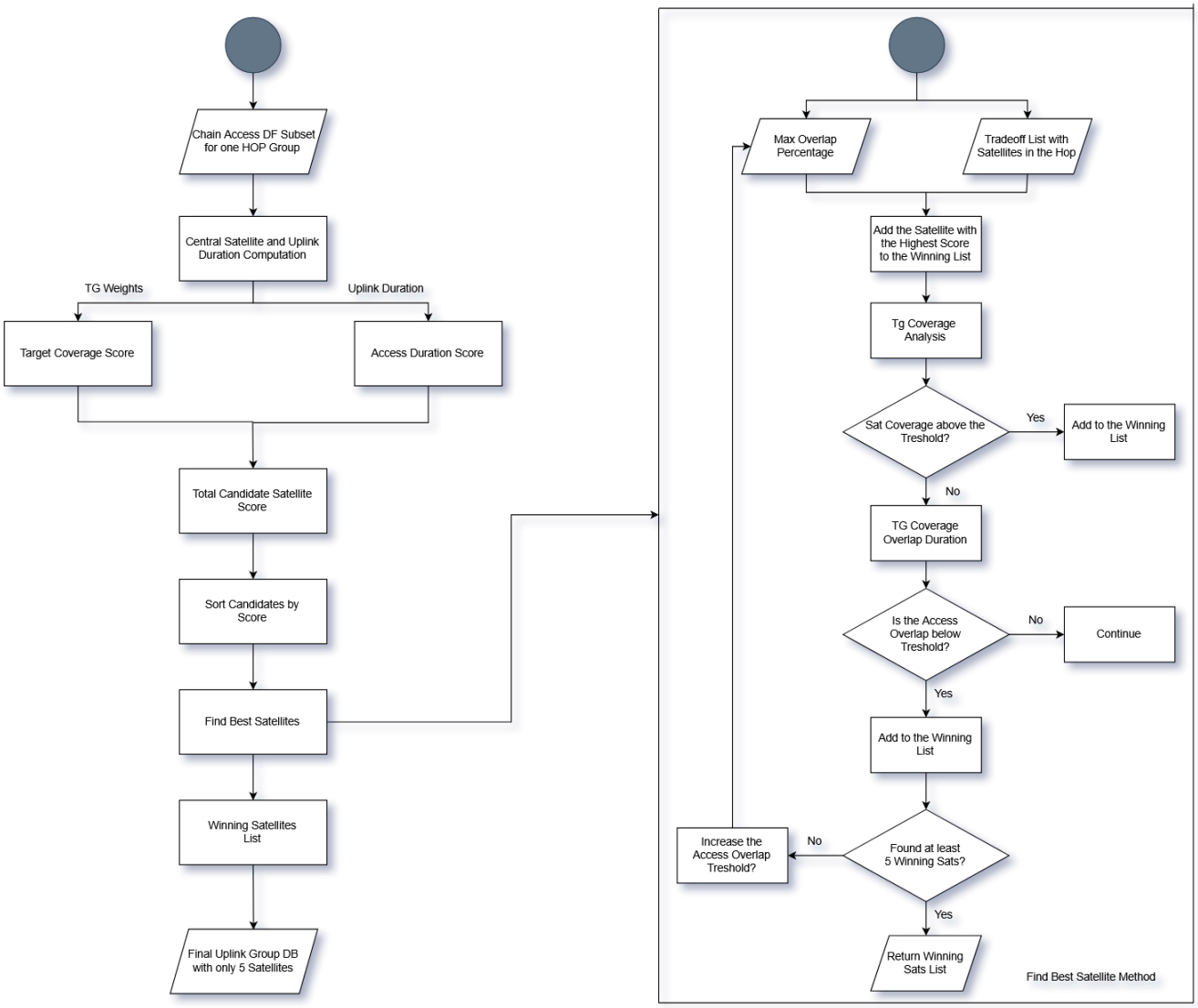

Figure 51: Flowchart of the *trade-off* tool to select the satellites to include in the hop of a specific Uplink group. On the right, the logic to find the 4 best satellites out of all the candidates satellites is represented. The procedure is iterated over each satellite in the candidate list.

9.3 Results of the tool

The Flexible OISL tool was initially tested on constellation A, on the original 8 networks of 5 OGSs.

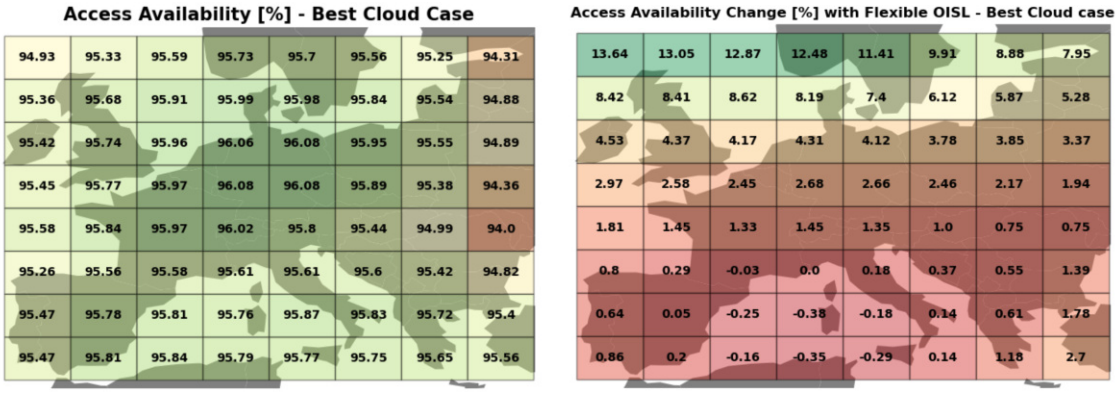

(a) Access Availability Percentage.

(b) Access Availability Improvement.

Figure 52: Constellation A, Best Cloud Network. Access Availability Percentage with flexible OISL (a) and Percentage Improvement in Access Availability from Classical OISL geometry to Flexible OISL geometry (b).

In figure 52 the Access Availability plot and the improvement plot from classical OISL geometry to this flexible OISL geometry are shown for the Best Cloud network. As can be seen, the implementation of flexible OISL made the entire network more homogeneous in terms of access availability, improving significantly the performance at higher latitudes, previous weak points of the Best Cloud network, and only slightly the already strong target areas. It can be seen that in a limited number of targets the access availability slightly decreased, but they are lower weight targets, so this decrease is completely aligned with the logic of the tool.
In the next phase bigger networks were tested using the NO tool, in order to see if this flexible geometry can produce an operable network even with less than 11 OGSs. The results are surprising, since all networks experienced significant improvements in their availability and overall scores, but really interesting is the 9 OGSs case.

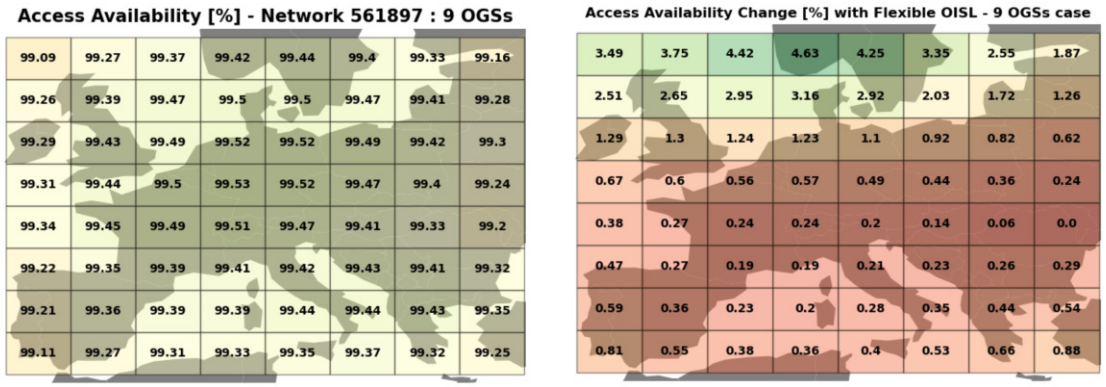

(a) Access Availability Percentage.

(b) Access Availability Improvement.

Figure 53: Constellation A, 9 OGSs. Access Availability Percentage with flexible OISL (a) and Percentage Improvement in Access Availability from Classical OISL geometry to Flexible OISL geometry (b).

In figure 53 the Access Availability plot and the improvement plot from classical OISL geometry to this flexible OISL geometry are shown for the most performing network of 9 OGSs already identified by the network optimization tool. This network had already a good performance with the classical OISL geometry, as can be seen from figure 38. However, the access availability percentage has a non-homogeneous distribution and displays values above 99% for low weights targets, while some of the most important targets don't reach this value. Also, the typical low performance at high latitudes and at the borders of the Europe target map is present. In the new flexible OISL version this network becomes operable, producing availabilities equal or above 99% on every single target.
Increasing again the number of OGSs leads to further increments in performance. The most performing network of 10 OGSs identified by the network optimization tool was tested, and the results are shown in figure 54.

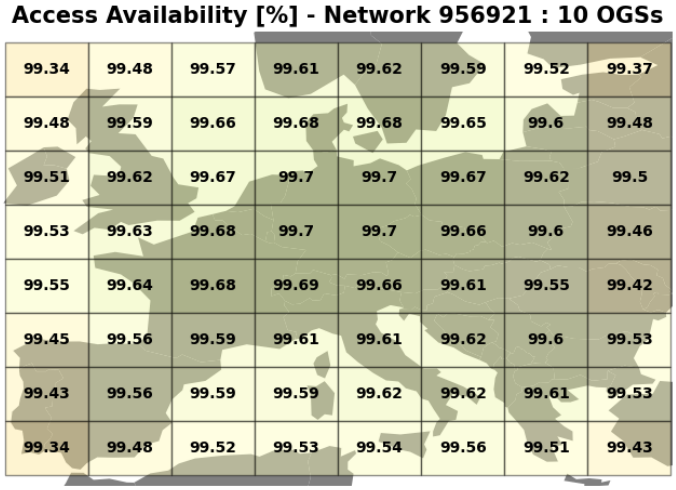

Figure 54: Constellation A. Access Availability percentage of the most performing network of 10 OGSs with Flexible OISL.

The access availabilities percentages oscillate between a minimum of 99.34%, for the low weighted targets, and 99.7%, for the high weighted targets.
Moving on to constellation B, since this constellation showed more weak areas than constellation A, especially in eastern Europe, it was decided to apply more aggressive weights to the targets in order to gain accesses at higher latitudes and higher longitudes.

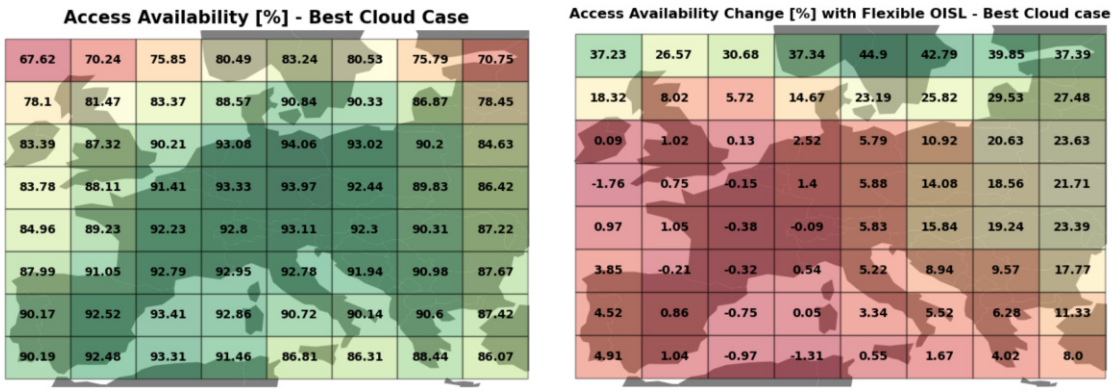

(a) Access Availability Percentage.

(b) Access Availability Improvement.

Figure 55: Constellation B, Best Cloud Network. Access Availability Percentage with flexible OISL (a) and Percentage Improvement in Access Availability from Classical OISL geometry to Flexible OISL geometry (b).

In figure 55 the Access Availability plot and the improvement plot from classical OISL geometry to this flexible OISL geometry are shown for the Best Cloud network. The first thing to notice is the substantial performance increase at higher latitudes and in eastern Europe, which were previous weak points of this particular network with a classical OISL geometry. We can see improvements up to 44% at high latitudes and from around 2 to around 24% in the most populated areas. Some low population density targets experience a decrease in availability, but this is to be expected, since those accesses have been 'redirected' to other targets with higher weight. The same trend repeats with bigger networks as well, with the situation for the best network of 16 OGSs previously identified showed in figure 56

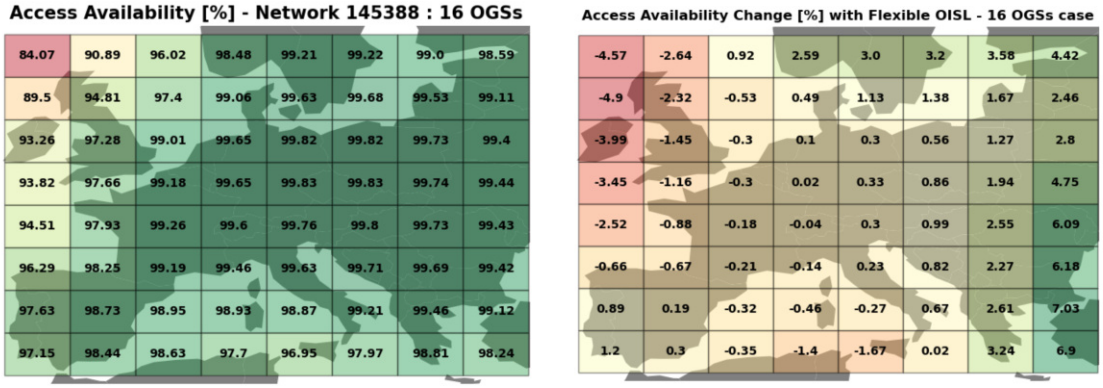

(a) Access Availability Percentage.

(b) Access Availability Improvement.

Figure 56: Constellation B, Best 16 OGSs Network. Access Availability Percentage with flexible OISL (a) and Percentage Improvement in Access Availability from Classical OISL geometry to Flexible OISL geometry (b).

Of particular interest is the best 15 OGSs network, showed in figure 57.

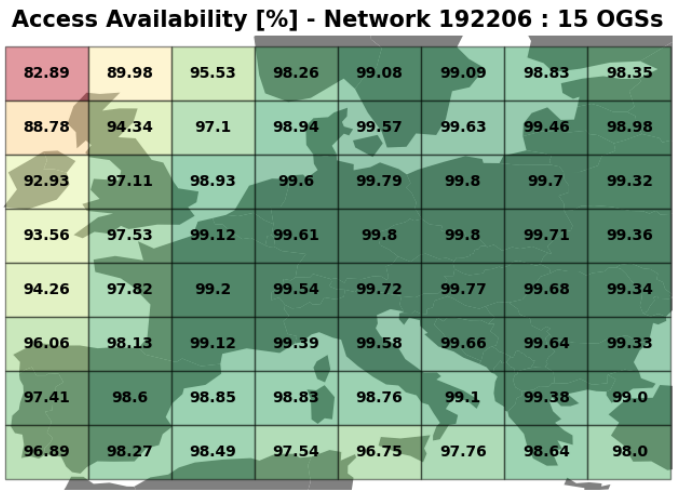

Figure 57: Constellation B. Access Availability percentage of the most performing network of 16 OGSs with Flexible OISL.

This network is indeed performing really well for the majority of the targets, and especially well for the most important targets, for which the access availability percentage reaches values up to 99.8%.

9.4 General Conclusions

Having analyzed the results of the flexible OISL tool, the following conclusions can be drawn:

- The implementation of a smarter flexible OISL geometry improved the performance of the networks in all cases. This is due to the possibility of selecting the satellites to include in the hop based on their target coverage performance, allowing the most important targets to reach higher access availability percentages.
- For constellation A the results are more homogeneous, with all the targets showing similar availability values, even at higher latitudes. On the other hand, for constellation B, the results are still pretty heterogeneous, with significant differences between the targets in densely populated areas close to the OGSs of the network, which show the highest availability percentages, and the targets located in sparsely populated areas and at the borders of the European area, which show the lowest availability percentages. The reason is once again the difference in altitude between the two constellations, which makes the satellites of Small LEO to span wider visibility cones on the European map, allowing for a larger decoupling between the geographical location of the OGSs and the position of the targets.
- This logic, although more complicated, would allow to reduce the number of OGSs required to have an operable network. Indeed, for constellation A this number would reduce from 11 to

9, while for constellation B 15 OGSs network would perform similarly to the 24 OGSs upper limit case.

- The best networks with flexible OISL coincide with the ones with classic OISL geometry identified by network optimization tool, as a further confirmation that the NO tool is able to pick the best OGSs networks independently on the OISL logic implemented. It is to be said, however, that a smaller number of networks have been tested since the chain DBs are larger, so it is possible that some small difference would appear after testing a larger number of networks.

This implementation of the tool is simply to be intended as a demonstration of the efficiency and potential of such a flexible OISL geometry since, as already said, no constraints on optical laser terminals allocation were considered. With such implementation, the performance of the networks is expected to decrease, but probably only by a limited amount. To find out how this OISL logic would perform in a more realistic situation, the constraints on payload allocation were implemented and tested. The results are presented in the following section.

9.5 Flexible OISL: Constraints on Payload Allocation

The implementation of a flexible OISL geometry, in which the central satellite is able to potentially link with every satellite within range, has been shown to lead to a significant increase in the performance of the networks, resulting to access availability percentages above 99% for all the targets located in densely populated areas while, at the same time, managing the higher latitudes way better than how a classical geometry could do. However, in the previously explored results, the physical disposition of the optical terminals hasn't been taken into account, making those results unrealistic. Indeed, the location of the terminals one a satellite is fixed and usually the payloads are located each on a different deck of the spacecraft. With the classical cross-like ISL geometry this requirement is by default satisfied, since the central satellite will be linked with the leading and following satellites on the same plane, via the two terminals located at its 'front' and 'back', and with the twins satellites on the adjacent planes, via the two terminals located on the opposite sides of the satellite.

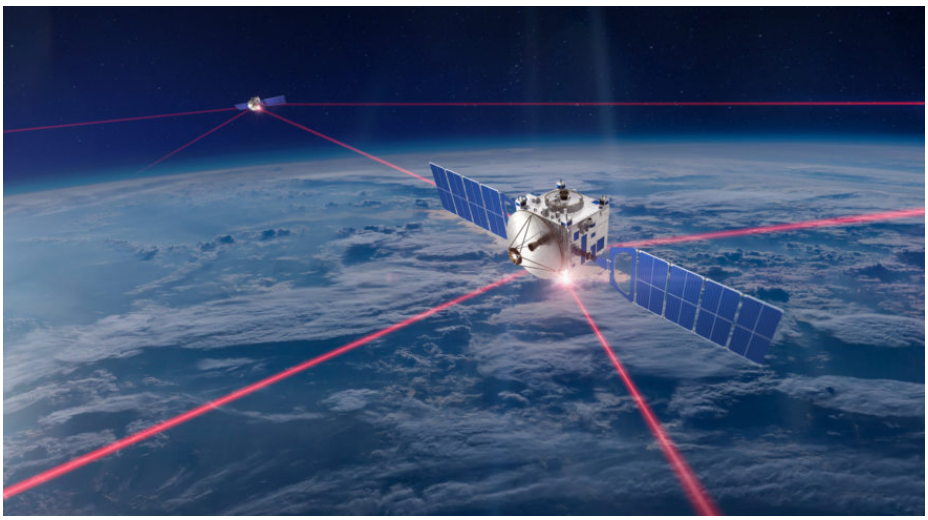

Figure 58: Artistic representation of two satellites linked via the classic OISL geometry [45].

Figure 58 shows a schematic representation of such situation. Those satellites are always within range constraint, so the resulting links are as stable as possible since they can be constantly maintained. With the flexible geometry the situation gets more complicated since the ISLs can be established also with satellites that are not always within range and not always visible from the same deck for the entire uplink duration. Also, the central satellite might be linked with multiple satellites visible only from one or two decks, a circumstance that implies all the terminals to be mounted on those two sides, which is a condition to be excluded from the simulation. We can imagine the terminals as antennas mounted on the spacecraft, with a specific visibility cone; only one of the satellites within the visibility cone can be connected with the central satellite by that terminal, meaning that the selection of the 4 satellites to link with must be divided into 4 sub selections, one for each deck.

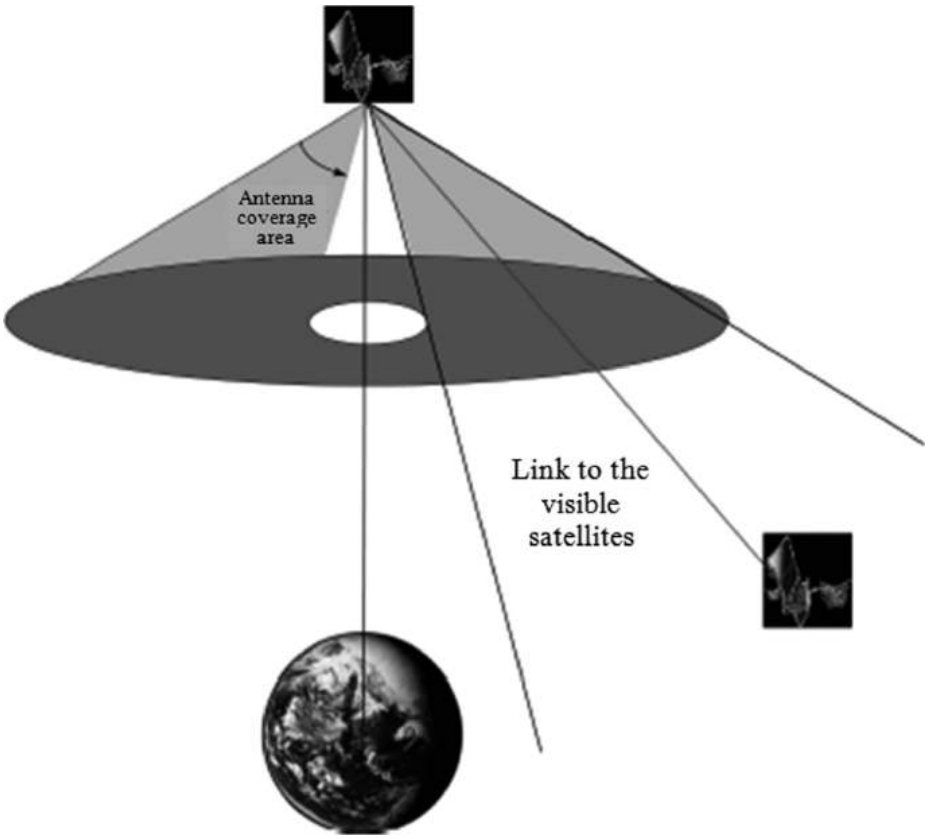

Figure 59: Projected visibility cone of an optical terminal for ISL. Only a satellite within visibility can be connected to the central satellite using that terminal [33].

Figure 59 shows the projected visibility cone of a terminal mounted on one deck. In the represented case that terminal will be used to link with that satellite, and so all the other satellites within the cone cannot be used to perform ISL. A logical implication of this physical constraint is that if the central satellite is flying over, let's say, Spain, the majority of the satellites within range will be visible from only one or two decks, while the remaining decks will include satellites that are outside of the Europe target area, leading to an incomplete hop of only three satellites instead of five. A decrease in performance over such areas is then expected. On the other hand, if a satellite is flying over central Europe, we don't expect a significant decrease in availability performance; indeed, due to the logic of the flexible OISL tool of selecting the satellites in order to guarantee the maximum target coverage with the minimum access overlap, the 4 satellites in the hop will probably be visible each from a different terminal, satisfying the payload allocation requirement.

9.6 Logic and Implementation of the tool

The logic of the tool is the same as in the first version of the flexible OISL tool, with their target coverage, target weight, chain duration and access overlap. The satellites are given a score based on these criteria and only the accesses of the four resulting 'winning' satellites will be considered in the availability analysis. The main difference is in the constraints that a satellite must satisfy in order

to be included in the list of possible candidates:

- The satellite must be within the range constraint for the entire duration of the uplink.
- The central satellite can link with a maximum of four satellites that must be connected to four different terminals, located on the four sides of the central satellite.
- Each terminal is mounted on a deck and it has a visibility cone of 180 degrees. In terms of altitude and azimuth, the terminal spans altitudes from -90 to 90 degrees and an azimuth range of 180 degrees, with the start and finish angles that depend on the deck on which the terminal is mounted.
- In order for a satellite to be considered as visible from a deck, it must stay within its visibility for at least 80% of the uplink duration. No switch between terminals is allowed.

To conduct the analysis an additional access report is needed: the AER (Azimuth, Elevation, Range) report, which shows the accesses of a given central satellite to all the satellites within range, not only in terms of distance but also in terms of azimuth and elevation. This type of report can be created using STK's report manager (see figure 13) and it has a time step of one minute. Before computing the AER report it is necessary to understand STK's default reference frame, since the 4 payloads will cover 4 different azimuth ranges depending on where they are mounted. In order to acknowledge this, a scenario with only two satellites has been created and the AER report has been computed. The velocity vector was introduced in the visualisation and from the joint analysis of the report and the 3d graphic window it was possible to establish the direction of pointing of the velocity vector.

(a) Azimuth angle close to 360 degrees.

(b) Azimuth angle close to 180 degrees.

Figure 60: AER access of a random satellite and a central satellite, showed with its velocity vector. In (a) the azimuth between the velocity vector the linked satellite is close to 360 degrees, while in (b) is close to 180 degrees, highlighting the default Eastern orientation of STK.

From the simple simulation analysis of figure 60 it emerges that the velocity vector is pointing toward East and identifies the east deck. Based on this, the satellite in figure 61 results to be visible from both the East and North terminals, but not from the West and South ones.

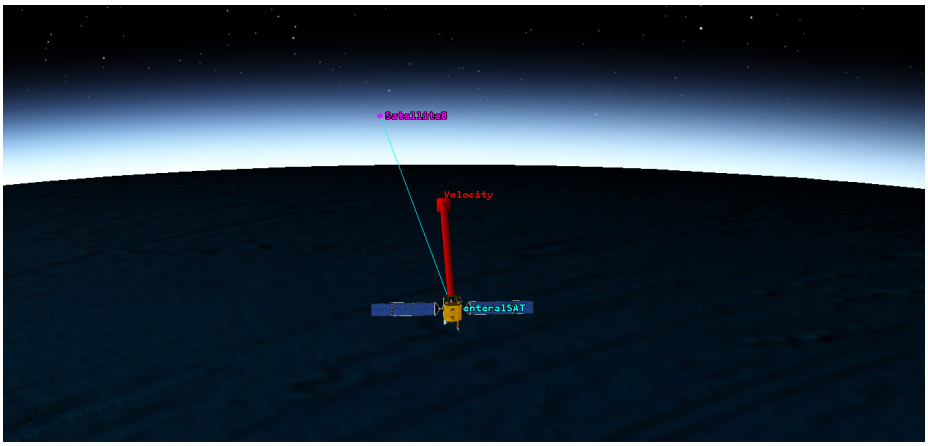

Figure 61: Satellite 8 visible from the Eastern and Northern decks.

The four payloads have been introduced in the configuration file with their specific ID and azimuth range. From the analysis of the report it emerged that the satellites within range are always in an elevation range between -15 and 15 degrees, so the elevation requirement is therefore always satisfied. Table 8 summarized the implementation of the terminals.

Table 8: ISL Terminals implementation.

Deck name	**ID**	**Minimum Azimuth**	**Maximum Azimuth**
East Deck 1	0	270	360
East Deck 2	0	0	90
West Deck	1	90	270
North Deck	2	180	360
South Deck	3	0	180

As for the previous version of the tool, a sample AER access with 1 day length for satellite 1 of plane 1 has been obtained and the information contained have been extracted and cleaned into a .csv file. This file will be read by the main script to get the terminal's visibility information of each candidate satellite. Within the access period of a satellite, i.e. the time interval in which that satellite is within the range of the central satellite, it enters and exits from the visibility cones of the different terminals. For example, at the beginning of the access it can be visible from the East and North decks, but then few minutes later is will be visible only from the North and West decks, making the identification of the deck's visibility along the simulation more complicated. However, thanks to the symmetrical properties of the orbits, a regularity and periodicity in the deck's visibility can be identified; for each satellite there are two different visibility groups which are one the mirror of the other. This means that if a satellite is visible from the North deck for a specific interval of time, in the second group it will be visible from the South deck in the same interval of time. An example is showed in table 9, where we can see that this symmetry is applied only for the lateral decks, not from the East and West decks.

Table 9: Example rows from the AER .csv file. The indexes in parenthesis represents the start and end minutes of the visibility per deck. A value of -1 means indicates that the visibility extends until the end of the access, while for a satellite outside range the indexes will be both 0.

Sat ID	**Group 1**	**Group 2**
Sat 9 Pl 9	E: [0:6] W: [7:-1] N: [4:-1] S: [0:3]	E: [0:6] W: [7:-1] N: [0:3] S: [4:-1]
Sat 9 Pl 10	E: [0:6] W: [7:-1] N: [0:7] S: [-1:-1]	E: [0:6] W: [7:-1] N: [-1:-1] S: [0:7]
Sat 9 Pl 11	E: [0:0] W: [0:0] N: [0:0] S: [0:0]	E: [0:0] W: [0:0] N: [0:0] S: [0:0]

These two groups are separated by the same access period previously identified, almost equal to half the orbital period of a satellite within the constellation.
The algorithms of the tool are the same as in the previous version, with the algorithm that identifies the candidate satellites, the one that scores them and the one that picks the best four. However, every candidate must now carry the deck's visibility information, meaning that each candidate should go through a method to find the deck's visibility. As already stated, a satellite is considered to be visible from a deck only if it is visible from that deck for at least 80% of the central satellite - hop satellite access duration, which coincides with the uplink duration, since only the candidates within range for the entire uplink duration are selected.

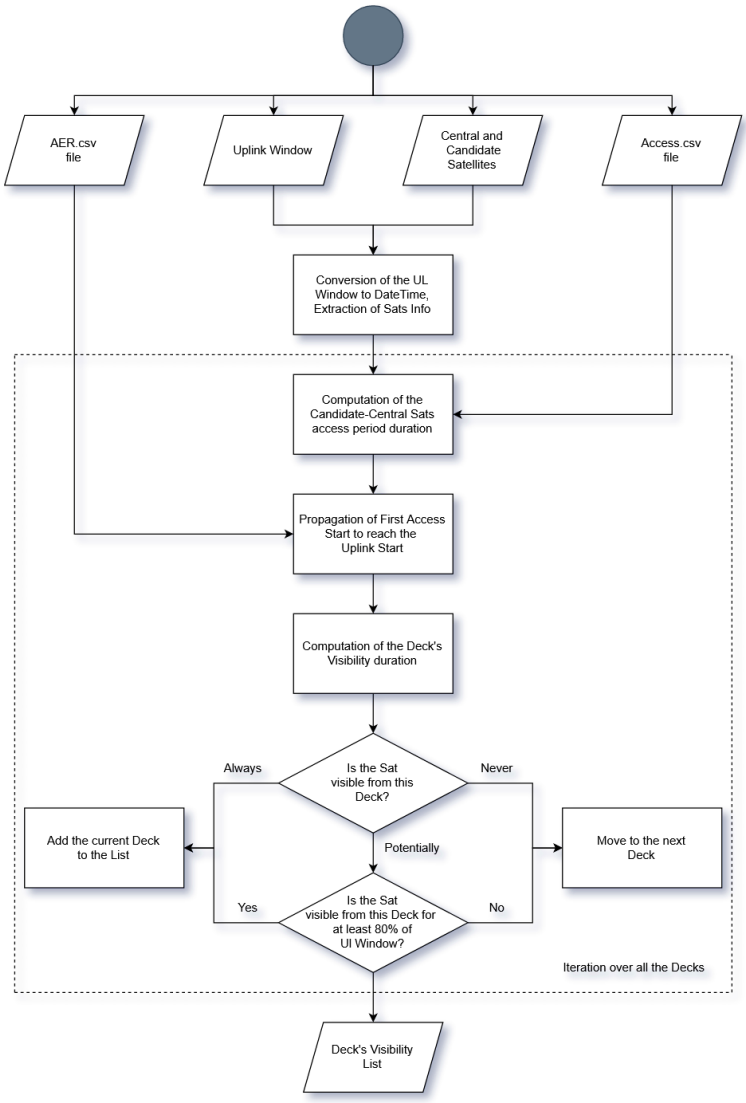

Figure 62: Flowchart of the Find Deck algorithm. The dashed figure represents the iteration over each deck.

The flowchart of the method used to find the deck's visibility is showed in figure 62.
Furthermore, the four winning satellites must be assigned to four different terminals, and so the method to find the best candidates has been modified in order to take this into account. Indeed, starting from the top of the ranking, the decks visibility of the satellite is taken into account and added to a list; if the next satellites in the ranking are visible from the same deck, they will be neglected, until the algorithm will found the first satellite visible from a different deck, and will add it to the list. This procedure will occur until all 4 decks are taken. If a satellite has a double visibility, meaning that it can be visible for more then one deck for at least 80% of the uplink duration, then the first deck will be considered as taken, but the second deck will count as a 'bonus deck'; if the

algorithm finds a satellite visible from the first deck of the two, i.e the one currently in the list, then the second one, i.e the one considered as bonus, will be added to the list, to mean that the first satellite added will be connected with the bonus deck, and the new satellite can added to the winning list as connected to its normal deck. In the end, the central satellite will have a hop of maximum 4 satellites, each connected to a different terminal and in range for the entire duration of the uplink. In figure 63 the flowchart of the flexible OISL tool with constraints is showed.

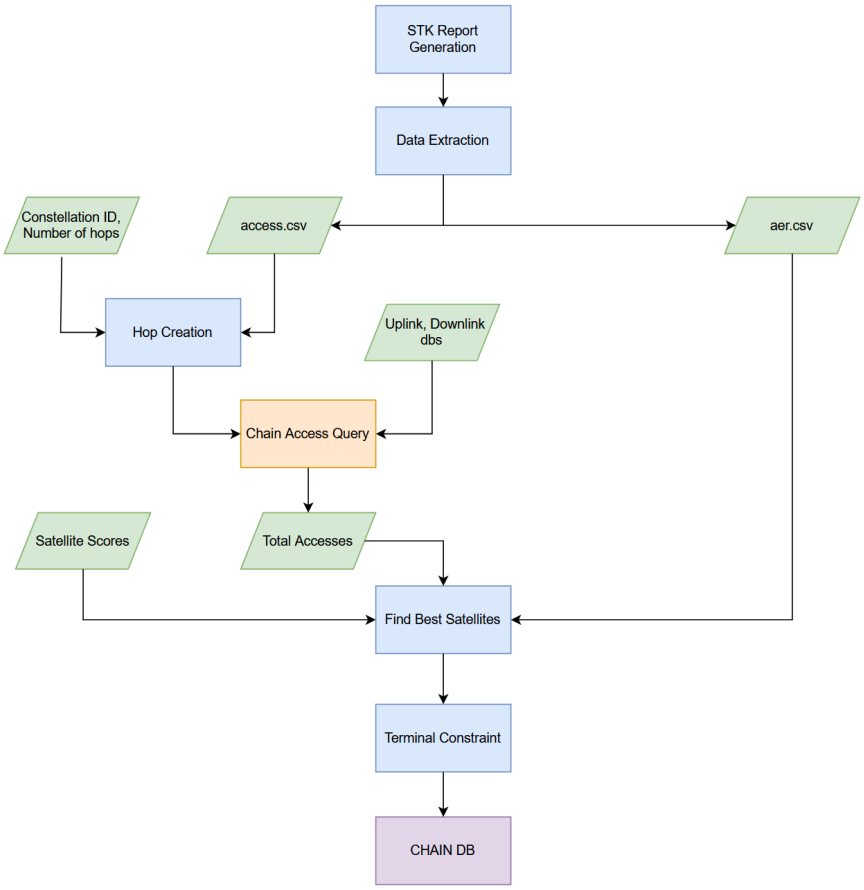

Figure 63: Flowchart of the Flexible OISL Tool with payload constraints.

9.7 Results of the tool

The new version of the tool has been tested on the 8 original networks of 5 OGSs each. Since at this point it appears evident that constellation A is the most interesting one, the results will be presented only for this constellation. The expected output is a general decrease in access availability performance with respect to the previous version of the tool, especially at the borders of the Europe target area, where a satellite linked with an OGS will have one or two terminals unused, since the satellites visible from them will be outside of the target area. As already stated, the decrease of performance in the central area is expected to be pretty limited, since a satellite flying over middle Europe will easily find itself linked with 4 satellites using all its terminals. These expectations were

indeed confirmed in all the networks, as we can see in figure 64, in which the Best Cloud network is taken as an example.

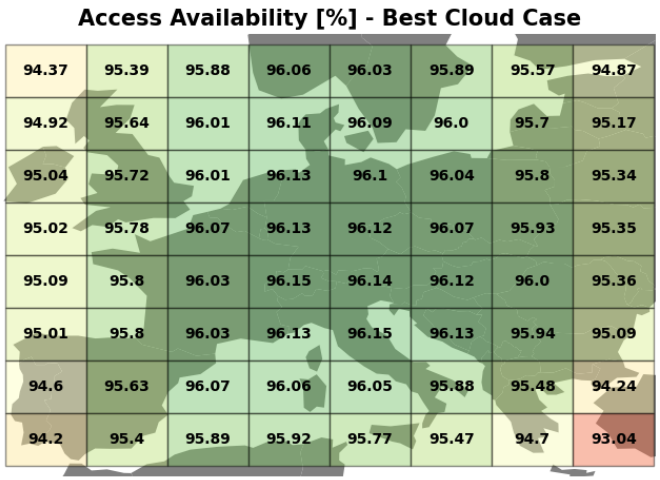

(a) Access Availability percentage.

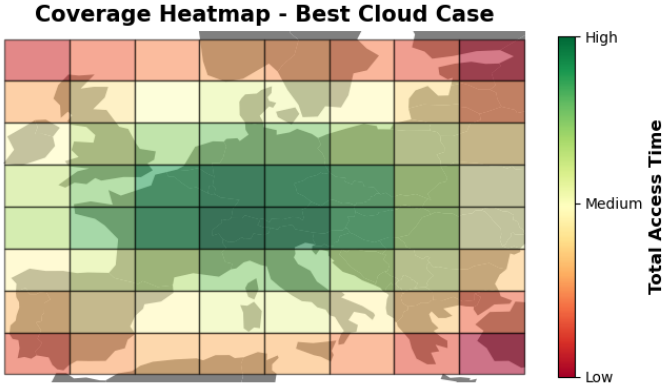

(b) Coverage Heatmap.

Figure 64: Access Availability percentage (a) and Coverage Heatmap (b) for the Best Cloud network in constellation A, with Flexible OISL and constraints on payload allocation.

Looking at the HM it is clearly evident how the majority of the accesses are in middle Europe, while the corners of the target area have a lower access density. It is interesting to confront this HM with the one of figure 20, which is the HM of the same network but without OISL. The largest density of accesses is not anymore in middle Europe but over the south-western area of Europe, the exact opposite of what we see in figure 64.

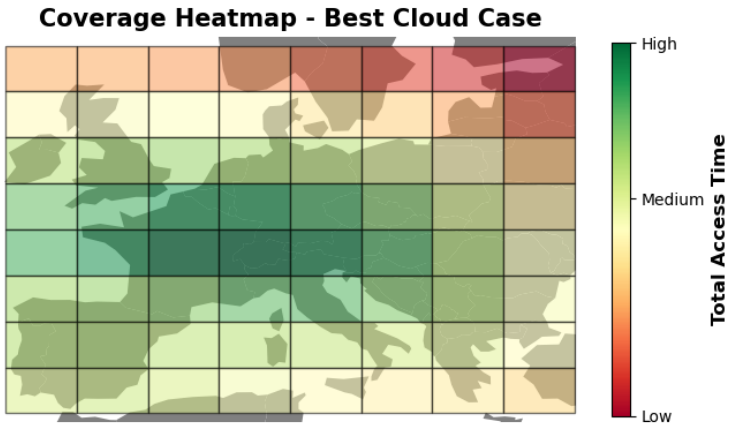

Figure 65: HeatMap for the Best Cloud network in constellation A, with flexible OISL but without constraints on payload allocation.

This change in access density from the south west to the central area is evident also in the HM of the same network for the previous version of the tool, without terminal allocation constraints, as can be seen from figure 65. The introduction of the constraints simply made this change more significant, since those regions lost even more accesses.

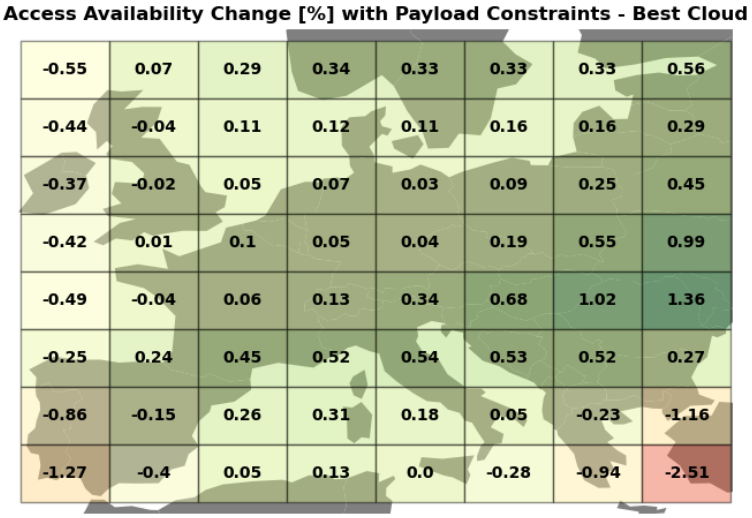

Figure 66: Access Availability percentage change after the introduction of the payload allocation constraint for the Best Cloud network in constellation A.

In figure 66 the access availability percentage change for the best cloud network after the introduction of the constraint is showed. The biggest decrease is located in the Spain area and in the Greece area, since this network hosts OGSs in both areas (Sevilla, Lisbon, Athens and Porto), so those were previously strong points of the network, but since they are located at the borders of the Europe area they experience the largest decrease in coverage and availability. On the other hand, it can be seen a small increase in middle and east Europe, which might seem weird. The reason behind this apparent increase in performance lies in an improved version of the algorithm for satellite selection: the previous version aimed at selecting the 4 best candidate satellites, but when it was not immediately possible to select 4 satellites due to the access overlap and target coverage constraints, this mechanism became less efficient, putting in a second place the score of the satellites trying to reach a full hop. In this version, the algorithm has been improved in order to limit the decrease in performance as much as possible; the goal is still to reach a full hop, but the quality of the satellites in the hop is still taking the first place in the ranking. The result is a slight increase in performance in some areas, which is fictitious since an higher performance would have been reached in the previous version of tool if this improved algorithm was deployed.
Since the main concern here is the gain in performance from a classic OISL geoemtry, figure 67 shows the changes in access availability from the classic OISL geometry to the flexible one with constraints on payload allocation, for the Best Cloud network. The little pentagons are positioned in correspondence of the locations of the OGSs.

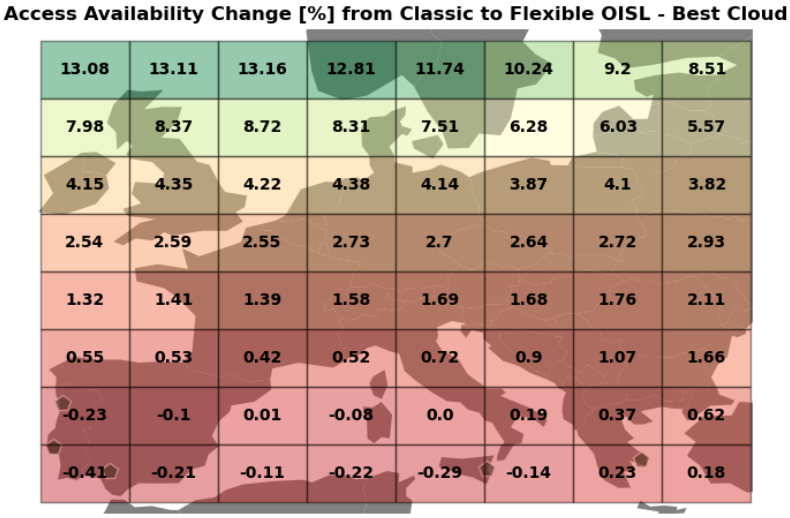

Figure 67: Access Availability improvements for the Best Cloud network in constellation A, from classic OISL to Flexible OISL with payload constraints.

It can be seen how the flexible OISL geometry, despite having implemented constraints on the payload allocation, offers a better performance for all the targets, with the exception of the Spanish area, where small decreases can be seen. The explanation behind this decrease lies in the weights of the targets and the overlap logic of the tool; indeed, a higher weight was attributed to central Europe, meaning that, if the central satellite is flying over that region, instead of picking the backward satellite, which would cover the Spanish area, it picks another satellite that provides a better coverage for other targets and minimizes the access overlap.
Figure 68 shows the Access Availability map of the best 9 OGSs network previously identified along with the changes in access availability from the classic OISL geometry to the flexible one with constraints

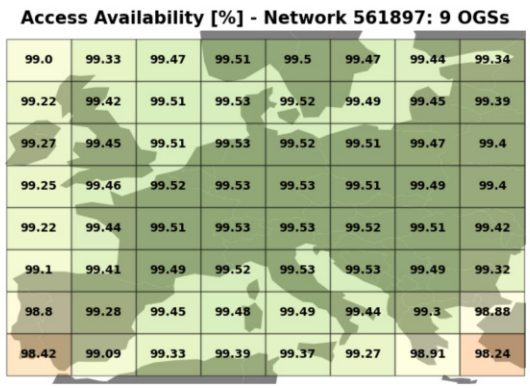

(a) Access Availability Percentage.

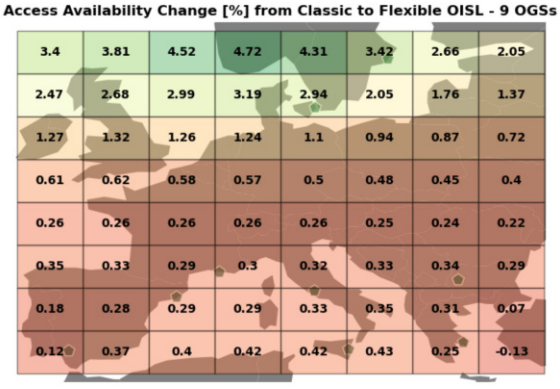

(b) Access Availability Improvement.

Figure 68: Access Availability percentage (a) and Improvements from Classic to Flexible OISL with constraints (b) for the best 9 OGSs network in constellation A.

For this network the improvements are present all over the European area, especially at the higher latitudes. The OGSs are represented by the small pentagons. Having included more OGSs, the Spanish area experienced an improvement, since now the OGSs are more uniformly distributed and only 1 out of 9 is in that area, versus the 3 out of 5 of the Best Cloud network, limiting the total access overlap in that specific region and thus leading to higher performance.
The improvements brought by moving to the classic OISL logic to the flexible one with constraints for the best 11 OGSs network is showed in figure 69.

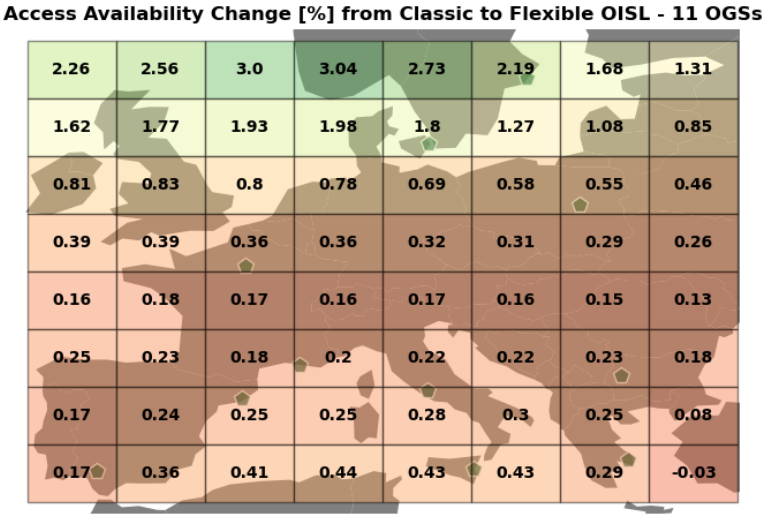

Figure 69: Access Availability improvements for the best 11 OGSs network in constellation A, from classic OISL to Flexible OISL with payload constraints.

The same trend is present also with 11 OGSs, with the only difference that the changes are now more limited, since the availabilities percentages are converging toward 100%.

9.8 General Conclusions

As a general conclusion, it can be said that the flexible OISL logic is a promising tool, able to increase the performance of the constellations by guaranteeing a more homogeneous access availability map and reducing the overall OGS number required to have a network with optimal availability. The introduction of the constraints on payload allocation made the situation more realistic, while at the same time reducing the scores of the network only by a small amount. Being this the first version of the tool, the approximations introduced biased the results in a negative way, since it has been observed that the propagation mechanism used by the hop generator method is sometimes excluding some satellites that, looking at the STK simulation, should be included. It is highly likely that a future version of the tool will lead to better results, as it is discussed in the final section of the thesis. Nonetheless, the results are still encouraging, showing the potential of such flexible logic. Indeed, table 10 shows the average access availability gain per target brought by the flexible OISL tool with payload constraints, as well as the minimum-maximum availability percentages for the same network in classic OISL and flexible OISL logic.

Table 10: Comparison between classic OISL and flexible OISL access availability results for networks of 5, 9 and 11 OGSs. The Average Availability Gain is a measure of the average improvement per target from a classic to a flexible OISL logic.

Network	**Minimum-Maximum Availability - Classic**	**Minimum-Maximum Availability - Flexible**	**Average Availability Gain**
Best Cloud	81.29-96.14%	92.53-96.07%	3.3%
Best Quadrant	82.50-94.80%	92.33-96.12%	3.3%
Northern	46.29-78.62%	67.88-78.61%	5.93%
Southern	80.90-97.28%	93.59-97.21%	3.34%
Best 9 OGSs	94.79-99.27%	97.48-99.52%	1.02%
Best 11 OGSs	96.77-99.66%	98.25-99.81%	0.68%

As it can be seen, in each network both the minimum and maximum availabilities show significant improvements, and the average gains range from 0.68% for the larger networks to 3.3% for the smaller ones, which, in the context of one year simulation period, accounts to respectively 2.5 and 10 more total days of connection, with a maximum of 5.93% (21 days) for the Northern network. The entity of the improvements decreases as the size of the network grows, as a consequence of the fact that the availabilities are getting closer to the limit of 100% and a sort of law of diminishing returns can be identified.

Table 11: Average Weighted Availability Gain from classic OISL to flexible OISL for networks of 5, 9 and 11 OGSs.

Network	**Weighted Availability Gain**
Best Cloud	2.73%
Best Quadrant	2.63%
Northern	5.18%
Southern	2.72%
Best 9 OGSs	0.80%
Best 11 OGSs	0.52%

To provide a more realistic measure of the average availability gain from classic to flexible OISL logic, a weighted average has been computed as well, taking into account the diffent weights attributed to the different targets. Table 11 shows the results for the 6 previously analyzed networks. Despite the decrease in average gain, the results are still impressive, ranging from 0.52 to 5.18%.

10 Conclusion

To conclude the work presented in this thesis, the following section sums up the content and results obtained so far and uses them to conduct a trade-off analysis between the two constellations. In the end, an outlook for the continuation of this work is provided, with focus on the developed tools.

10.1 Executive Summary

The aim of this work is to analyse the access availability and coverage performance of two satellite constellations that deploy optical uplinks and optical inter-satellite links. The two constellations mostly differ for their altitude, which makes for a different number of total satellites and a different ground coverage; Constellation A is a LEO constellation made of 256 satellites at 1200km altitude, while Constellation B is a LEO constellation made of 1152 satellites at 500km altitude.
Starting from orbital propagations done with STK and cloud databases containing the sky availability for all the 24 OGSs analyzed, these constellations have been assessed in order to create one chain database for each OGS, containing the accesses, meaning the time windows in which both the uplink and the downlink are available for each of the 64 targets in which the Europe area has been divided. Due to the introduction of a limitation in the number of terminals per OGS, an OGS HandOver logic was applied to maximize the access time. The 24 OGSs were first organized in networks of 5 OGS each in order to test the access availability performance of the constellations and highlight their first differences. It emerged clearly how the performance of constellation A is superior to the one of constellation B and that the best networks host the majority of their OGSs in southern Europe, where the weather conditions are better. OISL capability was investigated, testing 1 hop OISL on both constellations on each of the 8 networks of 5 OGSs, leading to an increase in performance and a decoupling between the geographical location of the OGSs and the access availability per target. At this point, further optimization algorithms have been developed to increase the access availability results of the constellations and optimize the OGS networks.
A chain access duration tool has been developed to investigate the average chain duration per target and to provide a further parameter to be used in the network optimization phase. It emerged that the chains of constellation A are in general way longer than those of constellation B, due to the higher constellation altitude that leads to longer visibility windows.
A network optimization tool has been developed to find the minimum number of OGS needed to reach availability percentages in the order of 99% on most targets and to find out the best combinations of the 24 OGSs. It emerged that constellation A needs 11 OGSs to reach an optimal performance, while constellation B struggles to reach higher availabilities on some targets even deploying all 24 OGSs.
A flexible OISL logic has been implemented to further improve the performance of the constellations, with the goal of selecting the 4 best satellites within the range constraint of the central satellite, independently on their orbital position. This tool showed that this logic has great potential, reducing the number of OGSs needed to guarantee an operable network to 9 for constellation A and 16 for constellation B. Later, a constraint on the payload allocation was introduced to make the situation more realistic, but the previous results came to be still valid, with only minor performance decreases.
Summing up, both constellations achieve huge access availability and coverage performance with the introduction of the different optimization tools developed, but constellation A seems to be way better than constellation B. The results gathered in the previous sections open the door for a quantitative trade-off analysis, which will be conducted in the next section. The modular implementation of the tools offers the possibility for further extension and optimization. As this could be a meaningful continuation of this work, the last section sums up options and opportunities.

10.2 Trade-Off

Even though the previously presented results seem to indicate that constellation A is more performing than constellation B, a trade-off analysis between the two constellations is here presented. Two trade studies are conducted; a qualitative one, implemented as a colour-coded table, and a quantitative one, implemented using a tool previously developed by DLR [49] and the results obtained in the previous sections.
The trade factors for the analysis are:

- **Access Availability performance (best) without OISL**: The access availability performance without OISL of the best network of 5 OGSs is taken for evaluation. Without OISL the most performing network is the Best Cloud per Quadrant for both constellations, since the performance is strictly dependent on the weather conditions of the OGS's location. A lower altitude constellation will perform worst on this trade factor.

- **Access availability performance (best) with OISL**: For this trade factor, the best network of 11 OGSs and the best network of 24 OGSs are taken as comparison terms, respectively for constellation A and constellation B. The idea is to find out the differences in access availability performance between the constellations, in the most likely scenario, that is a network with an OGS number sufficient to provide availabilities larger than 99% on most targets and with the deployment of a classical OISL geometry. The difference in the number of OGSs is not considered here, only the absolute performance quantified by the NO tool is taken into account.

- **Access availability performance (best) with flexible OISL**: For this trade factor, the best networks of 10 OGSs and 16 OGSs identified by the NO tool are taken as comparison terms, respectively for constellation A and B. In particular, the performance without constraints on payload allocation is considered. Being the situation less realistic, a lower trade score is attributed to this factor. As in the previous case, the difference in the number of OGSs is not considered.

- **Number of OGSs in the best network**: This trade factor confront the size of the best networks of the two constellation, attributing a score inversely proportional to the number of OGSs; indeed, a network with less OGSs is preferred to reduce mission complexity and the costs. The classic OISL geometry case is considered, so the numbers are 11 for constellation A and 24 for constellation B, since the score obtained by the NO tool by these two networks are comparable, while considering 16 OGSs for constellation B would be misleading, since the performance of that network is by far inferior to the one of the 11 OGSs network of constellation A, as presented in chapter 8.

- **Costs**: The total estimated cost of each constellation is obtained as a sum of the Capital Expenditure (CapEx) and the Operational Expenditure (OpEx). A higher score is assigned to the constellation that leads to the lower amount of expenditures.

- **Complexity**: Mission complexity increases with the number of total satellites in the constellation and with the number of OGSs that make the OGS network. Also, the deployment of flexible OISL would increase mission complexity, but since it will do it in the same way for both constellations, this is not considered in the analysis. Since constellation B has a higher number of satellites and requires more OGSs than constellation A, a lower score is attributed to the former and an higher score to the latter. Being mission complexity a complicated factor

to estimate, the scores have been manually attributed based on the number of satellites in the constellation and the number of OGSs in the best network.

- **Environmental Impact**: The environmental impact that a constellation will have is a fundamental factor to consider during the design process. Indeed, to guarantee a sustainable and durable use of space, factors like orbital pollution, space debris and impact on scientific observations and climate change are really important. The environmental impact has been computed as a sum of the following estimated parameters: amount of carbon dioxide introduced in the atmosphere by the process of building the satellites, the emission of exhausts from satellite burns and the fuel mass exhausted into the atmosphere to put satellites in orbit. The pollution has been quantified considering the collision risks and the negative impact on astronomical observations of the constellations. The information needed to estimate these factors is mostly provided by Hainaut and Williams [29].

- **Latency**: Latency is the transmission time of a signal from a transmitter to a receiver. The longer this time is, the worse is the constellation in terms of latency. As this amount highly depends on the position of the original transmitter and final receiver, when the satellites are further away from the transmitter (OGS) and the receiver (Target), so the constellation altitude is higher, the latency will also be higher. Furthermore, the introduction of OISL will increase the travel time, making the latency performance of both constellations worse. Since constellation B is at a lower altitude, its latency score is higher than the one of constellation A. To make the quantification comparable, the latency of the data transmission between two defined locations on Earth,is calculated for each constellation. In this thesis, the two European cities chosen to represent the calculation are Catania, which is thought as the OGS that provides the uplink, and Stockholm, thought as the end target of the chain.

To compute and quantify the environmental impact, the costs and the latency trade factors, the tool described in [49] was used.
The weights attributed to each trade factor ranges from 1 to 10 and are shown in table 12.

Table 12: Absolute rating values for the trade-off factors.

Parameter	**Id**	**Rating Value**
Access Availability performance w/o OISL	AAwoOISL	8
Access Availability performance Classic OISL	AAclOISL	10
Access Availability performance Flex OISL	AAflOISL	7
Number of OGSs in best Network	NumOGS	7
Costs	Cost	5
Complexity	Compl	4
Environmental Impact	EnvImp	6
Latency	Lat	5

A higher weight is assigned to the access availability performance with OISL, since this is the most likely implementation, followed by the no OISL and flexible OISL scores. More importance is attributed to the no OISL case versus the flexible OISL case, since the former is based on a technology already available, while the latter would require a new level of technology that, at the moment, is not there yet. A high level of importance is given also to the number of OGS deployed to achieve the best network and to the environmental pollution. Next, the cost, complexity and latency are assigned similar scores.

Each constellation is assigned a score from 1 to 10 for each of the trade factors and the final score is the weighted average of such scores. The results can be seen in the colour coded table 13, in which the performance of a constellation on each trade factor ranges from a red color (bad performance) to a green color (optimal performance).

Table 13: Qualitative trade study results.

	Constellation A	**Constellation B**
Access Availability performance w/o OISL		
Access Availability performance Classic OISL		
Access Availability performance Flex OISL		
Number of OGSs in best Network		
Costs		
Complexity		
Environmental Impact		
Latency		

The values for the trade factors of the constellations are showed in table 14 and the scores assigned to evaluate those performances are showed in table 15.

Table 14: Constellations values for each trade factor.

	Constellation A	**Constellation B**
Access Availability performance w/o OISL	0.788	0.433
Access Availability performance Classic OISL	0.991	0.974
Access Availability performance Flex OISL	0.996	0.985
Number of OGSs in best Network	11	24
Costs (bn EUR)	~ 113	~ 275
Complexity	Mid	High
Environmental Impact	Mid	High
Latency (s)	~ 0.029	~ 0.017

Table 15: Quantitative trade study results.

	Constellation A	**Constellation B**
Access Availability performance w/o OISL	7	4
Access Availability performance Classic OISL	9	8
Access Availability performance Flex OISL	10	9
Number of OGSs in best Network	9	2
Costs	4	3
Complexity	6	5
Environmental Impact	6	4
Latency (s)	7	10
Final Score	**7.58**	**5.73**

As it can be seen from the previously displayed tables, the performance of both constellations in the AAwoOISL case is sub-optimal, since all the networks of 5 OGSs tested were defective in the areas

far away from the OGS locations, especially for Large LEO, due to the narrower visibility cones of the satellites. Still considering purely the access availability performance, the situation drastically improves in the AAclOISL case, in which both constellations achieve availabilities above 99% on most targets, with respectively 11 and 24 OGSs. Lastly, in the AAflOISL case, the performance increases even more, reaching availabilities close to 100% on most targets. The values in table 14 are the target weighted availabilities scores provided by the NO tool, and we can see how they get really close to the maximum (1) in the OISL cases. However, while both constellations can achieve a great availability and coverage performance, only Small LEO is able to do so with a limited number of OGSs, equal to 11, while Large LEO requires respectively 24 and 16 OGSs for the AAclOISL and AAflOISL cases.
Regarding the costs, the estimated values are extremely high for both constellations, especially for Large LEO, whose cost is estimated to be around 275 billion dollars. Similar costs are expected when dealing with satellite constellations, but the values become higher and higher the larger the number of OGS and total satellites required, and the same is applicable for the complexity, who is estimated to be slightly above the average of LEO constellations for Small LEO, but above average for Large LEO.
The situation becomes more problematic for the environmental impact, since the estimated amounts of carbon dioxide emitted in the atmosphere are high for Small LEO, and extremely high for Large LEO; the values computed by the tool are 496 millions and 1030 millions kg of polluting substances, respectively for Small LEO and Large LEO. The same is true for the collision risk and the impact on astronomical observations, hence the red colors in table 13 and the low scores in table 15. Indeed, while the environmental impact is a downside for all satellite constellations, the situation is particularly worse than average for Large LEO, due to its high amount of satellites. Indeed, the collision risk, given by the product between the probability of having a collision and its consequence, amounts to 24.7 for Small LEO and 60.4 for Large LEO, a value almost three times higher. The astronomical impact, computed as the product between the number of visible satellites during the observation time multiplied by the magnitude of a single satellite, turned out to be equal to 887017 and 227065, for Large LEO and Small LEO respectively, indicating again a more negative performance for constellation B. Given all of the above, the environmental impact of Constellation A is indicated as Mid in table 14, while it is High for constellation B.
The only trade factor in favour of Large LEO came out to be the latency, which was estimated by the tool to be equal to only 0.017 seconds, versus the 0.029 seconds of Small LEO.
In the end, the final weighted scores for the two constellations are 7.58 for Small LEO and 5.73 for Large LEO. As expected, constellation A has higher scores for all the trade factors, with the exception of the latency, which is in favour of constellation B due to its lower altitude. The results clearly indicate that constellation A would be better suited for the mission, leading to higher access availabilities performances and lower costs, complexity and environmental pollution. It is to be said that the evaluation methodology is not free from uncertainty, however the final result is so strongly in favour of constellation A that this conclusion is not expected to change.

10.3 Suggestions for Future Research

The tools developed during the analysis have been realized with the goal of optimizing the access availability and coverage performance of the constellations, as well as the simulation time. However, while these tools proved to be useful and efficient, they are not free from improvements.
In particular, the Network Optimization tool is currently implemented via multiple building blocks: the requirements and the parameters for the analysis are defined in the config.py script, the main analysis is done by the joint work of the pre analysis and analysis.py scripts, while the trade-off

and the cloud blockage analysis are carried out by the tradeoff.py script. The improvements and suggestions of the tradeoff.py script are simply printed on the screen, and the user has to analyze and decide whether or not to apply them and start the analysis again from the beginning, after having modified the configuration file. A possible improvement would be the realization of a completely autonomous tool which, taking as input the constellation parameters and the goal of the user, is able to run itself until the accomplishment of the goal, which might be, for example, finding the minimum number of OGSs that guarantee availabilities above 99% on all the most important targets, as well as the locations of such OGSs, for each constellation. Another advancement might be evaluating multiple scenarios at a time, meaning that the best network is established considering its performance on the no OISL, classical OISL and flexible OISL databases, instead of only on one of these.
Another area of improvement is the flexible OISL tool, in particular the one with payload constraints. Indeed, the analysis done considering the optical laser terminals position, is an extremely complicated one, thus multiple approximations have been done: the computation of the satellites within the range constraint of the central satellite at a specific time is implemented taking the data of a 1 day long STK simulation of a reference satellite, the algorithm used to find the deck's visibility consider a satellite to be visible by a deck only if it is in its azimuth range for 80 % of the simulation time and no constraints on the time needed for a terminal to switch connection is implemented. An improvement (and a challenge) would be to get rid of these approximations and make the situation more realistic while, at the same time, keeping the simulation time under an acceptable threshold.
Implementing different models of Earth gravity in the STK simulations, computing the average bit rate per target, considering more OGSs in addition to those already analyzed and testing different yet realistic OISL geometries are only some of the additional steps that can be taken to progress this analysis.
In conclusion, just as a metaphor for life, no matter how many (cloud) blockages and issues we encounter along the way; if we stay positive and keep working hard, we will be able to build a system of 'full metal', solid and efficient enough to justify all the challenges we had to tackle.

References

[1] D.L. Fried. "Optical resolution through a randomly inhomogeneous medium for very long and very short exposures". In: *Journal of the Optical Society of America* 56 (1967), pp. 1372–1379.

[2] J. G. Walker. *Circular orbit patterns providing continuous whole Earth coverage*. Tech. rep. 70211. Royal Aircraft Establishment, UK, 1970.

[3] Peter O. Minott. "Scintillation in an earth-to-space propagation path". In: *Journal of the Optical Society of America* 62 (1972), pp. 885–888. URL: https://api.semanticscholar.org/CorpusID:120006841.

[4] A. H. Ballard. "Rosette Constellations of Earth Satellites". In: *IEEE Transactions on Aerospace and Electronic Systems* AES-16.5 (1980), pp. 656–673.

[5] J. G. Walker. "Satellite constellations". In: *Journal of the British Interplanetary Society* 37 (1984), pp. 559–571.

[6] Keith E. Wilson and James R. Lesh. "An Overview of the Galileo Optical Experiment (GOPEX)". In: *Communications Systems Research Section* (1993). URL: https://www.semanticscholar.org/paper/An-Overview-of-the-Galileo-Optical-Experiment-Wilson-Lesh.

[7] Paul A. Lightsey. "Scintillation in ground-to-space and retroreflected laser beams". In: *Optical Engineering* 33 (1994), pp. 2535–2543. URL: https://api.semanticscholar.org/CorpusID:120217114.

[8] M. Jeganathan, K. E. Wilson, and J. R. Lesh. "Preliminary analysis of fluctuations in the received uplink-beacon-power data obtained from the GOLD experiments". In: *TDA Progress Report 42-124*. Comm. Sys. and Research Sec., 1996, pp. 20–32.

[9] Keith E. Wilson. "An Overview of the GOLD Experiment Between the ETS-6 Satellite and the Table Mountain Facility". In: *Communications Systems Research Section* (1996). URL: https://api.semanticscholar.org/CorpusID:129678662.

[10] Keith E. Wilson et al. "Results of the Compensated Earth-Moon-Earth Retroreflector Laser Link (CEMERLL) Experiment". In: *Communications Systems Research Section* (1997). URL: https://api.semanticscholar.org/CorpusID:129678662.

[11] Keith E. Wilson et al. "Overview of the Ground-to-Orbit Lasercom Demonstration (GOLD)". In: *Photonics West*. 1997. URL: https://api.semanticscholar.org/CorpusID:33883421.

[12] J. H. Franz and V. K. Jain. *Optical Communications: Components and Systems: Analysis, Design, Optimization, Application*. Narosa Publishing House, 2000.

[13] Ray E. Sheriff and Y. Fun Hu. *Mobile Satellite Communication Networks*. Baffins Lane, Chichester, West Sussex, PO19 1UD, England: John Wiley Sons, LTD, 2001. ISBN: 0-471-72047-X.

[14] Vladimir Sidorovich. "Solar background effects in wireless optical communications". In: 4873 (Oct. 2002). DOI: 10.1117/12.456303.

[15] Toni Tolker-Nielsen and Gotthard Oppenhauser. "In-orbit test result of an operational optical intersatellite link between ARTEMIS and SPOT4, SILEX". In: *SPIE LASE*. 2002. URL: https://api.semanticscholar.org/CorpusID:61414144.

[16] M. Toyoshima. "Trends in satellite communications and the role of optical free-space communications". In: *J. Opt. Netw.* 4 (2005), pp. 300–311.

[17] Arun K. Majumdar and Jennifer C. Ricklin. *Free-Space Laser Communications: Principles and Advances*. Vol. 2. Optical and Fiber Communications Reports. Springer, 2008.

[18] H. Henniger and O. Wilfert. “An introduction to free-space optical communications”. In: *J. Radio Eng.* 19.2 (2010), pp. 203–212.

[19] Jill Tombasco. “Orbit Estimation of Geosynchronous Objects Via Ground-Based and Space-Based Optical Tracking”. In: (Jan. 2011).

[20] Shane M. Walsh, Skevos F. E. Karpathakis, et al. “Optical two-way time and frequency transfer over free space”. In: *Nature Photonics* 7 (2013), pp. 471–476.

[21] Katie Kriz. *ILS to Launch Eutelsat 9B Satellite in 2015*. 2014. URL: https://www.satellitetoday.com/business/2014/01/16/ils-to-launch-eutelsat-9b-satellite-in-2015/ (visited on 12/07/2023).

[22] X. Li, X. Zhang, X. Ren, et al. “Precise positioning with current multi-constellation Global Navigation Satellite Systems: GPS, GLONASS, Galileo and BeiDou”. In: *Scientific Reports* 5 (2015), p. 8328. URL: https://www.nature.com/articles/srep08328.

[23] Hemani Kaushal and Georges Kaddoum. “Optical Communication in Space: Challenges and Mitigation Techniques”. In: *IEEE Communications Surveys Tutorials* 19 (Aug. 2016), pp. 57–96. DOI: 10.1109/COMST.2016.2603518.

[24] Ahmed Hashim Mohammed et al. “HANDOVER IN LEO SATELLITE MOBILE NETWORKS.” In: 2016. URL: https://api.semanticscholar.org/CorpusID:63545165.

[25] Tyler Reid et al. “Leveraging Commercial Broadband LEO Constellations for Navigation”. In: Sept. 2016. DOI: 10.33012/2016.14729.

[26] Christian Fuchs. *ONUBLA Assessment of access availability of space-ground optical links*. Accessed: 2023-12-08. 2017. URL: https://nebula.esa.int/sites/default/files/neb_study/1189/C4000110718ExS.pdf.

[27] Hemani Kaushal and Georges Kaddoum. “Optical Communication in Space: Challenges and Mitigation Techniques”. In: *IEEE Communications Surveys & Tutorials* 19 (2017), pp. 57–96. URL: https://api.semanticscholar.org/CorpusID:19239549.

[28] De Gruyter. *Scaling capacity of fiber-optic transmission systems via silicon photonics*. 2020. URL: https://www.degruyter.com/document/doi/10.1515/nanoph-2020-0309/html (visited on 12/07/2023).

[29] Olivier R. Hainaut and Andrew P. Williams. “Impact of satellite constellations on astronomical observations with ESO telescopes in the visible and infrared domains”. In: *EDP Sciences Astronomy and Astrophysics* Apr. (2020).

[30] TechTarget. *What is line of sight?* 2020. URL: https://www.techtarget.com/whatis/definition/line-of-sight-LOS (visited on 12/07/2023).

[31] Vincent Billault et al. “Free space optical communication receiver based on a spatial demultiplexer and a photonic integrated coherent combining circuit”. In: *Optics Express* 29.21 (Sept. 2021), p. 33134. ISSN: 1094-4087. DOI: 10.1364/oe.433087. URL: http://dx.doi.org/10.1364/OE.433087.

[32] Soohyun Park and Joongheon Kim. *Trends in LEO Satellite Handover Algorithms*. 2021. arXiv: 2107.08619 [cs.NI].

[33] Jun Xie et al. “Satellite Navigation Inter-satellite Link Technology”. In: *Satellite Navigation Systems and Technologies*. Singapore: Springer Singapore, 2021, pp. 181–215. ISBN: 978-981-15-4863-5. DOI: 10.1007/978-981-15-4863-5_5. URL: https://doi.org/10.1007/978-981-15-4863-5_5.

[34] Saima Zafar and Hira Khalid. "Free Space Optical Networks: Applications, Challenges and Research Directions". In: *Wirel. Pers. Commun.* 121.1 (Nov. 2021), pp. 429–457. ISSN: 0929-6212. DOI: 10.1007/s11277-021-08644-4. URL: https://doi.org/10.1007/s11277-021-08644-4.

[35] National Aeronautics and Space Administration. *Deep Space Optical Communications (DSOC)*. https://www.nasa.gov/mission/deep-space-optical-communications-dsoc/. Oct. 2023.

[36] European Space Agency. *European Data Relay Satellite System (EDRS) Overview*. 2023. URL: https://connectivity.esa.int/european-data-relay-satellite-system-edrs-overview.

[37] European Space Agency. *European Data Relay Satellite System (EDRS) Overview*. 2023. URL: https://connectivity.esa.int/european-data-relay-satellite-system-edrs-overview (visited on 12/07/2023).

[38] European Space Agency. *Satellite frequency bands*. https://www.esa.int/Applications/Connectivity_and_Secure_Communications/Satellite_frequency_bands. Sept. 2023.

[39] Ciena. *Pioneering the path for quantum-secured long-distance communications: What's next?* 2023. URL: https://www.ciena.com/insights/blog/2023/pioneering-the-path-for-quantum-secured-long-distance-communications-whats-next.

[40] David J. Israel et al. "Early results from NASA's laser communications relay demonstration (LCRD) experiment program". In: *SPIE*. 2023. URL: https://www.spiedigitallibrary.org/conference-proceedings-of-spie/11536/1153619/Early-results-from-NASAs-laser-communications-relay/10.1117/12.2655481.short.

[41] Maureen Kaine-Krolak and Mark E. Novak. *An introduction to Infrared technology: Applications in the home, classroom, workplace, and beyond*. 2023. URL: https://park.org/Guests/Trace/pavilion/paper11.htm (visited on 12/07/2023).

[42] Colt Technology Services Group Limited. *IP Access Guide*. Accessed: 2023-12-08. 2023. URL: https://www.colt.net/solutions/on-demand/resources/ip-access-guide/.

[43] Catherine G. Manning and Katherine Schauer. *Optical Communications Overview*. https://www.nasa.gov/technology/space-comms/optical-communications-overview/. Sept. 2023.

[44] Edmund Optics. *Considerations in Collimation*. 2023. URL: https://www.edmundoptics.com/knowledge-center/application-notes/optics/considerations-in-collimation/ (visited on 12/07/2023).

[45] Profen. *The Future of Geostationary Satellites*. Accessed: December 18, 2023. 2023. URL: https://profen.com/en/future-of-geostationary-satellites/.

[46] Kateryna Sergeieva. *Satellite Constellations: Existing And Emerging Swarms*. 2023. URL: https://eos.com/blog/satellite-constellation/ (visited on 11/24/2023).

[47] *Using Waves to Communicate*. https://radio-waves.orange.com/en/using-waves-to-communicate/. Accessed: January 19, 2024. 2024.

[48] Samuele Raffa. *FL4NGSO - Technical Note 1 - Optical Link Scenarios*. DLR - KN, 2023-08-04.

[49] Karina Szych. *Optical Communication Payloads: Analysis for Sustainable Satellite Constellations*. FH Aachen, DLR - KN, 2023-06-20.